

UNIVERSITY OF OKLAHOMA
GRADUATE COLLEGE

POLYPHASIC TAXONOMY: A TOOL TO IDENTIFY AND CHARACTERIZE
MEMBERS OF COMPLEX MICROBIAL COMMUNITIES

A DISSERTATION
SUBMITTED TO THE GRADUATE FACULTY
in partial fulfillment of the requirements for the
Degree of
DOCTOR OF PHILOSOPHY

By
CRYSTAL NICOLE JOHNSON
Norman, Oklahoma
2014

POLYPHASIC TAXONOMY: A TOOL TO IDENTIFY AND CHARACTERIZE
MEMBERS OF COMPLEX MICROBIAL COMMUNITIES

A DISSERTATION APPROVED FOR THE
DEPARTMENT OF MICROBIOLOGY AND PLANT BIOLOGY

BY

Dr. Paul A. Lawson, Chair

Dr. Ralph S. Tanner

Dr. Richard Broughton

Dr. Boris Wawrik

Dr. Bradley S. Stevenson

© Copyright by CRYSTAL NICOLE JOHNSON 2014
All Rights Reserved.

“ *Natura non facit saltum* ”
Nature does not jump

Charles Darwin

Acknowledgements

It is with the deepest of gratitude that I acknowledge my support system of mentors, family, and friends that have lifted me up throughout this journey. My husband, Clayton Turner, whom I rely on for at least half of life; my parents, Derek and Jody Johnson, who may not have always understood how I could be in school so long but always supported my determination; and my grandparents, Joe and Judy Davis, who above anyone else inspire me to leave my mark on this world. I wish to thank my advisor, Dr. Paul Lawson, with whom I have grown into a scientist. I have appreciated your insight and advisement throughout my graduate research. I would also like to acknowledge my committee members for their guidance during my studies at The University of Oklahoma: Dr. Ralph Tanner, Dr. Boris Wawrik, Dr. Bradley Stevenson, and Dr. Richard Broughton. Many have played a role in this dissertation, and it truly represents a collaborative effort.

Table of Contents

Acknowledgements.....	iv
Table of Contents.....	v
List of Tables.....	viii
List of Figures.....	x
Abstract.....	xiii
Chapter 1: <i>Peptoniphilus stercorisuis</i> sp. nov. from a swine manure storage tank and description of <i>Peptoniphilus</i> fam. nov.....	1
Abstract.....	2
Introduction.....	4
<i>A preamble of taxonomy</i>	4
<i>Intragenetic relationships of Peptoniphilus</i>	9
Materials and Methods.....	11
<i>Bacterial strains and culture conditions</i>	11
<i>Morphological, physiological, and biochemical characterization</i>	11
<i>Determination of the 16S rRNA gene sequence and phylogenetic analysis</i> ...13	
<i>Chemotaxonomic characterization</i>	15
Results.....	17
<i>Description of Peptoniphilus stercorisuis</i> sp. nov.....	32
<i>Description of Peptoniphilaceae</i> fam. nov.....	33
Discussion.....	34
References.....	37
Chapter 2: <i>Savagea faecisuis</i> gen. nov., sp. nov., a tylosin- and tetracycline-resistant bacterium isolated from a swine-manure storage pit.....	41

Abstract	42
Introduction.....	43
Materials and Methods.....	45
<i>Bacterial strains and culture conditions</i>	45
<i>Morphological, physiological, and biochemical characterization</i>	45
<i>Determination of the 16S rRNA gene sequence and phylogenetic analysis</i> ...	47
<i>Chemotaxonomic characterization</i>	48
<i>Determination of tetracycline resistance genes</i>	51
Results.....	52
<i>Description of Savagea gen. nov</i>	65
<i>Description of Savagea faecisuis sp. nov</i>	66
Discussion.....	68
Acknowledgements.....	71
References.....	72
Chapter 3: <i>Proteiniphilum alaskensis</i> sp. nov., isolated from Alaskan petroleum pipeline effluent.....	76
Abstract	77
Introduction.....	79
Materials and Methods.....	81
<i>Bacterial strains and culture conditions</i>	81
<i>Morphological, physiological, and biochemical characterization</i>	82
<i>Determination of the 16S rRNA gene sequence and phylogenetic analysis</i> ...	84
<i>Chemotaxonomic characterization</i>	85
<i>Assessment of Corrosion potential</i>	85

Results.....	87
<i>Description of Proteiniphilum alaskensis sp. nov.</i>	99
Discussion.....	100
Acknowledgements.....	103
References.....	104
Chapter 4: Differential rates of corrosion measured between <i>Desulfovibrio alaskensis</i> and <i>Desulfovibrio indonesiensis</i> , a determination of microbial contributions to biocorrosion.....	
Abstract.....	107
Introduction.....	109
Materials and Methods.....	113
Material and Solution Preparation.....	113
<i>Biofilm Characteristics</i>	114
<i>Iron Liberation</i>	115
<i>Surface Analysis</i>	115
Results.....	117
Discussion.....	128
References.....	131
Appendix A: <i>Fodincurvata halophilus</i> sp. nov., a moderately halophilic bacterium from a marine saltern.....	
Appendix B: <i>Peptostreptococcus canis</i> sp. nov., isolated from subgingival plaque from canine oral cavity.....	153

List of Tables

Table 1.1: Morphological and physiological characteristics of strain SF-S1 ^T	19
Table 1.2: API Rapid ID 32A results for <i>P. stercorisuis</i> strain SF-S1 ^T	20
Table 1.3: API ZYM results for <i>P. stercorisuis</i> strain SF-S1 ^T	21
Table 1.4: Comparison of fatty acid profile of strain SF-S1 ^T with other members of the genus <i>Peptoniphilus</i>	26
Table 1.5: Comparison of Fatty acid profiles of SF-S1 ^T on different media with <i>P. methionivorax</i>	27
Table 1.6: Phenotypic characteristics useful in the differentiation of strain SF-S1 ^T from other members of the genus <i>Peptoniphilus</i>	29
Table 1.7: Morphological, biochemical and chemotaxonomic properties of <i>Peptoniphilaceae</i> and close relatives.....	30
Table 1.8: Morphological, biochemical and chemotaxonomic properties of genetically related taxa excluded from <i>Peptoniphilaceae</i> fam. nov.....	31
Table 2.1: Morphological and physiological characteristics of <i>Savagea faecisuis</i> Con12 ^T	53
Table 2.2: API ZYM results for <i>Savagea faecisuis</i> strain Con12 ^T	54
Table 2.3: Comparison of fatty acid profile of <i>Savagea faecisuis</i> strain Con12 ^T with type species of related genera.....	59
Table 2.4: Fatty acid profiles of <i>Savagea faecisuis</i> strain Con12 ^T grown on different media.....	60
Table 2.5: Characteristics that distinguish the genus <i>Savagea</i> from other closely related genera.....	64
Table 3.1: Comparison of the cellular fatty acid compositions (% of total identified) of <i>Proteiniphilum alaskensis</i> sp. nov. PE-10 ^T and phylogenetic relatives.....	94
Table 3.2: Characteristics comparison of strain PE-10 ^T , type strain of <i>Proteiniphilum acetatigenes</i> , and strain MH5.....	95
Table 4.1: Quantitative pit distribution obtained via profilometry for uninoculated control, <i>D. alaskensis</i> , and <i>D. indonesiensis</i> . Pit Density (grains/mm ²).....	127

Table A1.1: Characteristics that differentiate strain BA45AL ^T from related species of the genus <i>Fodinicurvata</i>	143
Table A1.2: Cellular fatty acid contents (percentages) of strain BA45AL ^T and the type strains of phylogenetically related species.....	145
Table B1.1: Cellular fatty acid compositions (%) of <i>Peptostreptococcus canis</i> sp. nov., <i>Peptostreptococcus anaerobius</i> , <i>Peptostreptococcus russellii</i> , and <i>Peptostreptococcus stomatis</i>	164
Table B1.2: Differential characteristics of <i>Peptostreptococcus canis</i> sp. nov., <i>Peptostreptococcus anaerobius</i> , <i>Peptostreptococcus russellii</i> , and <i>Peptostreptococcus stomatis</i>	165

List of Figures

Figure 1.1: Phase contrast image of strain SF-S1 ^T at 1000X magnification.....	18
Figure 1.2: Pairwise alignment of 16S rRNA gene sequences between <i>Peptoniphilus stercorisuis</i> strain SF-S1 ^T , the nearest cultivated neighbor <i>Peptoniphilus methioninivorax</i> , and other genetically similar species, <i>Peptoniphilus coxii</i> and <i>Peptoniphilus koenoeniae</i>	23
Figure 1.3: Phylogenetic dendrogram of 16S rRNA gene sequences indicating the position of <i>Peptoniphilus stercorisuis</i> sp. nov.....	24
Figure 2.1: Phylogenetic tree of 16S rRNA gene sequences indicating the position of <i>Savagea faecisuis</i> gen. nov. sp. nov. strain Con12 ^T within the <i>Planococcaceae</i> family.....	56
Figure 2.2: RAPD-PCR of <i>Savagea</i> strains using m13 primer.....	57
Figure 2.3: Two- dimensional total lipid profiles of <i>Savagea faecisuis</i> gen. nov. sp. nov. strain Con12 ^T	61
Figure 2.4: Amino acid analysis of strain Con12 ^T showing alanine (Ala), glutamic acid (Glu), glycine (Gly) and lysine (Lys).....	62
Figure 2.5: Chromatogram of isomer analysis for strain Con12 ^T	63
Figure 3.1: The complete 16S rRNA gene sequence of <i>Proteiniphilum alaskensis</i> strain PE-10 ^T	88
Figure 3.2: Pairwise alignment of the 16S rRNA gene sequences between <i>Proteiniphilum alaskensis</i> strain PE-10 ^T (query) and the nearest cultivated neighbor, <i>Proteiniphilum acetatigenes</i> strain TB107 (subject), showing 93.0% sequence similarity.....	88
Figure 3.3: Neighbor-joining phylogenetic tree showing the relationship between members of <i>Proteiniphilum</i> and related taxa based on 16S rRNA gene sequences.....	91
Figure 3.4: Phylogenetic analysis of a number of type trains, in addition to 16S rRNA sequence of PE-10 ^T and the OTUs obtained from the 454 pyrosequencing data.....	92
Figure 3.5: Carbon steel coupons imaged with SEM at 25 kV showing medium-only control (A), PE-10 ^T surface biofilm (B), and PE-10 ^T following biofilm removal (C). Scandium-generated line scan of PE-10 ^T incubated coupon after ASTM cleaning revealing surface roughness (D).....	98
Figure 4.1: SEM images of (a) <i>D. alaskensis</i> and (b) <i>D. indonesiensis</i> biofilms formed on the surface of metal coupons after 30 days in VMI medium.....	118

Figure 4.2: SEM images representative of all fields using an SE2 signal at 10 kV and 272 X magnification. (a) <i>D. alaskensis</i> and (b) <i>D. indonesiensis</i> colonized coupons after 90 days incubation.....	118
Figure 4.3: SEM images of bacterial growth taken with an SE2 signal at 10 kV and 272X magnification. (a) <i>D. alaskensis</i> and (b) <i>D. indonesiensis</i> colonized coupons after 30 days incubation, including (c) EDS spectrum layered for comparison of <i>D. alaskensis</i> and <i>D. indonesiensis</i> biomass and corrosion products.....	120
Figure 4.4: EDS comparison of biofilms (a) <i>D. alaskensis</i> spectra, 30 days (red) versus 90 days (yellow); (b) <i>D. indonesiensis</i> spectra, 30 days (red) versus 90 days (yellow).....	120
Figure 4.5: Biofilm thickness obtained from confocal microscopy using the reflective mode, showing statistically significant differences in colonization physiology between <i>D. alaskensis</i> and <i>D. indonesiensis</i> ($p < 0.05$) but not between <i>D. alaskensis</i> and the abiotic control (n=3).....	121
Figure 4.6: Rates of corrosion between <i>D. alaskensis</i> and <i>D. indonesiensis</i> after 30 and 90 days calculated from mass loss and iron liberation.....	122
Figure 4.7: Coupon topography using SEM (20kV at 500X) of metal surface after 30 days colonization with A ₁) <i>D. alaskensis</i> , A ₂) <i>D. indonesiensis</i> , showing; B _{1,2}) height profile for generating R _f , C _{1,2}) height thresholds (blue, depressed; red, elevated), and D _{1,2}) a 3-D plot of metal topography.....	123
Figure 4.8: Rates of corrosion between <i>D. alaskensis</i> and <i>D. indonesiensis</i> after 30 and 90 days calculated from roughness of metal after biofilm removal.....	124
Figure 4.9: A) 3-D contour map of <i>D. alaskensis</i> after 30 days B) <i>D. alaskensis</i> with thresholding at average mean height. C) Contour map of <i>D. indonesiensis</i> after 30 days D) <i>D. indonesiensis</i> with thresholding at average mean height.....	125
Figure 4.10: Metal coupon surface topography after 30 days incubation showing the pit depth, frequency, and distribution of (a) abiotic control (b) <i>D. alaskensis</i> and (c) <i>D. indonesiensis</i>	126
Figure A1.1: Phase-contrast micrograph of cells of strain BA45AL ^T grown in liquid medium under optimal conditions. Scale bar, 1 μm	138
Figure A1.2: Maximum-likelihood phylogenetic tree based on 16S rRNA gene sequences, showing the relationships between strain BA45AL ^T and representatives of the family <i>Rhodospirillaceae</i>	139

Figure A1.3: Two-dimensional thin layer chromatograms of the polar lipids of strain BA45AL ^T , <i>Fodinicurvata fenggangensis</i> DSM 21160 ^T and <i>Fodinicurvata sediminis</i> DSM 21159 ^T	147
Figure B1.1: Unrooted tree showing the phylogenetic relationships of <i>Peptostreptococcus canis</i> sp. nov., and other organisms within rRNA clusters XI and XIII.....	162
Figure B1.2: 16 rRNA gene sequence alignment of variable region 1 for <i>Peptostreptococcus canis</i> , <i>P. anaerobius</i> , <i>P. russellii</i> , and <i>P. stomatis</i>	164

Abstract

Systematics is a fundamental discipline that underpins the science of microbiology, providing a framework that allows for the identification, classification, taxonomy, and nomenclature of single cell organisms. Since the second half of the twentieth century, systematics has made revolutionary insights into microbial relationships, revealing the vast diversity on planet Earth. Culture-independent methods based on the small subunit of the ribosomal RNA (16S rRNA) gene have since been developing at an ever-accelerating rate. With what are now considered common technologies, Sanger sequencing, Pyrosequencing, and Next Generation sequencing have revealed that the majority of microbial life remains yet to be cultured in the laboratory. Consequently, taxonomists have realized the enormity of cataloguing this diversity and have developed a polyphasic methodology for the description and classification of new taxa.

Although molecular methods are freely available to researchers for identification purposes, novel organisms cannot be described in the scientific literature purely on sequence information alone. Instead, the application of a polyphasic taxonomic approach emphasizes the use of classical methods married with modern genetic fingerprinting. Traditional techniques include morphological and biochemical descriptions, as well as chemotaxonomic features that encompass cell wall, polar lipid, fatty acid, and respiratory menaquinones. These important diagnostic biomarkers aid in the general assignment of isolates to the correct taxa. Specifically, chemotaxonomic characteristics are especially useful in reflecting phylogenies at the genus/family level. Modern techniques use the 16S rRNA gene amplified by the polymerase chain reaction (PCR) as a useful tool for comparing evolutionary distances. Acting as a molecular time

chronometer, variable and conserved regions can then be mathematically assessed by comparing multiple sequence alignments and viewed as phylogenetic trees. But these taxonomic classifications do not necessarily define the expected physiological traits since closely related organisms isolated from different locations can have very distinct physiologies and metabolic processes. Therefore, laboratory investigations with these isolates and comparisons to reference strains of closely related organisms remain essential. When investigating any complex ecosystem, cultivation methods include the use of enrichment media that cast a nutritionally wide net through the use of various substrate and energy source amendments. Diverse conditions can be established by altering incubation temperatures, pH values, headspace compositions (N₂, H₂, and CO₂ gas) as well as internal vessel pressure during incubation. Some information on the types of organisms present within an environment may be derived from 16S gene sequence molecular inventories, and therefore microbial groups of interest may be specially targeted with particular media amendments and selective growth conditions. Isolates can then be obtained by subculturing single colonies from plates and roll tubes, as well as through the use of dilutions to isolate dominant organisms. While rRNA gene-based phylogenies have revolutionized microbial taxonomy, they continue to be reinforced by chemotaxonomic and biochemical considerations. A combination of bacterial isolation and cultivation, descriptive classical techniques, and modern molecular sequencing methods has thus resulted in the comprehensive classification of new taxa.

The laboratory studies presented in this dissertation used these evolved taxonomic tools to validate the discovery of a number of novel, or previously

uncultured, isolates from complex ecosystems. Chapters 1 and 2 describe the isolation of a novel bacterial species with family reclassification and the isolation of a novel genus, respectively. Pure cultures, obtained from swine manure storage pits, were found to represent previously uncultivated taxa. Physiological, biochemical, and genetic features were investigated in order to determine phylogeny and demonstrate uniqueness. One organism, strain SF-S1^T, was related to members of the genus *Peptoniphilus* which was accommodated within a new family, *Peptoniphilaceae* fam. nov. A second organism, strain Con12^T, was classified as a novel genus and species, *Savagea faecisuis* gen. nov., sp. nov.

Additionally, a new species from an Alaskan oil production pipeline was isolated in pure culture and characterized physiologically in order to investigate its role in the environment. This work stemmed from a collaborative effort within the OU Biocorrosion Center that focused on the molecular -dependent and -independent detection of microbial populations and their activities associated with biocorrosion. As such, the goal of the cultivation component presented here was to explore the microbiology of pipeline effluent for previously unidentified cultivars. Phylogenetic analysis based on 16S rRNA gene sequences from this isolate indicated that strain PE-10^T belonged within the genus *Proteiniphilum*, most closely to *Proteiniphilum acetatigenes* (94% similarity). Chapter 3 provides evidence that PE-10^T represents only the second cultivated species of this genus. Pyrosequencing and qPCR data suggested that *Proteiniphilum*-like organisms comprised 11% of the population of this particular sample. Furthermore, incubation experiments with carbon steel suggested that PE-10^T might be involved in biofilm production. The isolation of *Proteiniphilum alaskensis*

strain PE-10^T represented the cultivation of an abundant molecular phylotype, therefore providing a tangible microbe with which to conduct corrosion experiments.

Towards this effort, Chapter 4 provides an investigation of parameters useful in the assessment of Microbially Influenced Corrosion (MIC). The objectives were two-fold: first, to evaluate various ways to measure MIC, and second, to demonstrate these methods by measuring the differential corrosion activity between two model organisms. Accomplishment of these efforts helped structure the tools necessary for evaluating the nature of novel taxa found to be associated with pipeline corrosion. In this study, biofilm characteristics, metal dissolution, and the damage to steel surfaces were analyzed in order to demonstrate the biocorrosive potential of bacteria. *Desulfovibrio indonesiensis* and *Desulfovibrio alaskensis*, chosen because they are sulfate reducing bacteria (SRB) associated with oil production systems, were shown to interact differently with carbon steel as measured with various Scanning Electron Microscopy (SEM) techniques, iron analysis, and surface profilometry. The study presented here used a series of measurements to directly characterize the corrosive capabilities of microbial assemblages. Ultimately, these parameters will be essential for determining the risk of resident bacteria as well as for assessing the efficacy of current corrosion detection and mitigation strategies.

The entirety of my laboratory investigations is not limited to the data presented here, as many environments were probed for the potential to cultivate novel microorganisms. In the appendix, descriptions of two additional novel species are included. Here, previously uncultivated bacterial isolates were obtained from the water of a saltern in Santa Pola, Alicante, Spain and from the subgingival plaque of a canine Labrador Retriever. These species have been validated and appear in the formats of *The*

International Journal for Systematic Evolutionary Microbiology (IJSEM) and *Anaerobe*, respectively. The breadth of taxonomic discoveries has never been more realized, and remains an encouragement for scientists to continue to identify and characterize members of complex microbial communities.

Chapter 1

***Peptoniphilus stercorisuis* sp. nov. from a swine manure storage tank and
description of *Peptoniphilaceae* fam. nov.**

Abstract

The advent of molecular techniques has revealed that the majority of bacteria in nature have yet to be cultured or formally recognized in the universal tree of life. The present study builds upon various physiological and biochemical analyses, and utilizes a molecular systematic approach to determine useful diagnostic markers for the family, *Peptoniphilacea*. A species of previously unknown anaerobic bacteria was recovered from a swine manure storage tank and characterized using phenotypic, chemotaxonomic, and molecular taxonomic methods. Comparative 16S rRNA gene sequence studies and biochemical characteristics demonstrated that this organism was genotypically and phenotypically distinct, and represented a previously unknown sub-line within the order *Clostridiales*, within the *Firmicutes*. Pairwise sequence analysis demonstrated that the novel organism clustered within the genus *Peptoniphilus*, and was most closely related to *Peptoniphilus methionivorax*, sharing a 16S ribosomal RNA gene sequence similarity of 95.5%. Cells were Gram-stain positive and obligately anaerobic, growing in protein-containing media rather than with carbohydrates. The major long-chain fatty acids were found to be C_{14:0} (22.4%), C_{16:0} (15.6%), C_{16:1 ω 7c} (11.3%), and C_{16:0 ALDE} (10.1%), and the G +C mol % of the DNA was 31.8. Since cells were non-fermentative, conventional bacteriological tests that rely on carbohydrate fermentation reactions were of little value for identification. Therefore, chemotaxonomic methods helped provide a more robust description. Based upon the phenotypic and phylogenetic findings presented, a novel species *Peptoniphilus stercorisuis* sp. nov. was proposed. In addition, it was suggested that the genera *Peptoniphilus*, *Anaerococcus*, *Anaerosphaera*, *Finegoldia*, *Gallicola*, *Helcococcus*,

Murdochiella, and *Parvimonas* be accommodated within a new family for which the name *Peptoniphilaceae* fam. nov. was proposed. The type strain of *Peptoniphilus stercorisuis* sp. nov. was therefore established as SF-S1^T (DSM 27563^T = NBRC 109839^T). Though the exact role of SF-S1^T in swine feces remains unclear, this study confirmed that previously uncultured Gram-positive low mol % G+C bacteria exist in this complex ecosystem. Additionally, data suggested that strain SF-S1^T may be involved in the degradation of proteinacious material such as peptides and amino acids, an important process in the decomposition of organic material that results in alkaline and odorous compounds.

Introduction

A preamble of taxonomy:

The establishment of an orderly classification and nomenclature system for taxonomic purposes has been an evolving process since the late 1700's. The earliest approaches at systematically describing life forms barely meet the criteria used today to differentiate bacteria from multicellular organisms. Biologists who study higher order plants and animals may follow the course of evolution using fossil records and morphological details which serve as a basis for their phylogenetic classification. Unfortunately, these criteria are not available for bacterial investigations. Eventually using microscopy as a major tool, the descriptive phase of systematic bacteriology began in the early nineteenth century, though characterization was still limited to general cell shape, relative behavior, and habitat. Two notable events that altered the course of bacterial nomenclature was the recognition of six bacterial genera in 1872 followed by reclassification to include cyanobacteria and an additional 8 new genera in 1875 (Cohn, 1872; Cohn, 1875). This provided the foundational knowledge that organisms have specific, inheritable characteristics that could be used to draw conclusions on phylogenetic associations. With the growing awareness over the next decades that microbes were associated with human health and disease, came a rise in taxonomic contributions. Many subsequent attempts at logical classifications were made (Zopf, 1885; Schroeter, 1886; Trevisan, 1889). However logical, proper classification was limited by lack of organization based on biological markers. Without adequate descriptors, the identification of microbes and recognition of new species was nonspecific and unreliable. It was not until 1909 and 1921 that classifications provided

by Orla-Jensen included physiological data (Orla-Jensen, 1909; Orla-Jensen, 1921). These studies were the first to explore the species-boundary, assigning classification based on differences beyond morphology by focusing instead on information such as the fermentation of various sugars, generation of metabolic by-products, and growth habits in variable conditions. As the robustness of phenotypic-driven taxonomy increased, so too did the reliability of microbial phylogenetic relatedness.

With the late 1950s to early 1960s dawned the realization that large macromolecules such as proteins and DNA could contain information pertaining to evolutionary histories (Zuckerandl and Pauling, 1965). DNA was *the* biological constituent of life and became a focus of interest as a tool to be used in taxonomy. Values of mol% G+C were initially used to indicate the relatedness between microbes (McCarthy & Bolton, 1963). This genetic feature refers to the percentage of nitrogenous bases on a DNA molecule that are either guanine or cytosine. Organisms whose G+C values differed significantly were not considered to be related species, whereas similar G+C values *could be* considered the same species, but not under any certain terms. Though useful, G+C determination provided limited information with regard to identity and phylogeny. This ambiguity was addressed with a more direct and quantitative means of comparing genotypes. To obtain a more coherent picture, DNA- DNA hybridization was introduced. Separation between organisms at the species level was needed, and DNA-DNA hybridization provided techniques to assess the variability between two DNA strands through nucleotide reassociation calculations (McCarthy & Bolton, 1963). By definition, a measure based directly on the genome results in an average measure of the degree of homology of the entire genome between the

organisms concerned. However, the formation of DNA duplexes does not occur beyond 10-20% basepair mismatches, thereby limiting this method to species classification rather than for determining distant relationships (Stackebrandt & Goebel, 1994). It was the discovery by Doi and Igarashi (1965) that showed the small ribosomal subunit of RNA contained conserved regions that were slower to change than the rest of the genome. This allowed researchers to track the changes of specific nucleotide sequences over time, and to compare them across the microbial world. Ribosomal RNA gene sequences provided a useful biological marker for phylogenetic studies because ribosomes, responsible for protein synthesis, are critical to all domains of life. With this, variable regions of the rRNA gene could be compared in order to determine percent relatedness and phylogenetic relationships. By the 1970s, researchers, most significantly Carl Woese, had provided solid contributions to the phylogeny of bacteria and genetic relationships of all life forms (Woese and Fox, 1977).

The description of new taxa has been occurring at an accelerated rate within the last decade, driven by the rapid advances in sequencing technology. Systematic microbial biology is now based on a phylogenetic framework that marries the analysis of the nucleotide sequence of rRNA with phenotypic characteristics, resulting in significant advances in the understanding of relationships between taxa. The incorporation of molecular techniques has since revealed that the majority of bacteria in nature remain yet to be cultivated or described. Fundamental to understanding the complexity of ecological systems is the isolation and subsequent characterization of these microbes. Towards these efforts, molecular assays have been conducted in order to obtain censuses of community composition (Hugenholtz, 1998). Culture-independent

(molecular-based) methods best answer *who* grows within a given ecosystem, while culture-dependent methods allow researchers access to cultivars with which to study *how* these organisms contribute to their environment. In this way, molecular-based data is also useful for identifying “organisms of interest” to target for cultivation. Key players in important environmental processes may not necessarily be the dominant organisms, therefore the physiological impacts of these microbes can only be assessed by *in vivo* isolation and further characterization. The inability to successfully culture and maintain these organisms hindered many early investigations. Improvements in artificial media and cultivation techniques have provided encouragement for researchers to investigate specimens of anaerobic bacteria more carefully. An important step forward were the advances made by Hungate (1950), who developed a technique of cultivating anaerobic bacteria by placing them under a stream of deoxygenated carbon dioxide. When combined with the collection of specimens into pre-reduced, anaerobically sterilized media (Holderman and Moore, 1972) the isolation and subsequent identification of anaerobic bacteria was significantly improved.

Polar lipids and peptidoglycan cell-wall types remain powerful chemotaxonomic markers that allow delineation of strains to families, genera, and even species when 16S rRNA gene sequencing fails to do so with confidence (Busse *et al.*, 1996). These features have many different forms, thus providing powerful discriminatory tools that have historically been important in classifications schemes (Fahy *et al.*, 2005). Although not restrained by specialized equipment, these features have eluded a high throughput approach, and methods are now being performed in fewer and more specialized laboratories because such analytical expertise is required. Another major

impediment in the use of these cell-wall constituents in modern taxonomic approaches is the lack of any searchable and/or accumulative databases (Anderson and Wellington, 2001). This necessitates the repeated use of reference strains which is both time-consuming and expensive. Consequently, the integration of polar lipids and peptidoglycan data in the descriptions of novel taxa leads to fragmentary information that cannot be directly compared across related microbial groups.

Currently, the foci of a heated debate between microbiologists are the very concepts and methods used in prokaryotic systematics and how this should be approached in the future. Opinions vary from the classical view of collecting a plethora of phenotypic characteristics including morphology, biochemistry, and chemotaxonomy in tandem with phylogenetic analyses, to the provision of utilizing only genomic information with minimal phenotypic descriptors (Ramasamy *et al.*, 2014). Few would argue that a strong taxonomy must encompass sufficient biological markers to make the assignment of taxa to a particular group a robust process. Therefore, information from genomic analyses derived via affordable next generation sequencing must be embraced, but not at the expense of good taxonomic practices. Such advances now allow *in-silico* determination of G+C and DNA-DNA hybridization values, the “gold standards” of taxonomy. Furthermore, genomic sequences present a direct source of taxonomically relevant parameters such as cell features and metabolic potential (Siezen *et al.*, 2004). However, it is pertinent to note that databases that assign higher-level biological functions to this genomic information, such as the Kyoto Encyclopedia of Genes and Genomes (KEGG), often lack complete metabolic profiles or contain data that has not been experimentally confirmed (Altermann and Klaenhammer, 2005). Regardless, the

ability to compare the presence or absence of genes within whole genome sequences will provide greater resolution into the complexity of microbial ecosystems. With the sudden availability of large sequence datasets, microbiologists have been provided with valuable genetic information, allowing them to better explore bacterial diversity. As such, the discipline of taxonomy has made great strides in the last decade and is on the verge of a genomic transition.

Intragenetic relationships of Peptoniphilus

The genus *Peptoniphilus*, as it currently stands, consists of 12 species that include *Peptoniphilus asaccharolyticus* (Ezaki *et al.*, 2001), *Peptoniphilus coxii* (Citron *et al.*, 2012), *Peptoniphilus duerdenii* (Ulger-Toprak *et al.*, 2012), *Peptoniphilus harei* (Ezaki *et al.*, 2001), *Peptoniphilus indolicus* (Ezaki *et al.*, 2001), *Peptoniphilus ivorii* (Ezaki *et al.*, 2001), *Peptoniphilus koenoeniae* (Ulger-Toprak *et al.*, 2012), *Peptoniphilus lacrimalis* (Ezaki *et al.*, 2001), *Peptoniphilus methioninivorax* (Rooney *et al.*, 2011), *Peptoniphilus olsenii* (Song *et al.*, 2007), *Peptoniphilus gorbachii* (Song *et al.*, 2007) and *Peptoniphilus tyrrelliae* (Citron *et al.*, 2012). Almost all species have been isolated from human clinical material. However, *P. indolicus* was recovered from swine, cattle, and from insects associated with cattle, in addition to human clinical specimens (Ezaki *et al.*, 2001; Madsen *et al.*, 1991); while *P. methioninivorax* was isolated from retail ground beef (Rooney *et al.*, 2011). The nature of these habitats highlights a potential health-relevant role of the bacteria associated with these environments.

The exact relationship of this group of organisms with other close members of the *Firmicutes* is somewhat uncertain, and this is reflected in their placement within the Family XI *Incertae Sedis* (order *Clostridiales*, class *Clostridia*, phylum *Firmicutes*) in the current edition of *Bergey's Manual of Systematic Bacteriology* (De Vos *et al.*, 2009). Our studies demonstrate that the genus, *Peptoniphilus*, has a close relationship with *Anaerococcus*, *Anaerosphaera*, *Helcococcus*, *Finegoldia*, *Gallicola*, *Murdochiella* and *Parvimonas*. These organisms share consistent biochemical and chemotaxonomic traits that support the proposal to create a family with which to embrace these genera. In this chapter, the isolation and characterization of a novel species, *P. stercorisuis*, recovered from stored swine manure, demonstrates this need. This Gram stain-positive, obligately anaerobic, coccus-shaped organism was characterized using biochemical, chemotaxonomic, and phylogenetic methods. Based upon the findings presented here, a novel species, *Peptoniphilus stercorisuis* sp. nov. was proposed, in addition to the creation of a family to encompass genetically and physiologically similar taxa.

Materials and Methods

Bacterial strains and culture conditions

Strain SF-S1^T (DSM 27563^T = NBRC 109839^T) was isolated from a swine manure storage tank located at a pig production facility in central Oklahoma, USA. A sample of pig slurry was collected from a 3.0-meter depth using a tank sampler (NASCO, WI); the environmental conditions of the sample site were found to have a temperature of 28 °C, a pH of 7.3, and when allowed to settle, a particulate matter of approximately 50% (v/v). The sample was transferred to a nitrogen-flushed sterile bottle that was then sealed to maintain an anaerobic environment, and transported back to the laboratory on ice. A 10% (v/v) inoculum was used for enrichment in Brain Heart Infusion (BHI) (Oxoid, UK) broth at pH 7.0 and incubated at room temperature with H₂:N₂:CO₂ headspace (5:10:85) at 20 psi. Isolation was achieved through serial plate dilutions and subcultures on Tryptic Soy Agar (Becton, Dickenson and Company, MD) amended with 5% defibrinated sheep's blood, incubated in anoxic jars containing H₂:N₂:CO₂ headspace (5:10:85) at 37 °C. Colonies were picked and sub-cultured onto fresh medium until well isolated.

Morphological, physiological, and biochemical characterization

For phenotypic analysis, cells that had been grown anaerobically for 5 days at 37 °C on Brucella Blood agar (Oxoid, UK) were used for all tests unless otherwise stated. Cells were examined with an Olympus CX41 microscope using phase contrast at 1000X magnification (Fig. 1.1). For biochemical characterization, conventional tests and Rapid ID 32A and API ZYM (bioMérieux, Marcy L'Etoile, France) test systems

were used according to manufacturer's instructions, with all tests performed in duplicate (Jousimies-Somer *et al.*, 2002; Tindall *et al.*, 2007). For additional tests, the strain was incubated in Hungate tubes containing anoxic peptone-yeast extract (PY) medium (Holdeman *et al.*, 1977) supplemented with 0.1% cysteine sulfide. Additional tests included a temperature growth range that included broth incubations at 4, 10, 15, 20, 25, 30, 37, 43, 47, and 60 °C; pH values of 5.0, 5.5, 6.0, 6.5, 7.0, 7.3, 7.8, 8.0, 8.5 and 9.0; and NaCl concentrations of 0%, 0.5%, 1%, 2%, 3%, 4%, 5%, 6%, 7%, 8% and 9%. Optimum growth conditions were determined by measuring the rate increase in turbidity over time using a spectrophotometer at 600 nm (Spectronic 20D, Milton Roy). Fermentation tests were performed with fructose, mannose, glucose, sucrose, xylose, cellobiose, using pre-reduced, anaerobically sterilized carbohydrate broth tubes (Anaerobe Systems, CA). These pre-reduced tubes were inoculated with strain SF-S1^T inside an anaerobic glove bag (Coy, MI), incubated at 37 °C for 2 weeks and assessed for turbidity. Tests were considered positive if optical density (OD) measurements increased more than double the original OD. Antibiotic susceptibility was determined using discs (BBL[®]) impregnated with penicillin (P10, 10 units), chloramphenicol (C30, 30 mcg), bacitracin (B10, 10 units), trimethoprim (TMP5, 5 mcg), and ciprofloxacin (CIP5, 5 mcg). The diameter of growth inhibition was measured after incubation and resistance/ susceptibility was assessed using National Committee for Clinical Laboratory Standards (NCCLS) interpretive criteria. All tests were performed in duplicate.

Determination of the 16S rRNA gene sequence and phylogenetic analysis

For phylogenetic analyses, genomic DNA was extracted using phenol chloroform and precipitated with ethanol as described by Lawson *et al.* (1989). First, PY grown cells were pelleted and resuspended in 500 μ L TES buffer (0.05 M Tris, 0.05 M NaCl, 0.005 M EDTA; pH 8.0). Then 5 μ L of lysozyme (10 mg/mL) was added, and eppendorf tubes were incubated at 37 °C for 30 minutes in order to aid cell lysis. After 8 μ L of Proteinase K (10 mg/mL) and 8 μ L of RNase (10 mg/mL) was added, tubes were incubated in a 65 °C water bath for 1 hour in order to inhibit non-specific nucleases that would otherwise degrade DNA. Next, 120 μ L of 10% Sodium Dodecyl Sulfate (SDS) was added followed by further incubation at 65 °C for 10 minutes. Once cool, equal volumes of phenol: chloroform was mixed with samples until emulsions formed (~ 500 μ L). Tubes were then centrifuged at 4000 rpm for 10 minutes in order to promote phase separation of a lower solvent layer, a middle layer of protein and cell debris, and an upper aqueous layer containing the DNA. The top layer was pipetted into a new eppendorf tube and treated once more with the phenol: chloroform mix, centrifuged, and the upper layer removed. Finally, 2.5 volumes of ice- cold 100% ethanol were added in order to precipitate the DNA. Tubes were mixed well and centrifuged at 6500 rpm for 5 minutes before being dehydrated using a vacufuge (Eppendorf, Hamburg, Germany) for 25 minutes. DNA was resuspended in 100 μ L TE buffer (10 mM Tris, 1 mM EDTA; pH 8.0) and stored at -20 °C. The quantity of DNA was evaluated by gel electrophoresis, using known concentrations of Lambda DNA (100 ng/ μ L) for comparison. An agarose gel was made by mixing 0.4 g agarose with 50 mL 2-Amino-2-hydroxymethyl-propane-1,3-diol acetate Ethylenediaminetetraacetic acid (1x TAE).

This solution was heated for 2 minutes 50 seconds and allowed to cool before 2 μL ethidium bromide was added. Once the gel set, wells 1-5 received 1-5 μL Lambda DNA, representing 100 ng/ μL – 500 ng/ μL DNA, respectively. Each well contained 2 μL 10X Loading Dye, 2 μL DNA (except Lambda), and brought to 14 μL total volume using TAE buffer. After mixing, samples were loaded into the wells of the gel, and a constant current of 25 milliamps was applied. DNA was then visualized using a Transilluminator (UVP BioImaging Systems, Cambridge, UK) and quantified by means of visual comparison to Lambda standards. Next, DNA was diluted 1:10 and used as a template for the polymerase chain reaction (PCR) with universal primers 8F and 1492R. *E. coli* DNA was used as a positive control and no template DNA (volume replaced with molecular-grade H_2O) was used as the negative control. The PCR recipe included 100 ng DNA template, 0.5 μM each of forward and reverse primers, 0.2 mM deoxynucleotide triphosphates (dNTPs), 1X buffer, and 10 U Taq DNA Polymerase. Thermocycler conditions were as follows: Initial DNA denaturation at 94 $^{\circ}\text{C}$ for five minutes, then 30 cycles of denaturation for 30 seconds at 92 $^{\circ}\text{C}$, primer annealing for 30 seconds at 55 $^{\circ}\text{C}$, and DNA extension for 30 seconds at 72 $^{\circ}\text{C}$, followed by a final extension for five minutes at 72 $^{\circ}\text{C}$. After PCR amplification, products were visualized via gel electrophoresis in order to ensure that amplification was achieved, that amplicons were of appropriate size (~1400 bp), and that no contamination had been introduced. An agarose gel was made as mentioned before, however, instead of Lambda DNA, a 1 Kb Ladder was ran adjacent to PCR products of controls and test samples at 65 milliamps. Again, transillumination was used to reveal the presence and size of amplicons. Next, ExoSap-It was used to purify PCR products according to

manufacturer's instructions (Affymetrix, Inc.). For each of 5 sequencing primers, 2 μL PCR product, 3.25 μL H_2O , and 0.25 μL stock ExoSap-It were mixed and placed into a thermocycler using a one-cycle program of 37 $^\circ\text{C}$ for 30 minutes, 80 $^\circ\text{C}$ for 15 minutes, and a final hold at 4 $^\circ\text{C}$. Amplicons were then sent to The University of Oklahoma's Zoology Core Molecular Facility for sequencing using forward primers *pA* (bp positions 8 to 28), *anti-gamma* (bp 339 to 822), and *anti-three* (bp 1080 to 1492), and reverse primers *pD* (bp 539 to 8) and *three* (bp 1109 to 500) according to *Escherichia coli* nucleotide numbering. The closest known relatives of the new isolate based on the 16S rRNA gene sequence were determined by performing database searches of EMBL / GenBank using the program EzTaxon-e server (<http://eztaxon-e.ezbiocloud.net/>); (Kim *et al.*, 2012). The most related sequences were then selected for the calculation of pairwise sequence similarity using a global alignment algorithm (Myer & Miller, 1988). These sequences, and those of other related strains, were aligned with the sequence derived from SF-S1^T using the program ClustalW. Phylogenetic reconstructions were performed in MEGA (version 4) (Tamura *et al.*, 2007) using the neighbour-joining method (Saitou & Nei, 1987), applying evolutionary genetic distances that had been calculated by the Kimura two-parameter model (Kimura, 1980). Additionally, mol% G+C was determined according to the method of Mesbah *et al.* (1989).

Chemotaxonomic characterization

For chemotaxonomic analysis of cellular fatty acids, SF-S1^T biomass was collected from BHI Chocolate Agar (Oxoid, UK) after 72 hours of anaerobic growth at 37 $^\circ\text{C}$, and the analysis performed at the Center for Microbial Identification and

Taxonomy (University of Oklahoma). Fatty acid methyl esters were extracted using the Sherlock Microbial Identification System (MIDI) version 6.1 as described previously (Sasser, 1990; Kämpfer & Kroppenstedt, 1996). First, 8 mg of cells were collected from the third quadrant and spread around the bottom 1/8th of a GC vial. Triplicate samples were derivatized with 100 µL ammonia solution (Reagent Q1, proprietary concentrations), vortexed for 10 seconds at 3000 RPM, and heated for 10 minutes using a 100 °C heat block. The extraction was carried out by adding 500 µL of sulfuric acid/methanol (Reagent Q2, proprietary concentrations), and 200 µL hexane, followed by vortexing and centrifugation for 15 seconds at 3000 RPM. Finally, 70 µL of the upper hexane phase was removed and analyzed as the finished extract. Analysis was carried out with an Agilent Technologies 6890N gas chromatograph (GC) equipped with a phenyl methyl silicone fused silica capillary column (HP-2 25m x 0.2 mm x 0.33 µm film thickness) and a flame ionization detector. Hydrogen was used as the carrier gas. The temperature program was initiated at 170 °C and increased at 5 °C min⁻¹ to a final temperature of 270 °C. The relative amount of each fatty acid was expressed in terms of the percentage of total fatty acids. Q-FAME calibration standards were analyzed in conjunction to ensure proper peak naming.

Results

Morphological, physiological, and biochemical characteristics

The novel strain grew anaerobically but could not grow in oxic conditions. Cells stained Gram-positive, appeared coccus-shaped, and tended to cluster together in large aggregates (Fig. 1.1). Colonies were circular, grey, convex, entire, and opaque with a diameter of 1-2 mm on Brucella base agar (Oxoid, UK) plus defibrinated sheep's blood after 5 days of growth at 37 °C. Cells were catalase- and urease- negative and were also negative for nitrate reduction and indole production. Strain SF-S1^T was asaccharolytic and did not produce acid from the carbohydrates tested. Using antibiotic discs, the organism was susceptible to Penicillin, Chloramphenicol and Bacitracin but resistant to Trimethoprim and Ciprofloxacin.

The Rapid ID 32A profile for strain SF-S1^T was determined to be 2000053705 which corresponded to positive reactions for arginine dihydrolase, arginine arylamidase, phenylalanine arylamidase, leucine arylamidase, tyrosine arylamidase, alanine arylamidase, glycine arylamidase, histidine arylamidase, serine arylamidase, and a weak reaction for leucyl glycine arylamidase (Table 1.2). Using the API ZYM test system, positive reactions were obtained for leucine arylamidase, cystine arylamidase, and phosphohydrolase, with weak reactions obtained for α -galactosidase, and α -mannosidase (Table 1.3). All other ZYM tests were negative.

Figure 1.1: Phase contrast image of strain SF-S1^T at 1000X magnification.

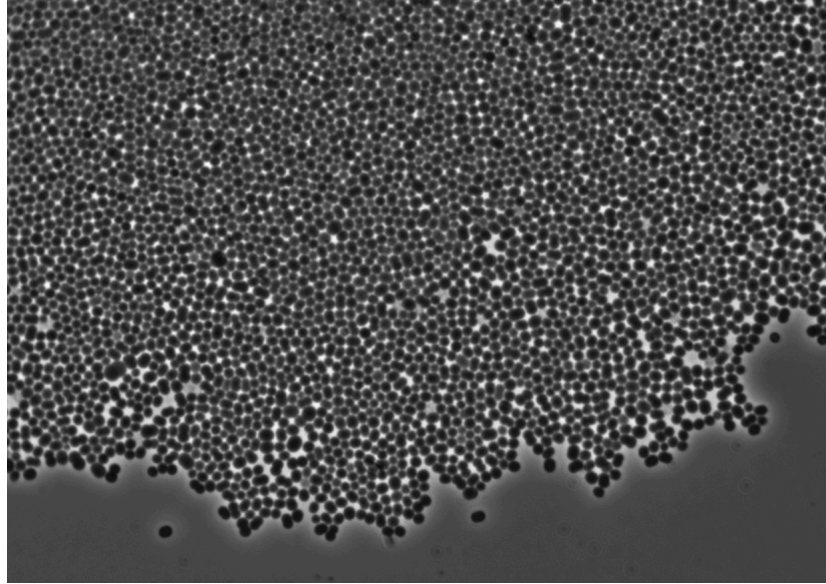


Table 1.1: Morphological and physiological characteristics of strain SF-S1^T.

Characteristics	SF-S1^T
Inhabiting niche	swine manure pit
Gram reactivity	positive
Cell shape	coccus
Cell size	0.7- 4.0um
Colony morphology	circular, grey, convex, entire
Colony size	1-2mm
Relation to O ₂	strict anaerobe
DNA G+C content (mol%)	31.8%
Motility	negative
Spore-formation	negative
Catalase	negative
Indole production	negative
Urease	negative
Nitrate reduction	negative
Sensitivity to bile	negative
Glucose fermentation	negative
Metabolic end products (volatile FA)	Butyrate Acetate
Antibiotic susceptibility	S - Penicillin S - Chloramphenicol S - Bacitracin R - Trimethoprim R - Ciprofloxacin

Table 1.2: API Rapid ID 32A results for *P. stercorisuis* strain SF-S1^T. +, positive; -, negative; w, weak.

ACTIVE INGREDIENTS	REACTIONS	SF-S1 ^T
Urea	Urease	-
L-arginine	Arginine DiHydrolase	+
4-nitrophenyl-DD-galactopyranoside	D-Galactosidase	-
4-nitrophenyl-βD-galactopyranoside	β-Galactosidase	-
4-nitrophenyl-βD-galactopyranoside-6-phosphate-2CHA	β-Galactosidase 6-Phosphate	-
4-nitrophenyl-DD-glucopyranoside	D-Glucosidase	-
4-nitrophenyl-βD-glucopyranoside	β-Glucosidase	-
4-nitrophenyl-DL-arabinofuropyranoside	D-Arabinosidase	-
4-nitrophenyl-βD-glucuronide	β-Glucuronidase	-
4-nitrophenyl-N-acetyl-βD-glucosaminide	N-Acetyl-β-Glucosaminidase	-
D-mannose	Mannose fermentation	-
D-raffinose	Raffinose fermentation	-
Glutamic acid	Glutamic acid DeCarboxylase	-
4-nitrophenyl-DL-fucopyranoside	D-Fucosidase	-
Potassium nitrate	Reduction of Nitrates	-
L-tryptophan	Indole production	-
2-naphthyl-phosphate	Alkaline Phosphatase	-
L-arginine-β-naphthylamide	Arginine Arylamidase	+
L-proline-β-naphthylamide	Proline Arylamidase	-
L-leucyl-L-glycine-β-naphthylamide	Leucyl Glycine Arylamidase	W+
L-phenylalanine-β-naphthylamide	Phenylalanine Arylamidase	+
L-leucine-β-naphthylamide	Leucine Arylamidase	+
Pyroglutamic acid β-naphthylamide	Pyroglutamic acid Arylamidase	-
L-tyrosine-β-naphthylamide	Tyrosine Arylamidase	+
L-alanyl-L-alanine-β-naphthylamide	Alanine Arylamidase	+
L-glycine-β-naphthylamide	Glycine Arylamidase	+
L-histidine-β-naphthylamide	Histidine Arylamidase	+
L-glutamyl-L-glutamic acid β-naphthylamide	Glutamyl Glutamic acid Arylamidase	-
L-serine-β-naphthylamide	Serine Arylamidase	+

Table 1.3: API ZYM results for *P. stercorarius* strain SF-S1^T. +, positive; -, negative; w, weak.

Hydrolyzed substrate	Enzyme	SF-S1 ^T
2-naphtyl-phosphate	Alkaline phosphatase	-
2-naphyl-butyrate	Esterase (C-4)	-
2-naphyl-caprylate	Esterase lipase (C-8)	-
2-naphyl-myristate	Lipase (C-14)	-
L-leucyl-2-naphtylamide	Leucine arylamidase	+
L-valyl-2-naphylamide	Valine arylamidase	-
L-cystyl-2-naphtylamide	Cystine arylamidase	+
N-benzoyl-DL-arginine-2-naphtylamide	Trypsin	-
N-glutaryl-phenylalanine-2-naphtylamide	Chymotrypsin	-
2-naphtyl-phosphate	Acid phosphatase	-
Naphtol-AS-BI-phosphate	Phosphohydrolase	+
6-Br-2-naphtyl- α D-galactopyranoside	α -Galactosidase	w
2-naphtyl- β D-galactopyranoside	β -Galactosidase	-
Naphtol-AS-BI- β D-glucuronide	β -Glucuronidase	-
2-naphtyl- α D-glucopyranoside	α -Glucosidase	-
6-Br-2-naphtyl- β D-glucopyranoside	β -Glucosidase	-
1-naphtyl-N-acetyl- β D-glucosaminide	N-Acetyl- β -glucosaminidase	-
6-Br-2-naphtyl- α D-mannopyranoside	α -Mannosidase	w
2-naphtyl- α L-fucopyranoside	α -Fucosidase	-

Determination of the 16S rRNA gene sequence and phylogenetic analysis

Results of the DNA databases searches showed the novel species to be a member of the phylum *Firmicutes* and within the genus *Peptoniphilus*. Pairwise comparisons revealed strain SF-S1^T was most closely related to *Peptoniphilus methioninivorax* sharing a 16S ribosomal RNA gene similarity of 95.5%, with all other species displaying 16S rRNA sequence similarity values of between 88.0 and 91.0% (Fig. 1.2). These values are well below the generally recognized divergence value of 3% used to facilitate the assignment of novel species (Stackebrandt & Goebel, 1994). The novel strain from the swine manure storage tank represents a new subline within the genus *Peptoniphilus* sharing the closest relationship with *Peptoniphilus methioninivorax* which was supported by a 100% bootstrap value and confirmed by the maximum-parsimony method (Fitch, 1971) using MEGA (version 4) (Fig. 1.3). It is interesting to note that *Peptoniphilus methioninivorax* is the only other species to date that has not been recovered from human clinical material but is associated with animals, albeit from ground beef.

Figure 1.2: Portion of the pairwise alignment of 16S rRNA gene sequences between *Peptoniphilus stercorisuis* strain SF-S1^T (referred to as *oklahomii*), the nearest cultivated neighbor *Peptoniphilus methioninivorax*, and other genetically similar species, *Peptoniphilus coxii* and *Peptoniphilus koenoenieniae*.

```

CLUSTAL W (1.83) multiple sequence alignment

oklahomii          TCCTGGCTCAGGACGAACGCTGGCGGCGCGCCTAACACATGCAAGTCGAGCGATGATATT
methioninivorax   -----TGCAGTCGAGCGATGA-AGC
coxii              -----CTCAGGACGAACGCTGGCGGCGCGCCTAACACATGCA-CTCGAGCGATGAAAGT
koenoenieniae     -----TGCAGTCGAGCGATGAAATT
                    **** *

oklahomii          TTTTCAGATTCTTCGGGATGACGAAAAGAAGGATTAGCGGGCAGCGGTGAGTAACACG
methioninivorax   TTTAAAAGATTCTTCGGAATGA-AATTAAGTGGATTAGCGGGCAGCGGTGAGTAACACG
coxii              TGTTCAGAT-CCTTCGGG-TGACGAACTTCCGGATTAGCGGGCAGCGGTGAGTAACCGG
koenoenieniae     TTAACAGATCCTTTCGGGGAGAAGATAAGATGGATTAGCGGGCAGCGGTGAGTAACACG
                    *   ****   ****   **   *   **** *

oklahomii          TGAATAACCTACCTTTGACACAGGGATAGCCTCGGGAAACTGGGATTAATACCAGATGAT
methioninivorax   TGAGTAACCTGCCTTTGACACAGGGATAGCCTCGGGAAACTGGGATTAATACCAGATGAA
coxii              TGAGGAACCTGCCTCTCACACAGGGATAGCCTCGGGAAACCGGGATTAATACCGTATGAC
koenoenieniae     TGAGTAACCTGCCTTTGACACAGGGATAGCCTCGGGAAACCGGGATTAATACCAGATAAC
                    ***   *****   * * * * *   ***** * * *

oklahomii          ATATCTTCATCACATGATAAAGATATTAAG-TGATTTAGCGGTCAAAGATGGATTTCGGC
methioninivorax   ACAGAATAATCGCATGATTAATCTGTAAAG-TGAATTAGCGGTCAAAGATGGACTCGCC
coxii              ACTATCAGATGGCATCATCAGGTAGTTAAAG-TG--CTAGCGGTGAGAGATGGCCTCGCC
koenoenieniae     ATTATCAGATCGCATGAGAAGATAATCAAAGCTGA---GGCGGTCAAAGATGGACTCGCC
                    *   **   * * * * *   *   * * * * *   * * * * *   * * * * *

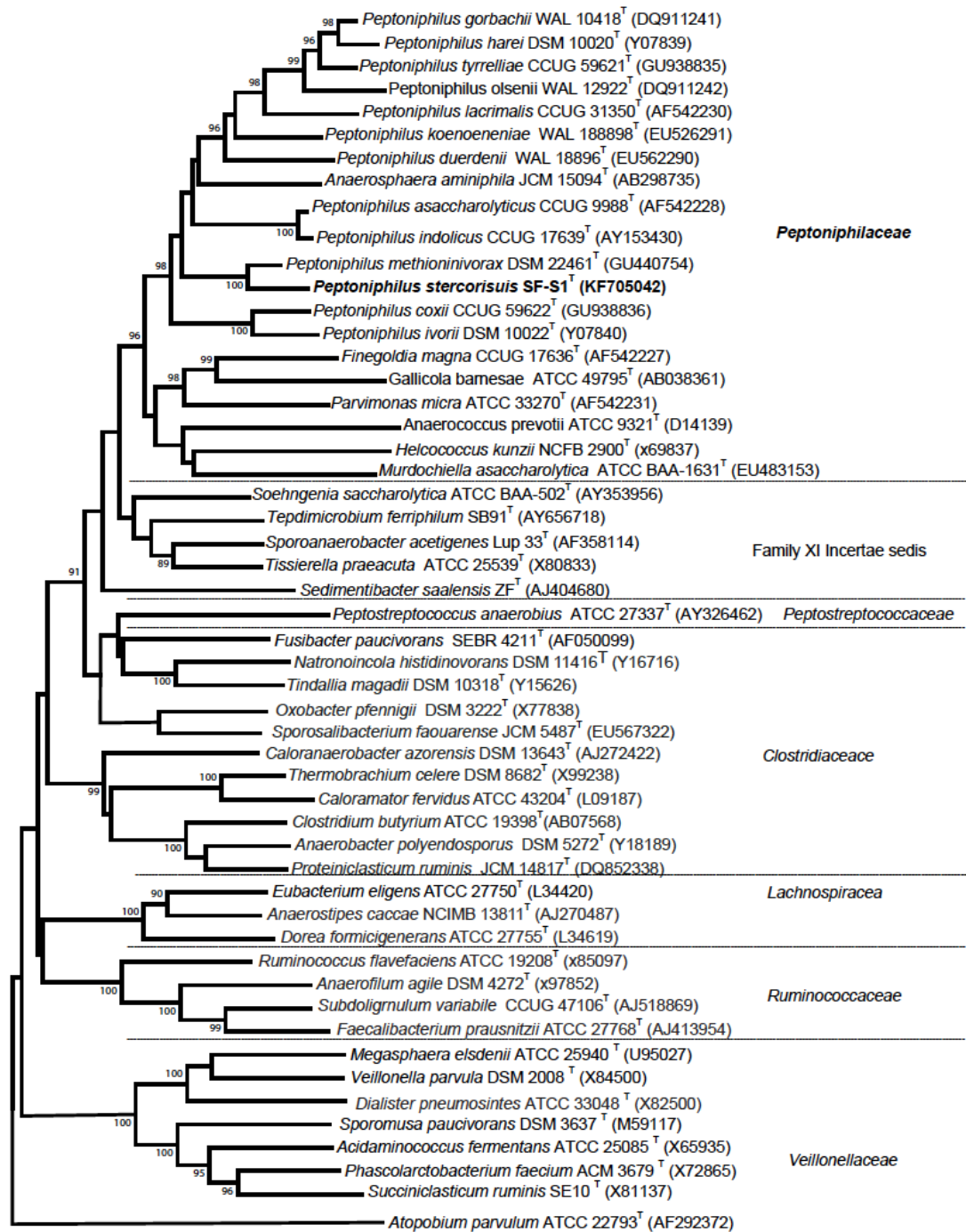
oklahomii          TCTGATTAGCTAGTTGTTGAGATAAAAGCTCACCAAGGCAACGATCAGTAACCGGCCCTGA
methioninivorax   TCTGATTAGCTGGTTGTTGAGATAACAGCCACCAAGGCAACGATCAGTAACCGGCCCTGA
coxii              TCTGATTAGTTAGTTGTTGGGTAACGGCCTACCAAGACGAGCATCAGTAACCGGCCCTGA
koenoenieniae     TCCCATTAGCTAGTTGTTAGAGTAATAGCCTACCAAGGCAACGATGGGTAGCCGGCCCTGA
                    **   ***** * *****   *** ** ***** * *****   *** *****

oklahomii          GAGGGTGAACGGTCACATTGGAACCTGAGACACGGTCCAAACTCCTACGGGAGGCAGCAGT
methioninivorax   GAGGGTGAACGGTCACATTGGAACCTGAGACACGGTCCAAACTCCTACGGGAGGCAGCAGT
coxii              GAGGGTGAACGGTCACATTGGAACCTGAGACACGGTCCAAACTCCTACGGGAGGCAGCAGT
koenoenieniae     GAGGGTGAACGGCCACATTGGAACCTGAGAAACGGTCCAAACTCCTACGGGAGGCAGCAGT
                    ***** * ***** * ***** * ***** * ***** * *****

oklahomii          GGGGAATATTGCACAATGGGGAACCTCTGATGCAGCGACGCCGCTGAGCGATGAAGGT
methioninivorax   GGGGAATATTGCACAATGGGGAAACCCTGATGCAGCGACGCCGCTGAGCGATGAAGGT
coxii              GGGGAATCTTGCACAATGGGGAAACCCTGATGCAGCGACGCCGCTGAGCGATGAAGGT
koenoenieniae     GGGGAATATTGCACAATGGGGAAACCCTGATGCAGCGACGCCGCTGAGCGAAGAAGGT
                    ***** * ***** * ***** * ***** * ***** * *****

```

Figure 1.3: Phylogenetic dendrogram of 16S rRNA gene sequences indicating the position of *Peptoniphilus stercorisuis* sp. nov. The tree was constructed using the neighbor-joining algorithm using MEGA (version 4) with *Atopobium parvulum* as the outgroup. Bootstrap values are displayed on their relative branches.



Chemotaxonomic characteristics

The quantitative fatty acid data of strain SF-S1^T was C_{14:0} (22.4%), C_{15:1}ω8c (8.7%), C_{16:0} (15.6%), C_{16:1}ω7c (11.3%), an C_{16:0} ALDE (10.1%) with minor amounts of C_{12:0} (2.2%), C_{13:1} (3.2%), anteiso-C_{15:0} (1.7%), C_{16:1}ω5c, (2.9%), C_{17:1}ω7c (1.8%), C_{17:1}ω8c (1.9%), C_{17:1}ω9c (1.1%), C_{17:0} (3.0%), and cyclo C_{17:0}/ C_{18:0} (2.9%). Trace amounts of C_{13:0} (0.8%), 2OH-C_{14:0} (0.9%), and isoH-C_{15:1} / 3OH-C_{13:1} (0.9%) were also detected in addition to a number of unknown products with estimated carbon lengths of C_{18:3} (0.8%), C_{16:3} (2.2%), and C_{13:8} (5.8%). Table 1.4 shows the fatty acid composition of strain SF-S1^T as well as some other type strains of the genus *Peptoniphilus*. The major products of C_{14:0} and isomers of C_{16:0} were consistent with the genus description however C_{16:0} ALDE was produced which was lacking, or only present in minor proportions, in some species (*Peptoniphilus asaccharolyticus*, *Peptoniphilus harei* and *Peptoniphilus olsenii*). Strain SF-S1^T also had an elevated level of C_{16:1}ω7c that was seen in *Peptoniphilus methionivorax* but not other species of the genus. Additionally, fatty acid analyses were performed on SF-S1^T using a number of different media for direct comparison with *P. methionivorax* grown on Columbia agar (Sigma-Aldrich, St. Louis, MO). Profiles obtained were remarkably stable, with C_{14:0}, C_{16:0}, and C_{16:1}ω7c always forming the major products (Table 1.5).

Table 1.4: Comparison of fatty acid profile of strain SF-S1^T with other members of the genus *Peptoniphilus*. Strains: 1, SF-S1^T; 2, *P. asaccharolyticus* CCUG 9988^T; 3, *P. duerdenii* WAL 18896^T; 4, *P. koenoenieniae* WAL 18898^T; 5, *P. gorbachii* CCUG 53341^T; 6, *P. harei* CCUG 38491^T; 7, *P. indolicus* CCUG 17639^T; 8, *P. ivorii* CCUG 38492^T; 9, *P. lacrimalis* CCUG 31350^T; 10, *P. methionivorax* NRRL B-23883^T; 11, *P. olsenii* CCUG 53342^T. Data from *Ulger-Toprak et al.*, 2012; *Rooney et al.*, 2011; CCUG (<http://www.ccug.se>).

Table 1.4:

Fatty acid ^a	1	2	3	4	5	6	7	8	9	10 ^b	11
C10:0			2.8			1.1	0.3				
C12:0	2.2	2.3				1.3	1.5			1.2	2.0
iso-2OH-C13:0							2.5				3.4
C14:0	22.4	5.4	4.4	3.1	2.9	3.6	12.5	4.4	1.5	10.9	8.2
iso-C15:0		2.6									
anteiso-C15:0	1.7										
C15:1 ω8c	8.7						1.0				
C16:0	15.6	14.4	33.0	22.6	24.0	18.8	11.3	29.5	20.2	25.1	13.1
C16:0 alde	10.1	0.7				1.8					0.7
C16:1 ω5c	2.9						1.5				1.1
C16:1 ω7c	11.3	3.9			2.7	3.3	5.3	1.0	3.4	14.1	4.8
C16:1 ω7c _{DMA}											1.5
C16:1 ω9c				3.3			3.1			3.4	1.3
C17:1ω9c	1.1					3.0					
iso-C17:1ω5c		3.0			2.6		18.5				
C17:0 _{DMA}	3.0										
iso-C17:1/ C16:0 _{DMA}				4.3		5.4					4.5
anteiso-C17:0		1.6				3.5	1.2	3.8		1.9	1.6
iso 3OH-C17:0				3.3	4.9		7.6	7.7		9.2	9.1
C18:0		9.4	16.2	12.1	8.1	4.0		4.8	12.3	3.0	6.3
C18:1 ω7c _{DMA}											1.1
C18:1 ω7c _{12/9t}							1.4				2.3
C18:1 ω9c		20.2	22.6	24.4	22.6	17.6	2.8	11.4	31.2	5.1	12.0
C18:1 ω9c _{DMA}		6.6		6.3	4.4	7.3		2.6	3.1		10.3
C18:2 ω6,9c / anteisoC18:0		22.0	21.1	20.6	26.8	19.8	9.7	24.0	25.7	8.5	12.2
iso-C19:1		1.5									1.0
Unknown C _{13:83}	5.52										
Unknown C _{16:31}	2.2										
Unknown C ₁₈₋₁₇		5.1				8.9			1.9		
Unknown C _{16:75}		1.4									2.1

^a Predominant products are shown in bold, values below 1% are not shown. Profiles for *P. coxii* and *P. tyrrelliae* have not been performed.

^b data taken from Rooney *et al.*, (2011), organism was grown on Columbia blood agar.

Table 1.5: Comparison of Fatty acid profiles of SF-S1^T on different media and with *P. methioninivorax*.

^a Fatty acid	Anaerobic Broth Agar	BHI Chocolate Agar	Brucella Blood Agar	Columbia Blood Agar	^b <i>P.methioninivorax</i> NRRL B-23883 ^T Columbia blood Agar
C10:0			1.79	0.96	
C12:0	1.38	2.15	2.02	2.39	1.2
C13:0		0.75	1.30	0.70	
C13:1	1.35	3.15	1.12	0.67	
C14:0	28.34	22.44	19.91	26.38	10.9
C14:0 2OH		0.86		2.73	
C15:0				4.01	
anteiso-C15:0	1.63	1.74	0.83	1.64	
C15:1 isoH/ 13:0 3OH		0.91		0.45	
C15:1 ω8c	6.98	8.74	3.88	1.09	
C15:1 ω6c			1.94	3.89	
C16:0	18.06	15.58	16.76	19.06	25.1
C16:0 alde	7.70	10.10	9.76		
C16:1 ω5c	2.98	2.88	2.78	2.84	
C16:1 ω7c	9.74	11.28	8.68	7.06	14.1
C16:1ω9c					3.4
C17:1ω8c	3.83	1.90	3.83	2.43	
C17:1ω9c		1.08	1.98		
C17:0	4.30	2.95	3.02	1.8	
anteiso-C17:0					1.9
iso-C17:0			0.78	1.69	
iso-C17:0 3-OH					9.2
iso-C17:1 / anteiso-C17:1					4.5
C17:0 cyclo/ C18:0	4.06	2.87	3.92		
C18:0				1.59	3.0
C18:1 ω7c DMA			1.23		
C18:1 ω7c					5.9
C18:1 ω9c			2.52	3.00	5.1
C18:2 ω6,9c /anteisoC18:0			1.09	2.06	8.5
Unknown C18:465			1.00	1.47	

Unknown C18:256	1.33	0.78	2.04		
Unknown C17:045			0.83	3.13	
Unknown C16:315	4.21	2.20	1.25		
Unknown C13:832	4.11	5.82	3.58	6.34	

^a Predominant products are shown in bold, values below 1% are not shown.

^b data taken from Rooney *et al.*, (2011).

In addition to its unique 16S rRNA gene sequence, traits useful in distinguishing the novel species from other *Peptoniphilus* species are shown in Table 1.6 and the species descriptions. Closely related taxa share negative catalase and indole activity, as well as positive results for the presence of leucine, phenylalanine, serine, and tyrosine arylamidases. Based on phenotypic, genotypic, and chemotaxonomic evidence, the bacterium from a swine manure storage tank represents a new species of the genus *Peptoniphilus*, for which the name *Peptoniphilus stercorisuis* sp. nov. was proposed. Furthermore, the family *Peptoniphilaceae* was proposed to encompass the genus *Peptoniphilus* and close relatives. Peripheral to this family are members belonging to the genera *Sedimentibacter*, *Soehngenia*, *Sporoanaerobacter*, *Tepidimicrobium* and *Tissierella* can be differentiated on the basis of their rod-shaped cell morphology and other features. The traits useful for distinguishing members of *Peptoniphilaceae* from surrounding taxa can be found in Tables 1.7 and 1.8.

Table 1.6: Phenotypic characteristics useful in the differentiation of strain SF-S1^T from other members of the genus *Peptoniphilus*.

Strains: 1, SF-S1^T; 2, *P. asaccharolyticus* CCUG 9988^T; 3, *P. coxii* CCUG 59622^T; 4, *P. duerdenii* WAL 18896^T; 5, *P. gorbachii* CCUG 53341^T; 6, *P. harei* CCUG 38491^T; 7, *P. koenoenieniae* WAL 18898^T; 8, *P. indolicus* CCUG 17639^T; 9, *P. ivorii* CCUG 38492^T; 10, *P. lacrimalis* CCUG 31350^T; 11, *P. methioninivorax* NRRL B-23883^T 12, *P. olsenii* CCUG 53342^T; 13, *P. tyrrelliae* CCUG 59621^T. Data from Ulger-Toprak *et al.*, 2012; Rooney *et al.*, 2011; Citron *et al.*, 2012. +, positive; -, negative; w, weak; nd, not determined.

Characteristic	1	2	3	4	5	6	7	8	9	10	11	12	13
Alanine arylamidase	+	-	-	-	-	-	-	-	-	+	W	+	-
Alkaline phosphate	-	-	-	-	-	W	-	+	-	-	+	+	-
Arginine dihydrolase	+	+	-	w	-	-	+	-	-	-	+	-	-
Catalase	-	-	-	-	-	+	-	+	-	-	nd	-	+
Glutamyl glutamic acid arylamidase	-	w	-	-	+	-	-	-	-	+	-	-	-
Glycine arylamidase	+	-	-	-	+	-	W	-	-	+	W	+	-
Indole	-	-	-	-	+	-	-	+	-	-	-	+	+
Leucine arylamidase	+	+	-	+	+	-	+	-	-	+	+	-	+
Phenylalanine arylamidase	+	+	-	-	W	-	+	-	-	+	W	+	-
Proline arylamidase	-	w	+	-	-	-	W	-	+	-	+	-	-
Pyroglutamic acid arylamidase	-	+	-	+	-	-	+	-	-	-	-	-	-
Serine arylamidase	+	+	-	-	+	-	+	-	-	+	W	+	-
Tyrosine arylamidase	+	+	-	-	+	-	+	-	-	+	+	+	+

Table 1.7: Morphological, biochemical and chemotaxonomic properties of *Peptoniphilaceae* and close relatives.

Characteristic	<i>Peptoniphilus</i>	<i>Anaerococcus</i>	<i>Anaerophæra</i>	<i>Fingoldia</i>	<i>Gallicola</i>	<i>Helcococcus</i>	<i>Murdochella</i>	<i>Parvimonas</i>
Gram-stain	+	+	+	+	+	+	+	+
Cell Morphology	cocci	cocci	cocci	cocci	cocci	cocci	cocci	cocci
Spore formation	-	-	-	-	-	-	-	-
Metabolism	Obligate anaerobe	Obligate anaerobe	Obligate anaerobe	Obligate anaerobe	Obligate anaerobe	Facultative anaerobe	Obligate anaerobe	Obligate anaerobe
End products from PYG	B, A	B	A, B	A	A, B	A, L	L	A
Major fatty acids	C _{18:1} , C _{16:0} , C _{18:0} , C _{16:1}	C _{18:1} , C _{16:1} , C _{18:0} , C _{16:0}	C _{17:1 ω8} , C _{18:1 ω7} DMA, C _{16:0}	C _{18:1} , C _{16:1} , C _{18:0} , C _{16:0}	C _{18:1} , C _{16:1} , C _{18:0} , C _{16:0}	ND	C _{14:0} , C _{16:0} , C _{18:1}	C _{18:0} /C _{18:2} , C _{18:1} /C _{16:0} , C _{16:1}
Cell-wall murein	Orn, D-Glu	Lys, D-Glu	Lys	Lys, D-Asp	D-Asp	D-Asp	ND	Lys
DNA G + C content (mol%)	30-34	30-35	32.5	32-34	27-34	ND	ND	27-28
Source	Human intestine and clinical material, vaginal discharges, ovarian, peritoneal and other bodily abscesses, cattle mastitis and swine manure	Human intestine, clinical material, vaginal discharges, ovarian, peritoneal and other bodily abscesses, skin, and nasal passage	Methanogenic cattle manure reactor	Vagina, oral cavity and other bodily abscesses	Chicken feces	Skin, human clinical material, sheep	Human clinical material	Oral cavity and human abscesses

Data taken from De Vos (2009); Ezaki *et al.* (2001); Rooney *et al.* (2011) and Ulger-Toprak *et al.* (2012).

Table 1.8: Morphological, biochemical and chemotaxonomic properties of genetically related taxa excluded from *Peptoniphilaceae* fam. nov.

Data taken from De Vos (2009); Ezaki *et al.* (2001); Rooney *et al.* (2011) and Ulger-Toprak *et al.* (2012).

Characteristic	<i>Sedimentibacter</i>	<i>Soehngenia</i>	<i>Sporoanaerobacter</i>	<i>Tepidimicrobium</i>	<i>Tissierella</i>
Gram-stain	+/-	+	+	+	+/-
Cell Morphology	rods	rods	rods	rods	rods
Spore formation	+	+	+	+	-
Metabolism	Obligate anaerobe	Anaerobe/ aerotolerant	Obligate anaerobe	Obligate anaerobe	Obligate anaerobe
End products from PYG	A, B	F, H ₂ , CO ₂ , A, E	A, H ₂ , CO ₂	A, E, B, H ₂ , CO ₂	A, B, IV
Major fatty acids	C _{14:0} , C _{16:1ω9} , C _{16:0}	ND	ND	ND	iso-C _{15:0} , C _{15:1} , C _{18:0} , C _{16:0}
Cell-wall murein	L-Lys	ND	Lys	ND	meso-DAP / D-orn
DNA G + C content (mol%)	34-35.5	43	32.2	33-36.2	28-32
Source	Methanogenic Freshwater Pond Sediment, freshwater river sediment, human blood	Anaerobic digester sludge	Upflow anaerobic sludge blanket	Freshwater hot spring, anaerobic digester thermophilic sludge	Human clinical material, human blood and feces, sugar-refinery waste water

Description of Peptoniphilus stercorisuis sp. nov.

ster.co.ri.su'is. L. masc. n. *stercus*, -*oris* feces, manure; L. gen. n. *suis* of a pig; N.L. gen. n. *stercorisuis* from pig feces/manure, referring to the isolation of the organism from pig faeces/manure.

Cells were anaerobic, Gram-stain positive cocci occurring singly or in pairs. Growth only occurred under strict anaerobic conditions. Cells were non-motile, non-sporeforming, and non-hemolytic. Growth was observed at 20 °C and 37 °C (optimum 30 °C), but not at 15 °C or 43 °C, at pH 6.0 and 9.0 (optimum pH 7.75), but not at pH 5.5 or 9.5, and with 0-5% (w/v) NaCl. Colonies were small (1-2 mm diameter), grey, circular, and convex on Brucella blood agar plates after 5 days of growth at 30 °C, while cells in liquid broths (PYG) aggregated into large floccules, visible by eye. Cells were both catalase and urease negative. Nitrate was not reduced and no indole was produced. Carbohydrates were not utilized. Using the API Rapid 32A kit, positive reactions were observed for arginine dihydrolase, arginine arylamidase, phenylalanine arylamidase, leucine arylamidase, tyrosine arylamidase, alanine arylamidase, glycine arylamidase, histidine arylamidase, serine arylamidase, and a weak positive for leucyl glycine arylamidase. Negative reactions were observed for α -galactosidase, β -galactosidase, β -galactosidase 6-phosphate, α -glucosidase, β -glucosidase, α -arabinosidase, β -glucuronidase, N-acetyl- β -glucosaminidase, raffinose and mannose fermentation, glutamic acid decarboxylase, α -fucosidase, alkaline phosphatase, proline arylamidase, pyroglutamic acid arylamidase, and glutamyl glutamic acid arylamidase. Using the API ZYM test system, positive reactions were obtained for leucine arylamidase, cystine arylamidase, and phosphohydrolase, weak reactions were obtained for α -galactosidase,

and α -mannosidase. Major fatty acids included C_{14:0}, C_{16:0}, C_{16:1 ω 7c} and C_{16:0ALDE}. The DNA G+C content was 31.8 mol% (HPLC). Cultures were sensitive to penicillin, chloramphenicol, and bacitracin but resistant to trimethoprim and ciprofloxacin.

The type strain, SF-S1^T (DSM 27563^T = NBRC 109839^T) was isolated from a swine manure storage tank located in the state of Oklahoma, USA.

Description of Peptoniphilaceae fam. nov.

Peptoniphilaceae (Pep.to.ni.phi.la.ce'ae. N.L. masc. n. *Peptoniphilus* type genus of the family; L. suff. *-aceae* ending to denote a family; N.L. fem. pl. n.

Peptoniphilaceae the family of the genus *Peptoniphilus*).

The delineation of the family, *Peptoniphilaceae*, was primarily made on basis of 16S rRNA gene sequence phylogeny and was supported by morphological, biochemical, and chemotaxonomic characteristics. The family falls within the order *Clostridiales* and includes the genera *Anaerococcus*, *Anaerosphaera*, *Finegoldia*, *Gallicola*, *Helcococcus*, *Murdochiella*, *Parvimonas* and *Peptoniphilus*. Organisms within this family stain Gram-positive and consist of strictly anaerobic cocci. Cells are negative for both motility and spore formation. While carbohydrates are not normally utilized, peptone and amino acids can be metabolized yielding butyrate, acetate, and lactate as major end products. Predominant fatty acids include C_{16:0}, C_{16:1}, C_{18:0}, and C_{18:1}. The cell wall may contain the diamino acids alanine, lysine, ornithine, or glutamic acid. Bacteria within this family are typically isolated from animal and bird feces or from human clinical samples. Organisms contain a DNA G +C (mol %) between 27-35. The type genus is *Peptoniphilus* Ezaki, Kawamura, Li, Li, Zhao and Shu 2001,1524^{VP}.

Discussion

The field of taxonomy faces several challenges when it comes to understanding bacterial diversity, particularly in the establishment of speciation criteria. These challenges include, but are not limited to, the lack of morphological features conserved among taxa, the occurrence of horizontal gene transfer within microbial communities, and the increased diversity of geographically evolving phenotypes that results. Though traditional measures of classification are somewhat laborious, the assessment of phenotypic and biochemical properties using classical laboratory tests remains important. One disadvantage of these techniques is the expensive and daunting task of acquiring genetically related neighbor strains from culture collections to be tested in conjunction with newly proposed taxa. While commercially available tests provide a rapid means of describing certain bacterial features, many, such as API test strips, rely on colorimetric result interpretation and require relatively unstable reagents. This manifests as a disadvantage because lack of continuity creates variable results among different laboratories. Another disadvantage of traditional characterization techniques is the uncertain terms of which properties are deemed relevant for the publication of a proposed organism. Currently, it is widely accepted to exclude chemotaxonomic information for novel species descriptions, but necessary in order to validate novel taxa at the genus level. Typically, tests are performed relative to the nearest-neighbor publication, in accordance with the conditions for growth. This limits the type of data generated and restricts the ability of researchers to compare different clades of microorganisms, especially those fastidious in nature.

Using a combination of such classical techniques and molecular identification methods, the classification of *Peptoniphilus stercorisuis* was revealed. Within the environment of stored swine manure, the discovery of *Peptoniphilus stercorisuis* represents a previously uncultivated bacterium capable of digesting proteinaceous compounds within fecal material. It is likely that the products from amino acid fermentation contribute to the odorous nature of animal operations, as experienced during laboratory cultivation. The genera *Anaerosphaera*, *Anaerococcus*, *Helcococcus*, *Finegoldia*, *Gallicola*, *Murdochiella*, *Parvimonas* and *Peptoniphilus* share a phylogenetic ancestry and form a robust group. In the current edition of *Bergey's Manual of Systematic Bacteriology*, the exact relationship of this group of organisms with other close members within the order *Clostridiales* is uncertain, and all are placed in the Family XI *Incertae sedis*. (De Vos *et al.*, 2009). From the phylogenetic data presented in Figure 1.3, it is clear that these genera form an rRNA gene super-cluster with members that also consistently share a number of biochemical and chemotaxonomic traits (Table 1.7). Peripheral to this group of organisms are members belonging to *Sedimentibacter*, *Soehngenia*, *Sporoanaerobacter*, *Tepidimicrobium* and *Tissierella* that can be differentiated on the basis of their rod-shaped cell morphology and other features shown in Table 1.8. Based on phylogenetic, biochemical, and chemotaxonomic information, the designation of *Peptoniphilaceae* fam. nov. was created in order to accommodate these genera. However, it is pertinent to note that the genus is not monophyletic with *Anaerosphaera* located within this group; this genus was originally circumscribed on the basis of Lysine presence rather than Ornithine as the diagnostic diamino acid of the cell-wall peptidoglycan as well as the presence of

thermotolerant cells (Ueki *et al.*, 2009). Additionally, *Anaerosphaera* was at one time phylogenetically located on the periphery of the *Peptoniphilus* cluster of organisms, but with the subsequent description of a number of *Peptoniphilus* species, *Anaerosphaera* became phylogenetically located within the center of this clade. Upon considering the internal structure present within this rRNA lineage, it is likely that further taxonomic revisions may be necessary in the future.

Rather than evaluating similarities between non-critical descriptive features, *in-silico* characterization seeks to compare information directly from the genome. Mining the genome for diagnostic phenotypic features could provide a wealth of data, but could also be negatively influenced by clonal mutations and limited by a lack of consideration for gene expression. Future efforts should focus on standardization of traditional protocols and the marrying of genomic and phenotypic information in publically available databases. Taxonomists must therefore meet this challenge by embracing new sequencing methods while maintaining the classical techniques that have provided a framework for proper microbial characterization for decades. The efforts presented here represent a continuing investigation into the ecosystem of manure storage pits as a rich source of novel microorganisms with human and animal health relevance. Ultimately, knowledge gained from studying laboratory isolates may aid in the use of compounds that interfere with fermentation processes, reducing the production of odorous and volatile compounds.

References

- Altermann, E. and Klaenhammer, T. R.** (2005). PathwayVoyager: pathway mapping using the Kyoto Encyclopedia of Genes and Genomes (KEGG) database. *BMC genomics* **6**(1), 60.
- Anderson, A. S. and Wellington, E. M.** (2001). The taxonomy of *Streptomyces* and related genera. *International Journal of Systematic and Evolutionary Microbiology* **51**(3): 797-814.
- Busse, H. J., Denner, E., & Lubitz, W.** (1996). Classification and identification of bacteria: current approaches to an old problem. Overview of methods used in bacterial systematics. *Journal of biotechnology* **47**(1), 3-38.
- Citron, D. M. D., Tyrrell, K. L. K. & Goldstein, E. J. C. E.** (2012). *Peptoniphilus coxii* sp. nov. and *Peptoniphilus tyrrelliae* sp. nov. isolated from human clinical infections. *Anaerobe* **18**: 244–248.
- Cohn, F.** (1872). Untersuchungen u̇ber Bakterien. Beitr Biol Pflanz 1, (Heft 2): 127–224 (in German).
- Cohn, F.** (1875). Untersuchungen u̇ber Bakterien. Beitr Biol Pflanz II, (Heft 3): 141–207 (in German).
- De Toni, J. B. and Trevisan, V.** (1889). Schizomycetaceae, in Saccardo's Sylloge Fungorum. **8**: 923-1087.
- De Vos, P., Garritty, G. M., Jones, D., Krieg, N. R., Ludwig, W., Rainey, F.A., Schleifer, K.-H. & Whitman, W. B. (Eds.)**. (2009). Family XI. *Incertae Sedis*. pp 1130-1149. In *Bergey's Manual of Systematic Bacteriology*. New York, NY: Springer New York.
- Doi, R. H. and Igarashi, R. T.** (1965). Conservation of ribosomal and messenger ribonucleic acid cistrons in *Bacillus* species. *Journal of bacteriology* **90**(2): 384-390.
- Ezaki, T., Kawamura, Y., Li, N., Li, Z. Y., Zhao, L. & Shu, S.** (2001). Proposal of the genera *Anaerococcus* gen. nov., *Peptoniphilus* gen. nov. and *Gallicola* gen. nov. for members of the genus *Peptostreptococcus*. *Int J Syst Evol Microbiol.* **51**:1521-1528.
- Fahy, E., Subramaniam, S., Brown, H. A., Glass, C. K., Merrill, A. H., Murphy, R. C., & Dennis, E. A.** (2005). A comprehensive classification system for lipids. *Journal of lipid research* **46**(5): 839-862.
- Fitch, W. M.** (1971). Toward defining the course of evolution: minimum change for a specified tree topology. *Systematic Zoology* **20**(4): 406-416.
- Holdeman, L.V. and Moore, W.E.C.** (1972). Anaerobe Laboratory Manual. Virginia: VPI Anaerobe Laboratory, Virginia Polytechnic Institute and State University.

- Hugenholtz, P., Goebel, B. M., & Pace, N. R.** (1998). Impact of culture-independent studies on the emerging phylogenetic view of bacterial diversity. *Journal of bacteriology*, **180**(18): 4765-4774.
- Hungate, R. E.** (1950). The anaerobic mesophilic cellulolytic bacteria. *Bacteriological Reviews* **14**: 1-49.
- Jousimies-Somer, H., Summanen, P., Citron, D. M., Baron, E. J., Wexler, H. M. & Finegold, S. M.** (2002). Wadsworth-KTL Anaerobic Bacteriology Manual, 6th ed., Belmont CA: Star Publishing.
- Kämpfer, P. and Kroppenstedt, R. M.** (1996). Numerical analysis of fatty acid patterns of coryneform bacteria and related taxa. *Can J Microbiol* **42**: 989-1005.
- Kim, O.-S., Cho, Y.-J., Lee, K., Yoon, S.-H., Kim, M., Na, H., Park, S.-C., Jeon, Y. S., Lee, J.-H. & other authors.** (2012). Introducing EzTaxon-e: a prokaryotic 16S rRNA gene sequence database with phylotypes that represent uncultured species. *Int J Syst Evol Microbiol* **62**: 716–721.
- Kimura, M.** (1980). A simple method for estimating evolutionary rates of base substitutions through comparative studies of nucleotide sequences. *J Mol Evol* 111-120.
- Madsen, M., Sørensen, G. H. & Nielsen, S. A.** (1991). Studies on the possible role of cattle nuisance flies, especially *Hydrotaea irritans*, in the transmission of summer mastitis in Denmark. *Med Vet Entomol* **5**: 421–429.
- McCarthy, B. J. and Bolton, E. T.** (1963). An approach to the measurement of genetic relatedness among organisms. *Proc Natl Acad Sci* **50**: 156-164.
- Mesbah, M., Premachandran, U. & Whitman, W. B.** (1989). Precise measurement of the G+C content of deoxyribonucleic acid by high-performance liquid chromatography. *Int J Syst Bacteriol* **39**: 159–167.
- Miller, D.N.** (2001). Accumulation and composition of odorous compounds in feedlot soils under aerobic, fermentative, anaerobic respiratory conditions. *J Anim Sci* **79**: 2503-2512.
- Myers, E. W. and Miller, W.** (1988). Optimal alignments in linear space. *Comput Appl Biosci* **4**: 11-17.
- Orla-Jensen, S.** (1909). Die Hauptlinien des natürlichen Bakteriensystems. *Zentbl. Bakteriol. Parasitenkd. Infektkrank. Hyg. Abt*, **2**(22): 305-346 (in German).
- Orla-Jensen, S.** (1921). The main lines of the natural bacterial system. *Journal of bacteriology* **6**(3): 263.

- Ramasamy, D., Mishra, A. K., Lagier, J. C., Padhmanabhan, R., Rossi, M., Sentausa, E., & Fournier, P. E.** (2014). A polyphasic strategy incorporating genomic data for the taxonomic description of novel bacterial species. *International journal of systematic and evolutionary microbiology* **64**(Pt 2): 384-391.
- Rooney, A. P., Swezey, J. L., Pukall, R., Schumann, P. & Spring, S.** (2011). *Peptoniphilus methionivorax* sp. nov., a Gram-positive anaerobic coccus isolated from retail ground beef. *Int J Syst Evol Microbiol* **61**: 1962–1967.
- Saitou, N. and Nei, M.** (1987). The neighbor-joining method: a new method for reconstructing phylogenetic trees. *Mol Biol Evol* **4**: 406-425.
- Sasser, M.** (1990). Identification of bacteria by gas chromatography of cellular fatty acids. MIDI, Inc. Newark, DE.
- Schroeter, J.** (1886). In Kryptogamenflora von Schlesien, Bd 3, Heft 3, Pilze, pp. 1-814. Edited by F.J Cohn. Breslau: J.U. Kern's Verlag.
- Siezen, R. J., van Enckevort, F. H., Kleerebezem, M., & Teusink, B.** (2004). Genome data mining of lactic acid bacteria: the impact of bioinformatics. *Current opinion in biotechnology* **15**(2): 105-115.
- Song, Y., Liu., C. & Finegold S.M.** (2007). *Peptoniphilus gorbachii* sp. nov., *Peptoniphilus olsenii* sp. nov., and *Anaerococcus murdochii* sp. nov. isolated from clinical specimens of human origin. *J Clin Microbiol.* **45**: 1746-1752.
- Stackebrandt, E. and Goebel, B. M.** (1994). Taxonomic note: a place for DNA-DNA reassociation and 16S rDNA sequence analysis in the present species definition in bacteriology. *Int J Syst Bacteriol* **44**: 846-849.
- Tamura, K., Dudley, J., Nei, M. & Kumar, S.** (2007). MEGA4: Molecular evolutionary genetics analysis (MEGA) software version 4.0. *Molecular Biology and Evolution* **24**:1596-1599.
- Tindall, B. J., Sikorski, J., Smibert, R. A. & Krieg, N. R.** (2007). Phenotypic characterization and the principles of comparative systematics. In *Methods for General and Molecular Microbiology*, pp. 330-393. Edited by C. A. Reddy, T. J. Beveridge, J. A. Breznak, G. A. Marzluf, T. M. Schmidt and R. L. Snyder. Washington, D. C.: ASM Press.
- Thompson, J. D., Higgins, D. G. & Gibson, T. J.** (1994). Clustalw: improving the sensitivity for progressive multiple sequence alignment through sequence weighting, position-specific gap penalties and weight matrix choice. *Nucleic Acids Res.* **22**: 4673-4680.

Ueki, A., Abe, K., Suzuki, D., Kaku, N., Watanabe, K., & Ueki, K. (2009). *Anaerosphaera aminiphila* gen. nov., sp. nov., a glutamate-degrading, Gram-positive anaerobic coccus isolated from a methanogenic reactor treating cattle waste. *Int J Syst Evol Microbiol*, **59**(12): 3161-3167.

Ulger-Toprak, N., Lawson, P. A., Summanen, P., O'Neal, L. & Finegold, S. M. (2012). *Peptoniphilus duerdenii* sp. nov. and *Peptoniphilus koenoenieniae* sp. nov., isolated from human clinical specimens. *Int J Syst Evol Microbiol* **62**: 2336–2341.

Whitehead T.R. and Cotta, M.A. (2004). Isolation and Identification of Hyper-Ammonia Producing Bacteria from Swine Manure Storage Pits. *Current Microbiology* **48**(1):20-26.

Woese, C. R., and Fox, G. E. (1977). Phylogenetic structure of the prokaryotic domain: the primary kingdoms. *Proceedings of the National Academy of Sciences* **74**(11): 5088-5090.

Zopf, W. (1885). *Zur Morphologie und Biologie der niederen Pilztiere (Monadinen) zugleich ein Beitrag zur Phytopathologie* (in German).

Zuckerlandl, E. and Pauling, L. (1965). Molecules as documents of evolutionary history. *Journal of Theoretical Biology* **8**: 357-366.

Chapter 2

***Savagea faecisuis* gen. nov., sp. nov., a tylosin- and tetracycline-resistant bacterium isolated from a swine manure storage pit**

Abstract

The management of swine manure storage facilities has become a focus within the farming community due to the health risks associated with fecal material processing. The scientific community has therefore turned to these environments in order to help understand the microbial processes responsible for the production of harmful and odorous compounds. Three strains of an unknown Gram-positive staining, non-sporeforming, motile, aerobic rod-shaped bacterium were isolated from a swine-manure storage pit. A polyphasic taxonomic study using morphological, biochemical, chemotaxonomic, and molecular methods was performed in order to identify and characterize these microbial inhabitants. In particular, pairwise analysis of the 16S rRNA gene demonstrated that the novel organism was most closely related to members of the genus *Sporosarcina* (92.8-94.5%), *Psychrobacillus* (93.5-93.9%) and *Paenisporosarcina* (93.3-94.5%). The predominant fatty acids consisted of iso-C_{15:0} and iso-C_{17:1} ω10c and the G +C mol % was 41.8. Based on biochemical, chemotaxonomic, and phylogenetic evidence, it was proposed that the unknown bacterium be classified as a novel genus and species, *Savagea faecisuis* gen. nov., sp. nov. with the type strain Con12^T (=CCUG 63563^T = NRRL B-59945^T). This study suggested that these organisms play a key role in the hydrolysis of peptides and release of amino acids from proteinaceous material found in swine manure storage systems. It also suggested that the novel species described here may contribute to the health risks associated with this ecosystem.

Introduction

Intensive livestock farming operations generate a large amount waste deposits that pose storage and disposal challenges. Modern animal confinement facilities have been condensed into fewer and fewer operations, while maintaining high numbers of domestication and processing. This has led to larger quantities of fecal material in concentrated areas, which results in longer storage periods before being used as fertilizer (Whitehead and Cotta, 2004). Specifically, the management system of swine manure employs large-scale storage methods such as lagoon treatment and deep pit storage, facilities that are subject to leaking contamination into local water sources. Also, the production of odorous compounds such as ammonia, sulfides, organic acids and alcohols is associated with the storage of swine feces. These biological metabolites affect the health of farmers and other animals while compromising the surrounding land through contamination. Therefore, a better understanding of the processes underlying production of these compounds remains the focus of ongoing research in swine manure management (Miller, 2001).

Ecosystems of the swine intestinal tract and the manure stored in large tanks are comprised of a complex assortment of known and novel bacterial species. Previous work in our laboratories (Cotta *et al.*, 2003; Whitehead and Cotta, 2001a) and by other researchers (Leser *et al.*, 2002; Snell-Castro *et al.*, 2005) has demonstrated that the predominant bacteria present in both ecosystems are Gram-positive staining, low mol% DNA G+C bacteria. Many of these organisms represent previously unidentified anaerobic bacterial genera and species (Cotta *et al.*, 2004; Whitehead and Cotta, 2001b; Whitehead *et al.*, 2005; Whitehead *et al.*, 2004; Whitehead and Cotta, 2004). The

identification of these organisms is fundamental to understanding the role of bacteria in the production of odorous compounds and greenhouse gas emissions from stored swine manure (Feilberg *et al.*, 2010; Miller and Varel, 2001). Another important topic of interest that may impact human health is the identification of antibiotic resistance genes in commensal bacteria of these ecosystems (Whitehead and Cotta, 2013). The cultivation of novel bacterial species and identification of their resistance genes can assist in determining the effects of prophylactic feeding of antibiotics to domestic swine. Many antibiotics are overused as growth promoters, and threaten the ability to regulate infections with regard to potential increases in resistance and gene transfer relating to human health. It has previously been demonstrated that a variety of resistance genes are present in the swine gastrointestinal (GI) tract and stored manure from the animals, and that new resistance genes are seen in isolated anaerobic bacterial strains (Whitehead and Cotta, 2013; Whitehead and Cotta, 2001a; Whitehead and Cotta, 2001b; Whittle *et al.*, 2003). As an extension of these investigations, we have initiated studies focused on the aerobic strains present in the swine GI tract and stored manure, which may also harbor antibiotic resistance genes. The present study describes the isolation and identification of 3 tylosin- and tetracycline-resistant, Gram-positive staining, aerobic, motile rod-shaped organisms. Based on phenotypic, chemotaxonomic, and phylogenetic considerations, it was proposed that the unknown organism originating from underground swine manure pits be classified as *Savagea faecisuis* gen. nov., sp. nov. (Type strain Con12^T = CCUG 63563^T = NRRL B-59945^T).

Materials and methods

Bacterial strains and culture conditions

Three isolates designated Con12^T (= CCUG 63563^T = NRRL B-59945^T), Tyl34 (= CCUG 63786) and Tyl40 (= CCUG 63787) were recovered from a swine manure storage pit located near Peoria, IL, USA. Isolations and enumerations were performed by plating samples that were serially diluted in BHI medium (BD, Sparks, MD) onto BHI-agar plates containing no antibiotics, tylosin (10 µg/ml) or tetracycline (10 µg/ml). Plates were incubated aerobically at 37 °C for up to two weeks. Single colonies were picked and repeatedly streaked out until pure cultures were obtained.

Morphological, physiological, and biochemical characterization

Strains Con12^T, Tyl34, and Tyl40 were cultured on Brain Heart Infusion (BHI; Bacto) agar plates at 37 °C for 48 hours. Gram staining was performed with the BD Gram Stain Kit (Sigma, St. Louis, IL), according to manufacturer's instructions. Cell morphology and motility were examined via phase contrast microscopy using an Olympus DP12 microscope. Motility was also assessed using semi-solid motility agar with Tetrazolium salt (TTC) as an indicator of respiration. Coagulase activity was determined using the Fluka Coagulase Test kit (Sigma, St. Louis, IL), according to manufacturer's instructions. Briefly, a loopful of log-phase growth was inoculated into 3 mL rabbit plasma in EDTA, incubated at 37 °C, and assessed for coagulation.

Staphylococcus aureus was used as a positive control. Other classical phenotypic tests were performed as described by Tindall *et al.* (2007). Starch hydrolysis was tested after 5 days incubation on starch agar using iodine to reveal the breakdown of starch as a

substrate. The casease test was performed by plating strains onto Milk agar containing powdered nonfat milk as the casein source and assessing the hydrolysis of casein after 5 days growth at 37 °C. In order to determine whether the large protein polymer, gelatin, could be catabolized, Nutrient Gelatin was stab-inoculated and observed for liquification after incubation. Urea hydrolysis was tested using Urea Broth which contained (g/L): urea, 20; trace amounts of yeast extract, 0.1; Na₂HPO₄ and KH₂PO₄ buffers, 9.5 and 9.1 respectively; and phenol red as the pH indicator, 0.01. The degree of alkaline end product accumulation was visualized as a rise in pH (bright pink) after 5 days incubation in order to determine whether the enzyme, urease, was present to break down urea into enough ammonia to sufficiently overcome the buffering capacity of the medium. Acid production from carbohydrates was carried out using Gordon medium as previously described (Gordon, 1973). Testing for the presence of spores was carried out using both the ethanol and heat shock methods as described by Koransky *et al.* (1978) following growth in BHI. In addition, strains were treated with decoyinine as described (Grossman and Losick, 1988; Mitani *et al.*, 1977) for potential induction of spore formation. The strains were biochemically characterized by using a combination of conventional tests, the API 50CH, API 20E, and API ZYM systems, according to the manufacturer's instructions (API bioMérieux, Marcy L'Etoile, France). First, log-phase growth was used to make a bacterial suspension in sterile diH₂O equivalent to McFarland Standard 0.5. Then 55 µL was pipetted into each cupule of API strips. The strip was incubated at 37 °C for 4 hours and examined for colorimetric changes according to API interpretive charts. All biochemical tests were performed in duplicate.

Resistance to antibiotics was determined by growth in BHI supplemented with filter-sterilized antibiotics.

Determination of the 16S rRNA gene sequence and phylogenetic analysis

For isolation of genomic DNA, the UltraClean Microbial Isolation Kit (Mo Bio, Solana Beach, CA) was used according to the manufacturer's instructions. DNA was diluted 1:100 in molecular-grade H₂O, then used as a template for PCR using the same recipe and thermocycler conditions as mentioned in Chapter 2. Gel electrophoresis and amplicon purification (ExoSap-It) were performed as previously mentioned. Sequencing was performed at The Oklahoma Medical Research Foundation (OMRF) using a series of five primers that covered the conserved and variable region of the 16S rRNA gene. To provide a rapid means of identification and to determine the phylogenetic position of the swine manure isolates, 16S rRNA gene sequence analysis was performed as previously described (Whitehead and Cotta, 2004). The closest known relatives of the new isolate based on the 16S rRNA gene sequence were determined by performing database searches of EMBL / GenBank using the program EzTaxon-e server (<http://eztaxon-e.ezbiocloud.net/>); (Kim *et al.*, 2012). The most related sequences were then selected for the calculation of pairwise sequence similarity using a global alignment algorithm (Myers and Miller, 1988). These sequences, and those of other related strains, were aligned with the sequence derived from Con12^T using the program ClustalW. Phylogenetic reconstructions were performed in MEGA (version 4) (Tamura *et al.*, 2007) using the neighbor-joining method (Saitou and Nei,

1987), applying evolutionary genetic distances that had been calculated by the Kimura two-parameter model (Kimura, 1980).

Determination of the DNA mol% G+C content of the Con12^T strain was performed at Deutsche Sammlung von Mikro-organismen und Zellkulturen GmbH (DSMZ) following the method of Cashion *et al.* (Cashion *et al.*, 1977). DNA was hydrolyzed using P1 nuclease and the nucleotides dephosphorylated with bovine alkaline phosphatase (Mesbah *et al.*, 1989). The resulting deoxyribonucleosides were analyzed by HPLC (Shimadzu Corp., Japan). The software package, CLARITY (Version 2.4.1.93) (DataApexLtd., Czech Republic) was then employed to analyze chromatograms. The G+C content was calculated from the ratio of deoxyguanosine (dG) and thymidine (dT) according to the methods described by Mesbah *et al.* (1989). Also, RAPD-PCR analyses were carried out with the m13 primer as described previously (Andrighetto *et al.*, 1998; Descheemaeker *et al.*, 1997).

Chemotaxonomic characterization

Fatty acid methyl ester (FAME) analysis was performed at the Center for Microbial Identification and Taxonomy (University of Oklahoma) using a MIDI System standardized protocol with Sherlock version 6.1 and the QTSA database as described previously (Miller, 1982; Sasser, 2001). Cells were derivitized and extracted as detailed in Chapter 1. Again, analysis was carried out with an Agilent 6890N GC using hydrogen as the carrier gas. The GC was equipped with a phenyl methyl silicone fused silica capillary column (HP-Ultra 2, 25m x 0.2 mm x 0.33 mm film thickness) and a flame ionization detector. The temperature program was initiated at 170 °C and

increased at 5 °C min⁻¹ to a final temperature of 270 °C. Integration of peaks and further calculations were performed by Sherlock Version 6.1. Fatty acid methyl esters were identified and quantified (relative to C7-C20 fatty acid standards), and the relative amount of each fatty acid was expressed in terms of the percentage of total fatty acids. In order to best compare FAME profiles with related taxa, cells were grown aerobically on Trypticase Soy Broth Agar (TSBA) for 24 hours at 37 °C and on TSA for 24-48 hours at 28 °C.

Additional chemotaxonomic analyses were performed with cells grown aerobically in flasks containing TSB medium on a rotary shaker for 48 hours at 30 °C, harvested by centrifugation at 3000 x g, and lyophilized. The polar lipids of strain Con12^T were analyzed as described by Groth *et al.* (Groth *et al.* 1996). Specifically, lipids were extracted from 100 mg lyophilized biomass using chloroform: methanol: 0.3% NaCl (1:2:0.8 v/v/v). The solution was degassed with nitrogen, sealed with a Teflon cap, and heated for 15 minutes at 80 °C. Once cooled to room temperature, cell debris was removed by centrifugation in 15 mL glass centrifuge tubes at 3000 rpm for 10 minutes. The supernatant was removed and further extracted with 5 mL of chloroform: 0.3% NaCl (1:1 v/v). Following a second centrifugation at 3000 rpm for 5 minutes, the lower chloroform phase was collected using a pasteur pipet and dried under a stream of nitrogen gas. This polar lipid extract was then resuspended in chloroform: methanol (2:1 v/v) and then spotted onto Silica backed, thin layer chromatography (TLC) plates using a Hamilton syringe in increments of 2 µL, with a total of 6 µL for each plate. Lipids were separated using two-dimensional TLC, with the first dimension consisting of chloroform: methanol: water (65:25:4 v/v/v) and the second dimension

consisting of chloroform: methanol: acetic acid: water (80:12:15:4 v/v/v). Plates were allowed to fully dry between chromatographies, and stored in the dark overnight before development. Dry plates were sprayed with Molybdenum Blue to develop phosphate-containing lipids, Dragendorff's reagent to show choline containing lipids, Ninhydrin to develop amino lipids, and Molybdophosphoric Acid to reveal total lipids.

Respiratory quinones were extracted and analyzed using the methods described by Altenburger *et al.* (1996) and Tindall *et al.* (1990a, b). Briefly, 100 mg of lyophilized biomass was placed in a 15 mL screw-top, Teflon-lined amber vial. 2.0 mL of methanol was added, followed by 1.0 mL hexane, before vials were degassed under N₂ in order to exchange headspace. After mixing for thirty minutes on a stir-plate, vials were placed into an ice bath for 10 minutes in order to observe hexane and methanol phase separation. Next, 1.0 mL of ice-cold hexane was added to yield a methanol: hexane (1:1 v/v) biphasic mixture before centrifuging at 3000 rpm for 5 minutes to enhance layer separation. The upper layer of hexane was then removed and transferred to another screw-top vial. The methanol phase was further extracted by the addition of 2.0 mL cold hexane and 0.3% NaCl, to give a ratio of 1:1:1 (v/v) hexane, methanol, 0.3% NaCl. Again, centrifugation was used to enhance phase separation before the upper hexane layer was removed and added to the first fraction. Finally, this hexane phase was concentrated under a stream of nitrogen gas and kept at -20 °C until analysis. Quinones were analyzed using high-performance liquid chromatography (HPLC) instrumentation reported by Stolz *et al.* (2007).

Peptidoglycan analysis was performed at the Biological Resource Center, National Institute of Technology and Evaluation (NBRC), Japan. Strain Con12^T was

grown in a flask containing TSB medium on a rotary shaker for 48 hours at 30 °C.

Amino acids and the isomers in the cell-wall hydrolysate were analyzed as described by Hamada *et al.* (2012).

Determination of tetracycline resistance genes

The presence of tetracycline resistance gene(s) was determined using PCR primers and protocols as described by Villedieu *et al.* (2003). PCR was carried out on genomic DNA (isolation described above) and plasmid DNA isolated with the QIAprep Spin Miniprep Kit (QIAGEN, Valencia, CA). *tet* PCR fragments were recovered using the MinElute PCR Purification Kit (QIAGEN, Valencia, CA) and sequenced using the same PCR primers from the initial reactions.

Results

Morphological, physiological, and biochemical characteristics

One isolate from the control Brain Heart Infusion (BHI) plating and two strains from the BHI-tylosin plating were found by 16S rRNA gene sequence analysis to belong to a single distinct group. The strains had a number of similar features that included being Gram-positive staining, motile rod-shaped cells in pairs or short chains. All strains were aerobic and catalase- and oxidase-negative. After 48 hours of aerobic growth at 37 °C on BHI-agar plates, colonies varied in size from 1-3 mm in diameter and were moist, cream-colored with raised centers. No hemolysis was observed on blood agar plates after one week, however, prolonged incubation (two weeks or more) led to the complete lysis of red blood cells. Growth was observed at 25 °C and 37 °C, but no growth occurred at 45 °C. Also, no growth was observed under anaerobic conditions, including fluid thioglycollate, deep agar stabs, and anaerobically incubated agar plates. Growth was seen in the presence of 6.5% NaCl and also in the presence of 10 µg/ml tetracycline. Con12^T was unable to grow with citrate as the sole energy source. The organism could not grow on starch plates and did not produce any casein clearings on Milk Agar plates. Urea Broth showed positive turbidity, but the medium remained a copper color, indicative of the culture maintaining a circumneutral pH. Partial liquefaction of the otherwise solid gelatin medium was observed after 5 days incubation. A summary of these traits can be seen in Table 2.1. Using the API ZYM test system, positive reactions were obtained for esterase (C4), leucine arylamidase, cystine arylamidase, and naphthol-AS-BI-phosphohydrolase, with weak reactions obtained for

esterase lipase (C8) and valine arylamidase (Table 2.2). All other ZYM tests were negative.

Table 2.1: Morphological and physiological characteristics of *Savagea faecisuis* Con12^T. +, positive; -, negative.

Characteristics	<i>Savagea faecisuis</i> Con12 ^T
Inhabiting niche	swine faeces
Gram reactivity	Gram (+)
Cell shape	irregular rod
Cell size	1 x 2-4 um length
Colony morphology	moist, cream-colored, raised center, odorous
Colony size	1-3 mm diameter
Relation to O ₂	obligately aerobic
Motility	motile
DNA G+C content (mol%)	41.8
Sporulation	-
Catalase	-
Oxidase	-
Coagulase	-
Growth on 6.5% NaCl	+
Citrate utilization (citrase)	citrase -
Blood hemolysis	γ-hemolytic
Casein hydrolysis	casease -
Gelatin hydrolysis	gelatinase +
Urea hydrolysis	urease -
Starch hydrolysis	-
Glucose fermentation	-
Acid from carbohydrates	-

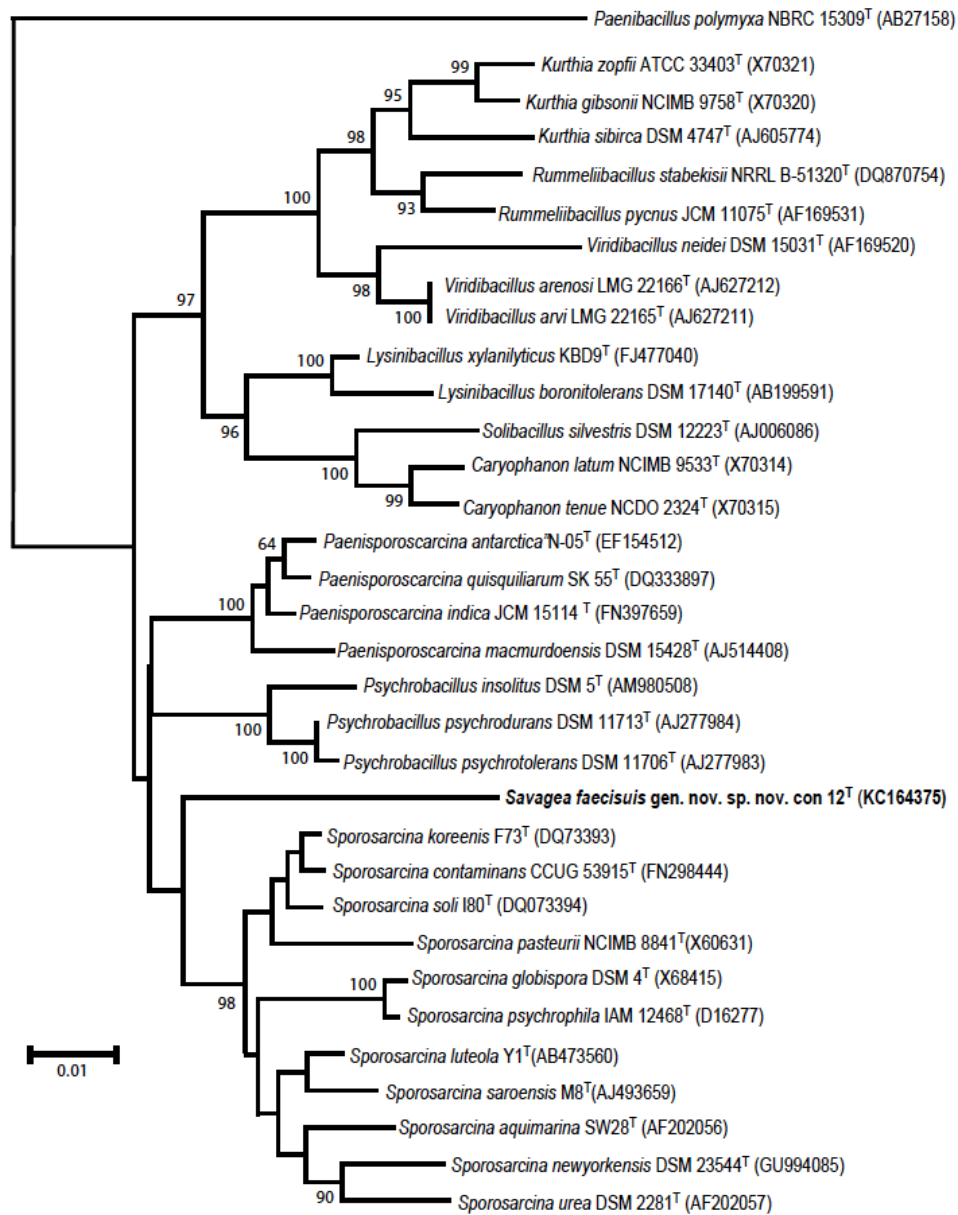
Table 2.2: API ZYM results for *Savagea faecisuis* strain Con12^T. +, positive; -, negative; w, weak.

Enzyme Activity	Con12 ^T
Alkaline phosphatase	-
Esterase (C-4)	+
Esterase lipase (C-8)	W
Lipase (C-14)	-
Leucine arylamidase	+
Valine arylamidase	W
Cystine arylamidase	+
Trypsin	-
Chymotrypsin	-
Acid phosphatase	-
Phosphohydrolase	+
α -Galactosidase	-
β -Galactosidase	-
β -Glucuronidase	-
α -Glucosidase	-
β -Glucosidase	-
N-Acetyl- β -glucosaminidase	-
α -Mannosidase	-
α -Fucosidase	-

Determination of the 16S rRNA gene sequence and phylogenetic analysis

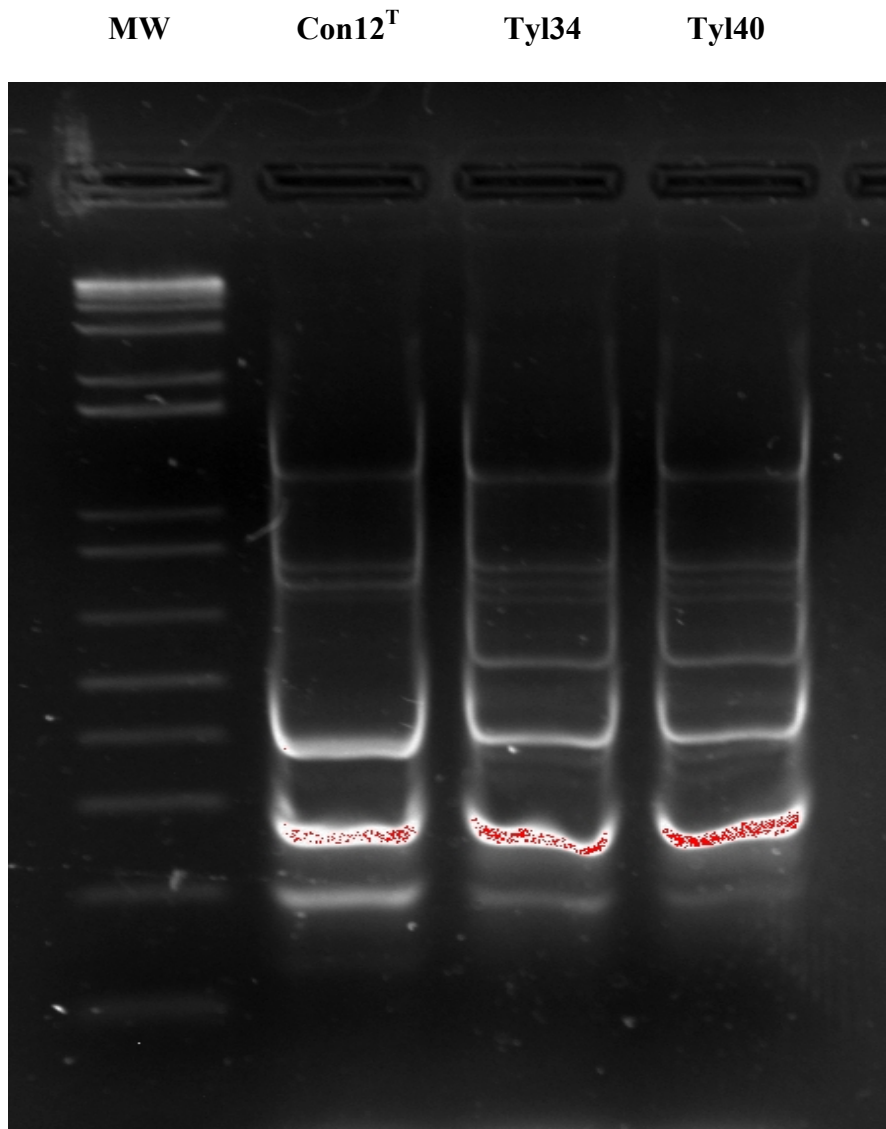
To investigate the phylogenetic affinity of the unknown isolates, the 16S rRNA gene was amplified by PCR and sequenced. The three strains were almost identical when their 16S rRNA genes were aligned (99.5-100% with 1420 nucleotides). A phylogenetic tree, constructed by the neighbor-joining method, depicting the phylogenetic affinity of strain Con12^T can be seen in Figure 2.1. The analysis demonstrated that the novel organism was a member of the *Firmicutes* phylum and located within the family *Planococcaceae*. It was most closely related to a cluster of organisms that contained members of the genera *Sporosarcina*, *Psychrobacillus*, and *Paenisporosarcina* and a neighboring clade that contained *Caryophanon*, *Kurthia*, *Lysinibacillus*, *Rummeliibacillus*, and *Solibacillus*.

Figure 2.1: Phylogenetic dendrogram of 16S rRNA gene sequences indicating the position of *Savagea faecisuis* gen. nov. sp. nov. Con12^T within the *Planococcaceae* family. The tree was constructed using the neighbour-joining algorithm from MEGA version 4 with *Paenibacillus polymyxa* as the outgroup. Bootstrap values are displayed at their relative nodes.



RAPD-PCR analysis of the strains using m13 primer demonstrated that the patterns were very similar, with Tyl34 and Tyl40 being identical with 5 fragments present, and Con12^T showing the same pattern with one of the fragments missing. Therefore, it appeared that strains Tyl34 and Tyl40 were very similar but of a separate clonal lineage from the Con12^T (Fig. 2.2).

Figure 2.2: RAPD-PCR of *Savagea* strains.



Chemotaxonomic characteristics

Cellular fatty acid analysis demonstrated that Con12^T, when grown on TSBA, contained two major products consisting of iso-C_{17:1} ω10c (14.2%) and iso-C_{15:0} (60.9%) with C_{16:1} ω11c being present in a lower amount (6.9%) . The full fatty acid profile, and a comparison with other close phylogenetic relatives, can be seen in Table 2.3. In addition, fatty acid analyses were also performed on Con12^T using a number of different media with and without the presence of blood (Table 2.4). The use of blood was thought important due to the fact that blood is often used in the growth media of clinically relevant strains, and this information will be of use for future studies. However, the profiles were found to be remarkably consistent, with iso-C_{17:1} ω10c, iso-C_{15:0}, and C_{16:1} ω11c always being the predominant products. All related genera produce either iso-C_{15:0}, anteiso-C_{15:0}, or a combination of both as a major product, but the strains of the proposed novel organism are unique in producing iso-C_{17:1} ω10c.

Table 2.3: Comparison of fatty acid profile of *Savagea facisuis* Con12^T with type species of related genera.

Strains: 1, Con12^T (this study); 2, *Caryophanon latum* NCIMB 9533^T (Fritze and Claus, 2009); 3, *Kurthia zopfii* DSM 20580^T (Ruan *et al.* 2014) ; 4, *Lysinibacillus boronitolerans* 10a^T (Ahmed *et al.* 2007); 5, *Paenisporosarcina quisquiliarum* SK 55^T (Krishnamurthi *et al.* 2009a); 6, *Psychrobacillus insolitus* DSM 5^T (Krishnamurthi *et al.* 2010); 7, *Solibacillus silvestris* DSM 12223^T (Krishnamurthi *et al.* 2009b); 8, *Sporosarcina urea* DSM 2281^T (Krishnamurthi *et al.* 2009a); 9, *Rummeliibacillus stabekisii* NRRL B-51320^T (Vaishampayan *et al.* 2009); 10, *Viridibacillus arvi* DSM 16317^T (Albert *et al.* 2007).

Fatty Acid	1	2 ^a	3 ^b	4	5	6	7	8 ^c	9 ^d	10
C14:0	1.0	3.3	1.4	ND	1.4	ND	ND	ND	2.6	0.8
C14:0 iso	0.5	4.9	8.3	2.9	4.7	34.2	2.9	4.6	6.7	1.4
C15:0	0.5	2.3	ND	ND	ND	ND	ND	ND	0.5	2.7
C15:0 anteiso	2.5	2.9	14.4	5.6	19.3	14.8	5.6	56.2	49.9	21.7
C15:0 iso	60.9	35.7	46.4	44.2	39.6	7.1	44.2	7.0	26.0	46.2
C15:1 iso ω _{9c}	1.0	ND	ND	ND	ND	ND	ND	ND	ND	ND
C16:0	1.5	4.3	2.6	ND	1.9	ND	ND	3.5		ND
C16:0 iso	0.5	2.1	3.3	6.2	4.0	1.1	6.2	2.8	4.7	0.8
C16:1 iso	ND	ND	ND	18.7	ND	ND	18.7	ND		ND
C16:1 ω _{7c} alcohol	1.3	8.8	ND	3.1	9.6	19.2	3.1	4.0	2.4	3.7
C16:1 ω _{11c}	6.9	25.7	3.0	ND	2.5	ND	ND	4.8	ND	3.9
C17:0 anteiso	0.9	0.9	tr	3.0	3.3	ND	3.0	12.1	7.0	4.8
C17:0 iso	2.8	1.2	1.2	5.1	1.6	ND	5.1	ND	ND	2.0
C17:1 ω _{10c} iso	14.2	3.4	tr	7.8	2.8	ND	7.8	ND	ND	5.2
C17:1 anteiso B/ iso I	1.8	ND	ND	2.8	5.6	ND	2.8	4.6	ND	6.8
C20:1 ω _{9c}	1.4	ND	ND	ND	ND	ND	ND	ND	ND	ND

Major fatty acids are shown in bold. ND, Not Detected; tr, trace amount.

Unless otherwise stated media used was Trypticase Soy Both Agar (TSBA)

^a medium no. 34 DSMZ http://www.dsmz.de/microorganisms/medium/pdf/DSMZ_Medium34.pdf

^b Nutrient Broth

^c marine agar

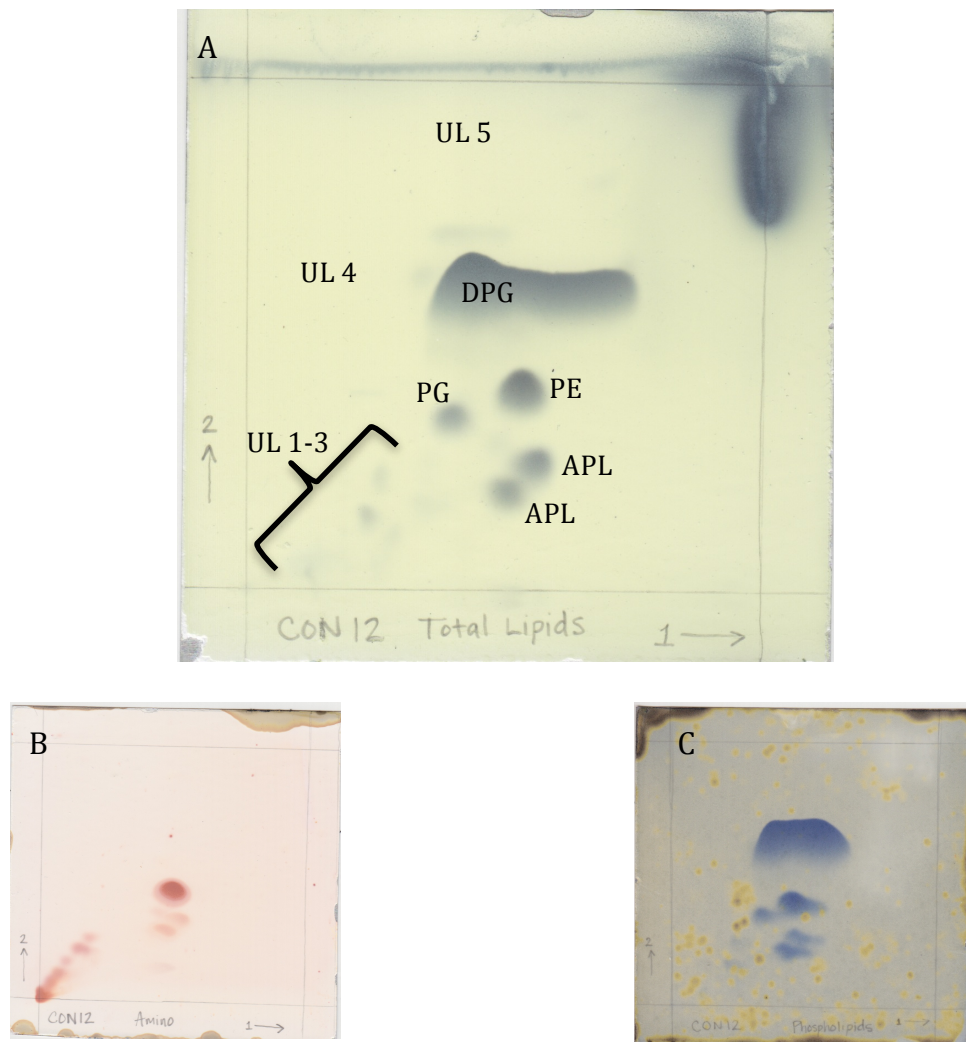
^d TSB

Table 2.4: Fatty acid profiles of *Savagea faecisuis* strain Con12^T grown on different media.

Fatty Acids	Blood Agar 37°C 24-48 hr	Brucella agar + 5% blood 30°C 24-48 hr	TSBA 30°C 24-48 hr	TSA 30°C 24-48 hr
C14:0	1.2	1.9	1.0	4.3
C14:0 iso	-	0.4	0.5	1.8
C15:0	1.5	1.5	0.5	1.8
C15:0 iso	60.2	57.9	60.9	35.5
C15:0 anteiso	4.6	2.7	2.5	8.8
C15:1 ω8c	-	1.4	0.6	-
C15:1 iso ω9c	-	0.5	1.0	-
C16:0	2.1	2.8	1.5	7.4
C16:0 iso	-	-	0.5	1.5
C16:1 ω7c alcohol	1.7	0.7	1.3	2.1
C16:1 ω11c	7.3	8.0	6.9	21.1
C17:0 iso	3.9	2.1	2.8	2.5
C17:0 anteiso	1.6	0.7	0.9	2.9
C17:1 ω10c iso		8.7	14.2	5.3
C17:1 iso I/ C16:0	1.8	-	-	2.1
C17:1 anteiso	-	1.6	1.8	-
C17:1 ω9c	-	1.2	0.8	1.51
C18:0/ C17:0 cyclo	-	1.2	-	-
C18:1 ω7c	-	0.5	-	-
C18:1 ω9c	-	4.2	-	-
C18:2 ω6,9c/18:0	1.0	-	-	-
C20:1 ω9c		1.0	1.4	1.4
Unknown ECL 14.761	2.0			
Unknown ECL 14.173	1.1	-	-	-
Unknown ECL 14.926	1.4	-	-	-

The two- dimensional lipid profiles of strain Con12^T revealed the presence of diphosphatidylglycerol (DPG), phosphotidylglycerol (PG), phosphotidylethanolamine (PE), aminophospholipid (UAPL), and unknown lipids (UL) (Figure 2.3). The major polar lipids DPG, PG and PE were revealed by molybdophosphoric acid spray and found to be comparable to related taxa in size, shape, and separation tendencies.

Figure 2.3: Two- dimensional total lipid profiles of *Savagea faecisuis* gen. nov. sp. nov. Con12^T. DPG – diphosphatidylglycerol, PG – phosphotidylglycerol, PE – phosphotidylethanolamine, APL – aminophospholipid, UL – unknown lipid. Shown, plates developed with Molybdophosphoric Acid to reveal total lipids, A; Ninhydrin to develop amino lipids, B; and Molybdenum Blue to develop phosphate-containing lipids, C.



Menaquinone-6 (MK-6) was found to be predominant compound in the quinone system. The peptidoglycan contained alanine (Ala), glutamic acid (Glu), glycine (Gly) and lysine (Lys) in a molar ratio of 2.0 : 2:0 : 1.1 : 0.9 (Figure 2.4). Enantiomeric analysis of the peptidoglycan amino acids revealed the presence of D-Ala, L-Ala, D-Glu, Gly and L-Lys (Figure 2.5). These results indicate that the cell-wall peptidoglycan of strain Con12^T is of the A4 α type with an interpeptide bridge comprising L-Lys–Gly–D-Glu. The DNA G+C content of the type strain Con12^T was determined to be 41.8 mol%.

Figure 2.4: Amino acid analysis of strain Con12^T showing alanine (Ala), glutamic acid (Glu), glycine (Gly) and lysine (Lys)

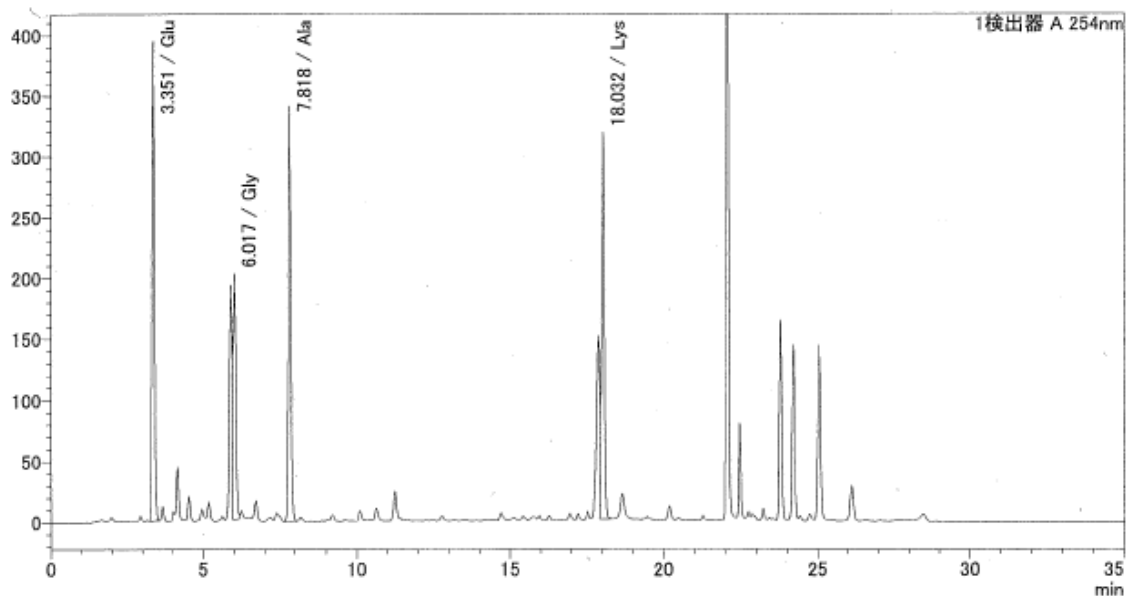


Figure 2.5: Chromatogram of isomer analysis for strain Con12^T.

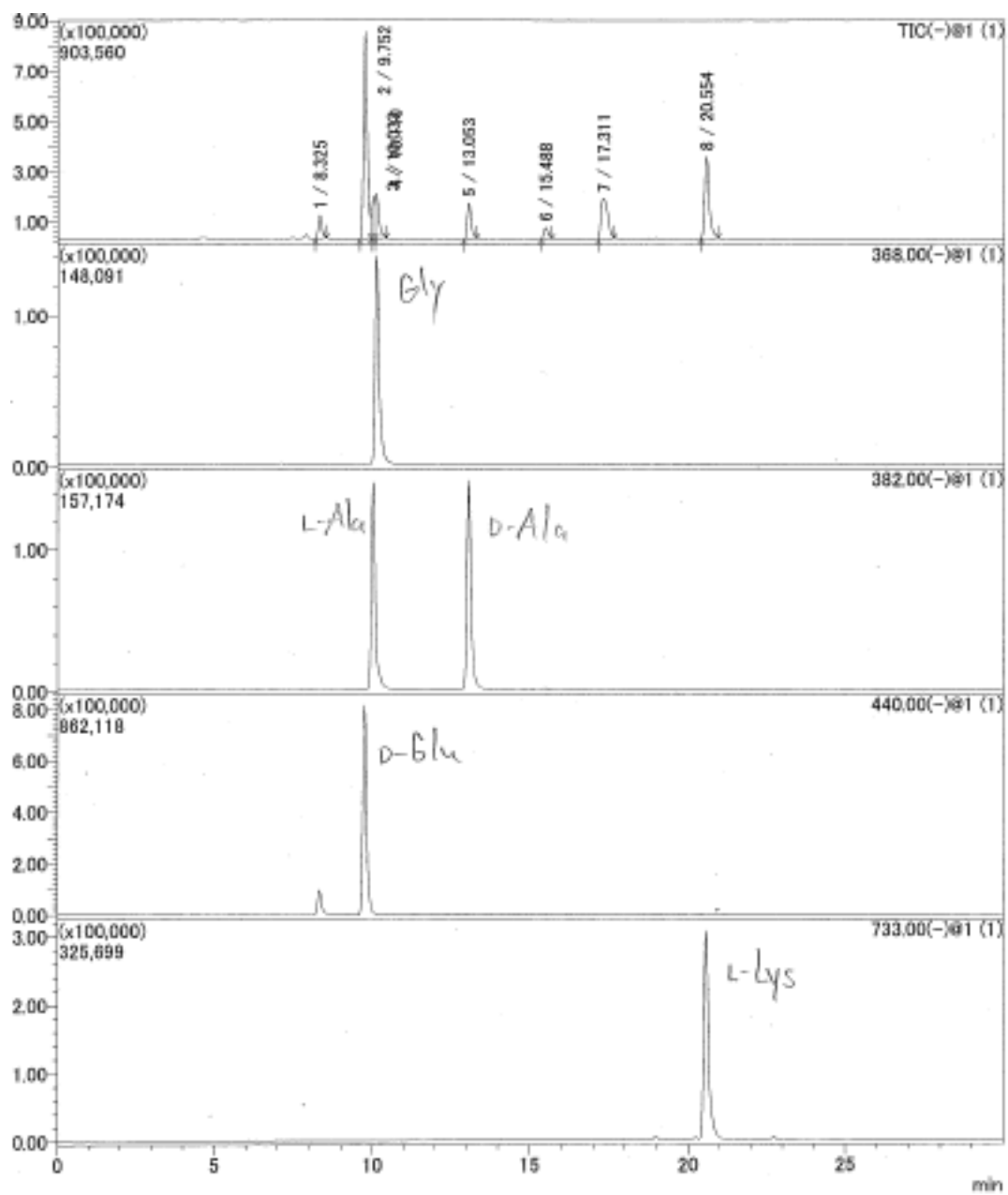


Table 2.5: Characteristics that distinguish the genus *Savagea* from other closely related genera.

Characteristics	<i>Savagea</i>	<i>Psychrobacillus</i> ^a	<i>Paenisporosarcina</i> ^b	<i>Sporosarcina</i> ^c	<i>Viridibacillus</i> ^d	<i>Lysinibacillus</i> ^e	<i>Kurthia</i> ^f	<i>Solibacillus</i> ^g
Cell shape	Rod/spherical	Rod/spherical	Rod/spherical	Rod/spherical	Rod	Rod	Rod	Rod
Spore formation	-	+	+	+	+	+	-	+
Peptidoglycan type	L-Lys-Gly-D-Glu	L-Orn-D-Glu	L-Lys-D-Asp	L-Lys-L-Ala-D-Asp/L-Lys-Gly-D-Glu/L-Lys-D-Glu	L-Lys-D-Asp/L-Lys-D-Glu	L-Lys-D-Asp	L-Lys-D-Asp	L-Lys-D-Glu
Quinone system	MK-6	MK-8, MK-7, MK-6, MK-9	MK-7, MK-8	MK-7	MK-7, MK-8	MK-7	MK-7	MK-7
Polar lipids	DPG, PG, PE, 5UL, 2APL	DPG, PG, PE, 2PL, 4UL	DPG, PG, PE, APL, UL	DPG, PG, PE, APL, 3UL	DPG, PG, PE, APL, 2PL	DPG, PG, APGL	DPG, PE, PG	DPG, PG, PE, PS, UPL
Major fatty acids	i-C _{15:0} , C _{17:1} ω ₁₀ c	at-C _{15:0} , C _{16:1} ω ₇ c alcohol, iso-C _{15:0} , iso-C _{14:0}	i-C _{15:0} , at-C _{15:0} , C _{16:1} ω ₇ c alcohol	at-C _{15:0} , (i-C _{15:0})	i-C _{15:0} , at-C _{15:0}	i-C _{15:0} , i-C _{16:0} , at-C _{17:0} , C _{16:1} ω ₇ c alcohol	i-C _{15:0} , at-C _{15:0}	i-C _{15:0} , i-C _{16:1}

Abbreviations: [MK, menaquinone; PG, phosphatidylglycerol; PE, phosphatidylethanolamine; APL, aminophospholipid; APGL, aminophosphoglycolipid; GBG, gentiobiosyl-diacylglycerol; UL, unknown lipid. Components listed in parentheses were present in major amounts in some members of the taxon.

Data for *Savagea* are from this study.

* Data from ^a (Krishnamurthi *et al.*, 2010); ^b (Krishnamurthi *et al.*, 2009a); ^c (Krishnamurthi *et al.*, 2009b); ^d (Albert *et al.*, 2007); ^e (Ahmed *et al.*, 2007); ^f (Ruan *et al.*, 2014); ^g (Krishnamurthi *et al.*, 2009b).

Tetracycline resistance genes

Results of PCR analyses of the genomic DNA from the three novel isolates using primers of various *tet* resistance genes revealed the presence of both *tetL* and *tetM* genes. Results from other primer sets were negative. DNA sequence analyses demonstrated that the *tetL* fragments from the Tyl364 and Tyl40 strains were 98% similar, but both were only 93% similar with the *tetL* fragment from Con12^T. Similarly the *tetM* fragment from Tyl34 and Tyl40 were 100% similar, but only 90% similar to that from Con12^T. This data suggests again that Tyl34 and Tyl40 strains are similar but of different clonal lineage from the Con12^T. It is also interesting to note that PCR analyses using plasmid DNA revealed a similar pattern, suggesting the *tet* resistance genes may be carried on plasmid(s) by the strains (data not shown). The GenBank accession numbers for the *tetL* sequences are Con12^T: KM610309; Tyl34: KM610310; and Tyl40: KM610311, respectively. The GenBank accession numbers for the *tetM* sequences are Con12^T: KM610312; Tyl34: KM610313; and Tyl40: KM610315, respectively.

Description of Savagea gen. nov.

Savagea (Savagea: Sa.va'ge.a. N.L. fem. n. *Savagea*, named in honour of Dwayne C. Savage, an American microbiologist, for his contributions to gastrointestinal microbiology)

Members of this genus have cells that Gram-stain positive, and are catalase- and oxidase-negative. Cultures are obligately aerobic and contain motile rods. No spore formation is observed within this genus. Major fatty acids include iso-C_{17:1} ω10c and

iso-C_{15:0}. MK-6 has been the predominant quinone detected among species. Instead of utilizing carbohydrates, proteinacious material is consumed. Cell-wall peptidoglycan is of the A4 α type, where Diphosphatidylglycerol (DPG), phosphatidylglycerol (PG), and phosphatidylethanolamine (PE) are present, in addition to a number of unidentified products. The G+C content of the type species is 41.8 mol%. 16S rRNA gene analysis indicates that the genus is a member of the family *Planococcaceae*. The type strain is *Savagea faecisuis*.

Description of Savagea faecisuis sp. nov.

(*faecisuis*: fa.e.ci.su'is. L. n. *faexfaecis*, *faeces*; L. gen. n. *suis*, of swine, pig; N.L. gen. n. *faecisuis*, from pig faeces/manure).

Cells consisted of Gram-stain positive, motile rods arranged as single cells, pairs, or short chains. After 48 hours of aerobic growth at 37 °C on BHI-agar plates, colonies varied in size from 1-3 mm in diameter and were moist, cream-colored with raised centers. No growth was observed under anaerobic conditions, therefore *Savagea faecisuis* was considered an obligate aerobe. Although no hemolysis was observed on blood agar plates after one week, β -hemolysis was seen after two weeks. Growth was viable at 25 °C and 37 °C, but no growth occurred at 45 °C. Growth also occurred in BHI with 6.5% NaCl. No spore formation was observed and nitrate was not reduced. Cells tested negative for both catalase and oxidase activity. Coagulase activity was also negative. Con12^T was unable to grow with citrate as the sole energy source, and therefore considered negative for both of the enzymes, citrate permease and citrase. No growth was observed on starch-agar plates. Thus, *Savagea faecisuis* was negative for

the secretion of α -amylase, as no starch was hydrolyzed. Cells were considered negative for the secretion of the casease enzyme. Cells were also considered negative for urease because urea hydrolysis, and the subsequent production of ammonia and CO₂, was not observed. Results from the gelatin hydrolysis test were positive for a gelatinase enzyme due to the partial liquefaction of solid gelatin-containing medium after 5 days incubation. No acid production was observed when grown in Gordon Medium with the following carbohydrates: glucose, xylose, arabinose, maltose, fructose, cellobiose, and mannitol. Strains were resistant to tylosin and tetracycline at 10 μ g/ml. Using the API 50CH test system, all reactions were negative. Employing the API 20E system, a positive reaction was noted for acetoin production and a weakly positive for oxidase. Negative reactions were obtained for all other reactions. Using the API ZYM test system, positive reactions were obtained for esterase (C4), leucine arylamidase, cystine arylamidase, and naphthol-AS-BI-phosphohydrolase, with weak reactions obtained for esterase lipase (C8) and valine arylamidase. All other ZYM tests were negative. *Savagea faecisuis* produced the major fatty acids, iso-C_{17:1} ω 10c and iso-C_{15:0} and contained MK-6 as the predominant quinone. The peptidoglycan contained alanine (Ala), glutamic acid (Glu), glycine (Gly) and lysine (Lys), and was of the A4 α type with an interpeptide bridge comprising L-Lys-Gly-D-Glu. The G+C content of the DNA of the type strain was 41.8 mol%. All strains were susceptible to Tylosin (10 μ g/mL), Erythromycin (10 μ g/mL), and Tetracycline (10 μ g/ mL), yet resistant to Ampicillin (25 μ g/mL), Novobiocin (25 μ g/mL), and Gentamicin (25 μ g/mL). The type strain is Con12^T (=CCUG 63563^T = NRRL B-59945^T). The GenBank accession numbers

for the 16S rRNA gene sequences of *S. faecisuis* strains are Con12^T: KC164375; Tyl34: KC511961; and Tyl40: KC511960, respectively.

Discussion

Phenotypic, phylogenetic and chemotaxonomic methods clearly demonstrated that the novel organisms isolated from swine manure can be separated from all known related taxa. Therefore, the unidentified bacteria merit classification of a novel genus and species named *Savagea faecisuis* gen. nov. sp. nov. This data suggested that Tyl34 and Tyl40 strains were similar but of different clonal lineage from Con12^T. Though the type strain Con12^T, and other strains, Tyl34 and Tyl40, were all isolated from a swine manure storage pit, the official habitat is not known.

Phylogenetic analysis based on the 16S rRNA gene demonstrated that the novel species was most closely related to the family *Planococcaceae* (Ludwig *et al.*, 2009). *Planococcaceae* falls within the order *Bacillales*, which now embraces 16 genera: *Savagea*, *Bhargavaea*, *Caryophanon*, *Chryseomicrbium*, *Filibacter*, *Jeotgalibacillus*, *Kurthia*, *Paenisporosarcina*, *Psychrobacillus*, *Planococcus*, *Planomicrobium*, *Rummeliibacillus*, *Solibacillus*, *Sporosarcina*, *Ureibacillus*, and *Viridibacillus* (Krishnamurthi *et al.*, 2010). Though close in genetic relatedness, the *Savagea* type strain Con12^T formed a separate clade from members of closely related genera. In particular, pairwise analysis demonstrated that the novel organism was most closely related to members of the genera *Sporosarcina* (92.8-94.5%), *Psychrobacillus*

(93.5-93.9%), and *Paenisporosarcina* (93.3-93.9%). This phylogenetic coherence was supported with further characterization.

Physiological investigations revealed that all strains were negative for acid production from glucose, xylose, arabinose, maltose, fructose, cellobiose, and mannitol. Rather than carbohydrate utilization, *Savagea* species grew on peptone, tryptone, and other proteinaceous substrates. Positive reactions were obtained for leucine arylamidase and cystine arylamidase, with a weak reaction obtained for valine arylamidase. The arylamidase enzyme catalyzes the hydrolysis of N-terminal amino acids from peptides or amides, and the presence of these enzymes indicate that *Savagea* species may play a key role in the release of amino acids from organic fecal material (Macfarlane *et al.*, 1989). These amino acid products are then likely to be utilized by other members of this complex microbial community that possess aminohydrolase enzymes for nitrogen mineralization. Urease broth containing peptone, potassium phosphate, and phenol red remained orange after incubation, indicating an alkaline pH above 8.4 was not achieved. The enzyme urease was not present, therefore urea (the product of amino acid decarboxylation) cannot be hydrolyzed. Cells were considered negative for urease because the production of ammonia and CO₂ was not observed. Therefore, *Savagea faecisuis* was unable to break the peptide bonds between adjacent amino acids to hydrolyze urea, a common component of swine manure storage tanks. Cells were also considered negative for the secretion of casease because milk agar plates containing the phosphoprotein, casein, showed no zone of clearing around growth. This was an important test because it revealed the inability of *Savagea* to break down large

polypeptides into individual amino acids. While it appeared that calls were largely capable of proteolysis, they lacked secretion of the specific exoenzyme, casease.

The oxidase test showed that no oxidation of tetramethyl-p-phenylenediamine occurred, therefore Con12^T lacked the respiratory enzyme cytochrome c oxidase that transfers electrons to oxygen, reducing O₂ to water. Since Con12^T was capable of aerobic respiration, cells must have a different terminal oxidase system. Using the Coagulase test with rabbit plasma, a negative result for both bound and free (extracellular) coagulase was revealed. There was no fibrinogen precipitation and no agglutination of cells, therefore plasma was not coagulated. While this virulent trait was not detected, blood hydrolysis and DNase activity indicated that *Savagea* species were capable of lysing red blood cells and cleaving the phosphodiester bonds that link nucleotides within DNA. These attributes may raise the risk of these species in human and animal health safety. Finally, antibiotic studies revealed that all strains were susceptible to Tylosin, Erythromycin, and Tetracycline, yet resistant to Ampicillin, Novobiocin, and Gentamicin. Closely related *Sporosarcina* species, however, remained resistant to Tetracycline. This information could be particularly valuable if future investigations reveal a greater health concern for *Savagea* species.

This study suggests that these organisms are intimately involved in the multi-step process of the breakdown of organic matter, ultimately resulting in an odorous alkaline environment. It also reinforces that the novel species described here, along with other Gram-positive cocci, are commonly found within this ecosystem. The activity of these organisms deserves further attention because they play key roles in the release of amino acids from proteinaceous material found in waste disposal systems, and therefore

may aid in a better understanding of the nitrogen cycling occurring within these complex microbial communities.

Acknowledgements

The authors wish to acknowledge the valuable technical assistance by Rhonda Zeltwanger. We also thank Ken-ichiro Suzuki at the Biological Resource Center, National Institute of Technology and Evaluation (NBRC) for facilitating the analysis of the peptidoglycan. Antibiotic sensitivity tests and RAPD-PCR data of *Savagea* strains using the m13 primer was performed by Dr. Terence Whitehead. Funding for this study was provided by the United States Department of Agriculture.

References

- Ahmed I, Yokota A, Yamazoe A, Fujiwara T.** (2007). Proposal of *Lysinibacillus boronitolerans* gen. nov. sp. nov., and transfer of *Bacillus fusiformis* to *Lysinibacillus fusiformis* comb. nov. and *Bacillus sphaericus* to *Lysinibacillus sphaericus* comb. nov. *Int J Syst Evol Microbiol* **57**:1117–1125.
- Albert RA, Archambault J, Lempa M, Hurst B, Richardson C, Gruenloh S, Duran M, Worliczek HL, Huber BE, Rosselló-Móra R, Schumann P, Busse H-J.** (2007). Proposal of *Viridibacillus* gen. nov. and reclassification of *Bacillus arvi*, *Bacillus arenosi* and *Bacillus neidei* as *Viridibacillus arvi* gen. nov., comb. nov., *Viridibacillus arenosi* comb. nov. and *Viridibacillus neidei* comb. nov. *Int J Syst Evol Microbiol* **57**:2729–2737.
- Altenburger P, Kämpfer P, Makristathis A, Lubitz W, Busse H-J.** (1996). Classification of bacteria isolated from a medieval wall painting. *J Biotech* **47**:39–52.
- Andrighetto C, De Dea P, Lombardi A, Neviani E, Rossetti L, Giraffa G.** (1998). Molecular identification and cluster analysis of homofermentative thermophilic lactobacilli isolated from dairy products. *Res Microbiol* **149**:631–643.
- Cashion P, Holder-Franklin MA, McCully J, Franklin M.** (1977). A Rapid Method for the Base Ratio Determination of Bacterial DNA. *Analyt Biochem* **81**:461–466.
- Cotta MA, Whitehead TR, Collins MD, Lawson PA.** (2004). *Atopostipes suicloacale* gen. nov., sp. nov., isolated from an underground swine manure storage pit. *Anaerobe* **10**:191–195.
- Cotta MA, Whitehead TR, Zeltwanger RL.** (2003). Isolation, characterization and comparison of bacteria from swine faeces and manure storage pits. *Environ Microbiol* **5**:737–745.
- Descheemaeker P, Lammens C, Pot B, Vandamme P, Goossens H.** (1997). Evaluation of arbitrarily primed PCR analysis and pulsed-field gel electrophoresis of large genomic DNA fragments for identification of enterococci important in human medicine. *Int J Syst Evol Microbiol* **47**:555–561.
- Feilberg A, Liu D, Adamsen APS, Hansen MJ, Jonassen Ken.** (2010). Odorant emissions from intensive pig production measured by online Proton-Transfer-Reaction Mass Spectrometry. *Environ Sci Technol* **44**:5894–5900.
- Fritze D, and Claus D.** (2009). Genus II. *Caryophanon*. In: de Vos P, Garrity GM, Jones D, Krieg NR, Ludwig W, Rainey FA, Schleifer K-H, Whitman B (eds) *Bergey's Manual of Systematic Bacteriology*, 2nd ed. Vol 3 *The Firmicutes*. pp 354–359.
- Gordon RE.** (1973). The genus *Bacillus* (Agriculture handbook ; no. 427).

Grossman AD, Losick R. (1988). Extracellular control of spore formation in *Bacillus subtilis*. *Proc Natl Acad Sci USA* **85**:4369-4373.

Groth I, Schumann P, Weiss N, Martin K, Rainey FA. (1996). *Agrococcus jenensis* gen. nov., sp. nov., a new genus of actinomycetes with diaminobutyric acid in the cell wall. *Int J of Syst Bacteriol* **46**:234–239.

Hamada M, Yamamura H, Komukai C, Tamura T, Suzuki K-I, Hayakawa M. (2012). *Luteimicrobium album* sp. nov., a novel actinobacterium isolated from a lichen collected in Japan, and emended description of the genus *Luteimicrobium*. *J Antibiotics* **65**:427–431.

Kim O-S, Cho Y-J, Lee K, Yoon S-H, Kim M, Na H, Park S-C, Jeon YS, Lee J-H, Yi H, Won S, Chun J. (2012). Introducing EzTaxon-e: a prokaryotic 16S rRNA gene sequence database with phylotypes that represent uncultured species. *International Journal of Systematic Bacteriology* **62**:716–721.

Kimura M. (1980). A simple method for estimating evolutionary rates of base substitutions through comparative studies of nucleotide sequences. *J Mol Evol* **16**:111–120.

Koransky JR, Allen SD, Dowell Jr VR. (1978). Use of ethanol for selective isolation of sporeforming microorganisms. *Appl Environ Microbiol* **35**:762-765.

Krishnamurthi S, Bhattacharya A, Mayilraj S, NamesforLife, LLC, Saha P, Schumann P, Chakrabarti T. (2009a). Description of *Paenisporosarcina quisquiliarum* gen. nov., sp. nov., and reclassification of *Sporosarcina macmurdoensis* Reddy *et al.* 2003 as *Paenisporosarcina macmurdoensis* comb. nov. *Int J Syst Evol Microbiol* **59**:1364–1370.

Krishnamurthi S, Chakrabarti T, Stackebrandt E. (2009b). Re-examination of the taxonomic position of *Bacillus silvestris* Rheims *et al.* 1999 and proposal to transfer it to *Solibacillus* gen. nov. as *Solibacillus silvestris* comb. nov. *Int J Syst Evol Microbiol* **59**:1054–1058.

Krishnamurthi S, Ruckmani A, Pukall R, Chakrabarti T. (2010). *Psychrobacillus* gen. nov. and proposal for reclassification of *Bacillus insolitus* Larkin & Stokes, 1967, *B. psychrotolerans* Abd-El Rahman *et al.*, 2002 and *B. psychrodurans* Abd-El Rahman *et al.*, 2002 as *Psychrobacillus insolitus* comb. nov., *Psychrobacillus psychrotolerans* comb. nov. and *Psychrobacillus psychrodurans* comb. nov. *Syst Appl Microbiol* **33**:367–373.

Leser TD, Amenuvor JZ, Jensen TK, Lindecrona RH, Boye M, Møller K. (2002). Culture-independent analysis of gut bacteria: the pig gastrointestinal tract microbiota revisited. *Appl Environ Microbiol* **68**:673–690.

- Ludwig W, Schleifer K-H, Whitman B.** (2009). Revised road map to the phylum *Firmicutes*. In: de Vos P, Garrity GM, Jones D, Kreig NR, Rainey FA, Schleifer K-H, Whitman B (eds) *Bergeys Manual of Systematic Bacteriology*. 2nd, Vo. 3, The *Firmicutes*. Springer, pp 1–13.
- Macfarlane, G. T., Hay, S., & Gibson, G. R.** (1989). Influence of mucin on glycosidase, protease and arylamidase activities of human gut bacteria grown in a 3-stage continuous culture system. *Journal of applied bacteriology* **66**(5): 407-417.
- Miller DN, Varel VH.** (2001). In vitro study of the biochemical origin and production limits of odorous compounds in cattle feedlots. *J Animal Scien* **79**:2949–2956.
- Miller LT.** (1982). Single derivatization method for routine analysis of bacterial whole-cell fatty acid methyl esters, including hydroxy acids. *J Clin Microbiol* **16**:584–586.
- Mitani T, Heinze JE, Freese E.** (1977). Induction of sporulation in *Bacillus subtilis* by decoyinine or hadacidin. *Biochem Biophys Res Comm* **77**:1118-1125.
- Mesbah M, Premachandran U, Whitman W.** (1989). Precise measurement of the G+C content of deoxyribonucleic acid by high performance liquid chromatography. *Int J Syst Bact* **39**:159-167.
- Myers EW, Miller W.** (1988). Optimal alignments in linear space. *Comput Appl Biosci* **4**:11–17.
- Ruan Z, Wang Y, Song J, Jiang S, Wang H, Li Y, Zhao B, Jiang R, Bin Zhao.** (2014). *Kurthia huakuii* sp. nov., isolated from biogas slurry, and emended description of the genus *Kurthia*. *Int J Syst Evol Microbiol* **64**:518–521.
- Saitou N, Nei M.** (1987). The neighbor-joining method: a new method for reconstructing phylogenetic trees. *Mol Biol Evol* **4**:406–425.
- Sasser M.** Identification of bacteria by gas chromatography of cellular fatty acids: Technical Note #101.
- Snell-Castro R, Godon J-J, DelgenÃ s J-P, Dabert P.** (2005). Characterisation of the microbial diversity in a pig manure storage pit using small subunit rDNA sequence analysis. *FEMS Microbiology Ecology* **52**:229–242.
- Tamura K, Dudley J, Nei M, Kumar S.** (2007). MEGA4: Molecular Evolutionary Genetics Analysis (MEGA) software version 4.0. *Mol Biol Evol* **24**:1596–1599.
- Tindall BJ.** (1990). Lipid composition of *Halobacterium lacusprofundi*. *FEMS Microbiol Lett* **66**:199–202.

Tindall BJ, Sikorski J, Smibert RA, Krieg NR. (2007). Phenotypic characterization and the principles of comparative systematics. In: Reddy CA, Beveridge TJ, Marzluf GA, Schmidt TM, Synder LR (eds) *Methods for General and Molecular Microbiology*, 3rd ed. ASM Press. pp 330–393.

Vaishampayan P, Miyashita M, Ohnishi A, Satomi M, Rooney A, La Duc MT, Venkateswaran K. (2009). Description of *Rummeliibacillus stabekisii* gen. nov., sp. nov. and reclassification of *Bacillus pycnus* Nakamura *et al.* 2002 as *Rummeliibacillus pycnus* comb. nov. *Int J Syst Evol Microbiol* **59**:1094–1099.

Villedieu A, Diaz-Torres ML, Hunt N, McNab R, Spratt DA, Wilson, M, Mullany P. (2003). Prevalence of tetracycline resistance genes in oral bacteria. *Antimicrob Agents Chemother* **47**:878-882.

Whitehead TR, Cotta MA. (2001a). Characterization and Comparison of Microbial Populations in Swine Faeces and Manure Storage Pits by 16S rDNA Gene Sequence Analyses. *Anaerobe* **7**:181–187.

Whitehead TR, Cotta MA. (2001b). Sequence analyses of a broad host-range plasmid containing *ermT* from a tylosin-resistant *Lactobacillus* sp. isolated from swine feces. *Curr Microbiol* **43**:17-20.

Whitehead TR, Cotta MA. (2013). Stored swine manure and swine faeces as reservoirs of antibiotic resistance genes. *Lett Appl Microbiol* **56**:264–267.

Whitehead TR, Cotta MA. (2004). Isolation and Identification of Hyper-Ammonia Producing Bacteria from Swine Manure Storage Pits. *Curr Microbiol* **48**:1–7.

Whitehead TR, Cotta MA, Collins MD, Falsen E, Lawson PA. (2005). *Bacteroides coprosuis* sp. nov., isolated from swine-manure storage pits. *Int J Syst Evol Microbiol* **55**:2515–2518.

Whitehead TR, Cotta MA, Collins MD, Lawson PA. (2004). *Hespellia stercorisuis* gen. nov., sp. nov. and *Hespellia porcina* sp. nov., isolated from swine manure storage pits. *Int J Syst Evol Microbiol* **54**:241–245.

Whittle G, Whitehead TR, Hamburger N, Shoemaker NB, Cotta MA, Salyers AA. (2003). Identification of a new ribosomal protection type of tetracycline resistance gene, tet(36), from swine manure pits. *Appl Environ Microbiol* **69**:4151–4158.

Chapter 3

***Proteiniphilum alaskensis* sp. nov., isolated from Alaskan petroleum pipeline effluent**

Abstract

Microbially influenced corrosion (MIC) of pipelines and other associated metal infrastructure is a problem that continues to increase as human oil dependency increases. However, little is known about the microbial populations responsible for these corrosive activities. Anaerobic enrichment cultures were constructed with the goal of cultivating and characterizing microorganisms related to MIC. The inoculum was obtained from a pipeline undergoing physical corrosion mitigation (pigging) on the North Slope of Alaska. A number of known and novel members of the *Firmicutes* and *Bacteroidetes* were isolated under strict anaerobic conditions and identified using 16S rRNA gene sequencing. In particular, one Gram-negative staining organism, strain PE-10^T, shared only 93.0% 16S rRNA gene sequence similarity to the closest validated species, *Proteiniphilum acetatigenes* TB107^T, yet represented 11% of the microbial population within the sample. This pipeline sample was enriched in biofilm-associated microorganisms, and contained a 49.2 – fold increase in *Proteiniphilum*-like OTUs compared to bulk fluids. Cells of PE-10^T were non-motile and non-spore-forming, with optimal growth occurring in proteinacious media without NaCl, at pH 7.6, and incubated at 37 °C. The end products identified during growth in pre-reduced Peptone-Yeast Extract (PY) medium were formate and acetate. Predominant fatty acids consisted of anteiso-C15:0 (38.3%) and C16:0 (14.9%).

In addition to phenotypic and phylogenetic characterization, the physical capacity of PE-10^T to cause MIC was investigated using Scanning Electron Microscopy (SEM). While no signals of corrosive activity were observed, PE-10^T formed a recalcitrant biofilm on metal surfaces during anaerobic incubation. Compared to abiotic

controls (and other organisms tested, see Chapter 4), the overall roughness of the metal surface following biofilm removal remained low. On the basis of polyphasic evidence from this study, a new species, *Proteiniphilum alaskensis* sp. nov., was proposed, with strain PE-10^T as the type strain. The cultivation of this novel species was significant because it represents a cultivated molecular signal from which to approach corrosion studies.

Introduction

Mitigation of corrosion in gas and liquid pipelines is expensive both in time and money costing \$7 billion per year, resulting in severe disruptions and delays in fuel delivery (Biezma and San Cristóbal 2005). The scientific community is becoming increasingly aware that reservoir microorganisms can not only degrade hydrocarbons but also actively participate in microbially influenced corrosion (MIC) of pipelines and other associated metal infrastructure (Ropital 2010; Stipanicev, Turcu *et al.* 2014). Little is known about the microbial populations responsible for these activities, which often exist as complex biofilms. Samples of surface associated biofilms likely contain populations that play a role in biocorrosion, whether by acid production, metabolically driven electron transfer, or by acting as primary colonizers and facilitating the recruitment of others (Lloyd, Mabbett *et al.* 2001; Purish, Koptieva *et al.* 2006; Vu, Chen *et al.* 2009). Biofilms are thought to be particularly harmful to pipeline integrity due to their metabolic proximity to the metallic infrastructure and increased resistance to mitigation practices such as the use of biocides and PIGs (pipeline inspection gauges) (Sheng, Ting *et al.* 2008). Biocide refers to the chemical control of microbial growth, while pigging efforts include specialized devices that physically remove accumulated material as they run the interior length of a pipeline. The effluent resulting from the physical removal of pipeline build-up is known as the PIG envelope, and contains many particulates such as scraped biomass and pipeline scalings (corrosion products). As such, it has been hypothesized that the microbial community within these biofilms may be associated with biocorrosive activities (Zuo 2007; Melo, Urtiga Filho *et al.* 2011).

Therefore, in addition to being of taxonomic importance, the cultivation of these resident microbes is pivotal to understanding the mechanisms involved in biocorrosion.

Currently, there exists only one validated species of *Proteiniphilum*, *P. acetatigenes* TB107^T, which was isolated from the granule sludge of an upflow anaerobic sludge blanket reactor treating brewery wastewater (Chen and Dong 2005). While not much is known about this genus, *P. acetatigenes* TB107^T was shown to produce acetic and propionic acid from the fermentation of yeast extract, peptone, pyruvate, and L-arginine. From the scope of a complex community, these two metabolic products may also act as substrates, providing carbon and energy sources to other members of a bacterial population. Otherwise, the role of *P. acetatigenes* TB107^T in brewery wastewater treatment remains unknown.

Recently, however, two strains (MH5 and MH1) of an additional *Proteiniphilum* species were recovered from oil tars of the Shengli oil field, China (Biogas Institute of Ministry of Agriculture, Sichuan University). MH5 and MH1 were isolated from a hexadecane-degrading methanogenic enrichment inoculated with contaminated soil (unpublished). While no studies have been reported on their isolation or subsequent characterization, the presence of MH5 and MH1 within geographically distinct oil-field sites may help shed light onto *Proteiniphilum*'s ecological role.

Cultivation-based characterization of these microorganisms is an important step in understanding the metabolic capabilities and potentially corrosive mechanisms of the microbial communities in these unique, extreme ecosystems. The knowledge gained through these studies could lead to better mitigation strategies to combat deleterious microbial processes.

Materials and Methods

Bacterial strains and culture conditions

PE-10^T was isolated in a basal medium, amended with 1% peptone and 5 mM benzoate, from a PIG envelope sample collected from a produced water line off the North Slope of Alaska, USA. Samples were collected anaerobically by University of Oklahoma researchers and shipped to associated laboratories for culture- dependent and -independent analyses. Upon receipt of this sample, anaerobic enrichments were constructed with the goal of cultivating and characterizing microorganisms related to MIC. Specifically, a pure culture of PE-10^T was obtained via serial dilutions in anaerobic tubes sealed with butyl rubber stoppers under a gaseous atmosphere of 80:20 N₂:CO₂ (10psi) at 37 °C. Purity was checked by plating on general anaerobic agar (Difco) supplemented with 0.1% hemin, whereupon isolated colonies were examined microscopically. The basal medium contained the following constituents at the indicated final concentrations in percent (v/v): Pfennig's mineral solution I, 5.0; Pfennig's mineral solution II, 5.0; Wolin's Trace metal solution, 0.5; Balch vitamin solution, 1.0; resazurin, 0.0001 (w/v); NaHCO₃ solution, 7.0; 1.25% cysteine-HCl – 1.25% Na₂S·9H₂O solution, 2.0. It was prepared under an 80% N₂: 20% CO₂ gas phase and autoclaved at 121 °C for 20 minutes. The NaHCO₃ solution was added to the cooled sterile medium, which was then dispensed in 9.0 ml aliquots into 18 x 150 mm culture tubes, sealed, and sterilized. Media was reduced with the cysteine sulfide one day prior to inoculation. 1.0 mL inoculations were used for serial dilutions and routine transfers, where the headspace was exchanged with 100% N₂. Following repeated transfers, isolate PE-10^T no longer grew well on this basal medium, therefore all

subsequent characterization and routine cultivation was carried out in Peptone-Yeast medium (PY).

Morphological, physiological, and biochemical characterization

The morphology of colonies was observed on PY agar incubated anaerobically for 7 days at 37 °C. Gram staining was performed using the BD Gram Stain Kit (Sigma, St. Louis, IL), according to the manufacturer's instructions. Cell morphology and motility was assessed using phase contrast microscopy with an Olympus DP12 microscope. Spore formation was tested using malachite green staining and steam to induce sporulation, followed by safranin counterstain. Further characterization of strain PE-10^T was performed using hungate tubes containing anoxic PY medium (Holdeman *et al.*, 1975) supplemented with 0.1% cysteine sulfide. First, the cardinal growth parameters were determined for temperature, pH, and salinity ranges. The conditions tested included temperatures 4, 10, 15, 20, 25, 30, 37, 43, 47, and 60 °C; pH values 5.0, 5.5, 6.0, 6.5, 7.0, 7.3, 7.8, 8.0, 8.5, 9.0; and NaCl concentrations of 0%, 0.5%, 1%, 2%, 3%, 4%, 5%, 6%, 7%, 8%, and 9%. The pH range was adjusted with several buffers (0.1 M final concentration): sodium acetate buffer for pH 5.0-6.0, potassium phosphate buffer for pH 7.0-8.0, and Tris/HCl buffer for pH 8.5 and 9.0. Optimum growth conditions were determined spectrophotometrically at 600 nm (Spectronic 20D, Milton Roy). All tests were performed in duplicate.

Next, substrate utilization was determined using a basal medium amended with 20 mM (final concentration) of the following: glucose, sucrose, arabinose, cellobiose, maltose, mannose, fructose, melibiose, ribose, xylose, lactate, crotonate, methanol,

starch, and yeast extract. The basal medium consisted of (g/L): NH_4Cl , 1.0; K_2HPO_4 , 0.3; KH_2PO_4 , 0.3; NaCl , 0.6; $\text{CaCl}_2 \cdot 2\text{H}_2\text{O}$, 0.1; MgCl_2 , 0.2; KCl , 0.1; and resazurin, 0.0001. Tubes were incubated for 14 days at 37 °C then measured spectrophotometrically for growth. The isolate was considered able to utilize a substrate if it resulted in a significant increase in optical density compared to abiotic controls ($n = 3$). Carbohydrate utilization was confirmed using API CH50 according to manufacturer's instructions (bioMérieux, Marcy L'Etoile, France).

In order to further assess the organism's dependency on yeast extract, anaerobic PY medium was made with varying concentrations of yeast extract. Typically, PY contains 1.05% yeast extract, therefore, the range of 1.0, 0.8, 0.6, 0.4, 0.2, 0.1, 0.01 and 0.0% yeast extract was tested. Tubes were incubated for 14 days at 37 °C then measured spectrophotometrically for growth.

Finally, the production of short chain volatile fatty acids was examined following the methods mentioned in previous chapters. Cells were grown at 37 °C in PY and PYG (20mM glucose amended post sterilization from a sterile anoxic stock solution) media under strict anaerobic conditions, with cysteine sulfide used as the reducing agent. Following 14 days of incubation, 1.0 mL was removed from triplicate tubes and centrifuged in order to pellet cells. The supernatants were transferred into glass vials and stored at -20 °C until analysis, whereupon a 1: 20 dilution was treated with Dowex before HPLC injection. Metabolic end products were determined by HPLC using an Aminex HPX-87H column (4.6 x 250 mm, 5 μm particle size) and a mobile phase of 0.015 N HCL. The expected end product retention times were correlated with standards to determine the presence of end products.

Determination of the 16S rRNA gene sequence and phylogenetic analysis

For phylogenetic analysis, cells were grown in PY for 5 days and biomass was collected by centrifugation. Genomic DNA was extracted using phenol chloroform and precipitated with ethanol as detailed in Chapter 1 (Lawson *et al.*, 1989). The quantity of DNA was evaluated by gel electrophoresis using known concentrations of lambda DNA for comparison. Undiluted DNA was then used as a template for PCR with universal primers 8F and 1492R. Thermocycler conditions were the same as mentioned previously. After PCR amplification, products were visualized via gel electrophoresis and processed with ExoSap-It (Affymetrix, Inc.) to eliminate unincorporated nucleotides. Amplicons were then sent to The University of Oklahoma's Zoology Core Molecular Laboratory for sequencing using the suite of primers mentioned in Chapter 1. In order to ascertain the taxonomic position of the isolate, the manually concatenated 16S rRNA gene sequence of PE-10^T was compared to the most similar sequences retrieved from database searches using the program FASTA (Lipman and Pearson, 1985). Sequences of closely related taxa were selected for pairwise sequence similarity calculations using a global alignment algorithm with the program, ClustalW (Thompson *et al.*, 1994). A phylogenetic tree was constructed using the neighbor-joining method of Saitou and Nei (1987) from evolutionary distances computed using the two-parameter model of Kimura (1980). The topology of the phylogenetic tree was evaluated by bootstrap analysis using 1,000 replicates (Felsenstein, 1985).

Chemotaxonomic characterization

Cellular fatty acid profiles of strain PE-10^T were analyzed using the Sherlock Microbial Identification system (MIDI) as described by Sasser (1990). Cells were cultured anaerobically on PY agar at 37 °C for 3 days and then harvested from the third quadrant. As mentioned previously, fatty acids extracts were obtained using a series of ammonia, sulfuric acid/methanol, and hexane treatments and analyzed by GC (Aligent 6890N).

Assessment of Corrosion potential

A microscopy approach at investigating biocorrosive characteristics was employed. Two biological replicates of PE-10^T monocultures were inoculated into separate tubes containing carbon steel coupons in reduced anaerobic media. In order to examine surface-association, SEM was used to visualize the formation of biofilms after two weeks incubation at 37 °C. Two separate tubes were also investigated once the organisms had been removed to look for evidence of corrosion on the coupon surface. Cells were removed by sonication in soapy water followed by acid immersion for ten minutes. The acid solution consisted of 500 mL concentrated HCl, 500 mL DiH₂O, and 3.5 g hexamethylene tetramine. Coupons were rinsed with DiH₂O, acetone, then methanol, and finally blow-dried with nitrogen (ASTM Standard G1-03). Using duplicate samples of abiotic controls, chemical corrosion was assessed in order to see the latent effects of an aqueous environment. Secondary and backscattered images were taken to visualize biofilm features and sample topography (Zeiss DSM-960). Coupons were visualized by magnification of one random site each to show relative

compositional differences based off atomic number and to provide the template images with which to calculate surface roughness. For this purpose, stereo image pairs were taken at 20 kV on a $\pm 5^\circ$ tilt, digitally stacked, and analyzed for quantitative height reconstruction (Scandium Solution Height, Olympus). Line scans were also performed to generate height profiles, which showed feature size and thickness. These SEM tools were used to visualize biofilm localization, monitor topographical changes on metal surfaces, and ultimately to assess the corrosive capacity of PE-10^T.

Results

Morphological, physiological, and biochemical characteristics

Cells of strain PE-10^T were short to long rods depending on growth conditions and usually occurred singly or paired end-to-end. Single pinpoint colonies formed on PY agar after 4 to 5 days incubation at 37 °C. PE-10^T was a Gram-stain negative obligate anaerobe. Microaerophilic and aerobic growth did not occur. Growth was seen from 18 to 70 °C with a 37 °C optimum, at pH ranging of 6.0 to 8.8 with a 7.6 optimum, and in 0% to 2% NaCl with 0% optimum. Cultures of PE-10^T grown in anoxic PY broth (pH 7.6, 0% NaCl) at 37 °C have a doubling time of 25.1 hours. PE-10^T grew with 100% N₂ headspace, and did not require H₂ or CO₂. Yeast extract could not be used as a sole carbon substrate. In fact, no other carbohydrates or short chain fatty acids tested were shown to support growth; these included glucose, fructose, ribose, xylose, lactate, starch, sucrose, maltose, rhamnose, cellobiose, crotonate, yeast extract, mannose, arabinose, melibiose, raffinose, acetate, methanol. No methane was produced.

Determination of the 16S rRNA gene sequence and phylogenetic analysis

The 16S ribosomal RNA gene of strain PE-10^T was amplified by PCR and sequenced. Five overlapping contigs were concatenated, yielding the FASTA sequence seen in Figure 3.1. This nearly full nucleotide sequence was then used to identify the taxonomic neighbors of strain PE-10^T through NCBI sequence database comparisons. The most closely related 16S rRNA sequence belonged to *Proteiniphilum acetatigenes* strain TB107^T, sharing 93.0% similarity with 98% query coverage and a 0.0 E value (Fig. 3.2).

Figure 3.1: The complete 16S rRNA gene sequence of *Proteiniphilum alaskensis* strain PE-10^T.

```

>PE-10
CTATCGGTACGATNTCAGGNACCCCCGGCTCCCATGGCTTGACGGGCGGTGNNNNCAAGGCCNNGGAACGTATTCACCG
CGCCGTGGCTGATGCGCGATTACTAGCGAATCCAGCTTCACGGAGTCGAGTTGCAGACTCCGATCCGAACCTGAGAGTGG
TTTTGGAGATTAGCATCCTGTCGCCAGGTAGCTGCCCTTTGTACCACCCATTGTAACACGTGTGTCGCCCCGGACGTAA
GGGCCnGTGCTGATTTGACGTATCCCCACCTTCCCTCGCATCTTACGATGGCAGTCTCGCCAGAGTCCCAGCTTTACC
TGATGGTAACTGACGATGAGGGTTGCGCTCGTTATGGCACTTAAGCCGACACCTCACGGCACGAGCTGACGACaACCAT
GCAGCACCTACACATCTGCCCCGTAGGGAATATCCGTTTCCGAATACGTCAGATGCATTTCAAGCCCCGGTAAGGTTCC
TCGCGTATCATCGAATTAACCACATGTTCCCTCCGCTTGTCGGGCCCCCGTCAATTCCTTTGAGTTTCATTCTTGCGA
ACGTACTCCCAGGTGGATTACTTAACGCTTTCGCTCAGCCGCTTACATTGTATCGCAAACAGCCAGTAATCATCGTTT
ACTGCGTGGACTACCAGGGTATCTAATCCTGTTTGATCCCCACGCTTCGTCATGAGCGTCAGTTATGGTTTAGTAAG
CTGCCTGCGCAATCGGTGTTCTTTGTGATATCTATGCATTTACCGCTACACCACAAATTCGCTACTTCATCCACAC
TCAAGCTTGCCAGTTTCGAAGGCTCTTTACAGTTGAGCTGCAAAATTTACCGCCGACTTAACATGCCGCTGCGCAC
CCTTTAAACCCAATAAATCCGGATAACGCTCGGATCCTCCGATTACCGCGGCTGCTGGCACGGAGTTAGCCGATCCTT
ATTCGTAAGGTACCTGCAACGTCTTAGCGCGTAAGACTATTTATCCCTTACAAAAGAAGTTTACAACCCGTAGGGCCG
TCTTCCCTTACGCGACTTGCTGGTTCAGACTCTCGTCCATTGACCAATATTCCTCACTGCTGCCTCCCCTAGGAGTCT
GGACCGTGTCTCAGTTCAGTGTGGGGGATCaCCCTCAGTTCCCcTATCCATCGTTGCCTTGGTGAGCCGTTACCTC
ACCAACAAGCTAATGGAACGCATGCCCATCTACTACCGATAAATCTTTAACAAATATATCCATGCGGATCCCCTGTGTT
ATAGGGTATTAGTCCGCTTTCAACGGGTTATCCCTTGTAGTAGGCAGGTTGCATACCGGTTACTCACCCGTGCGCCG
GTCGCCACCCGTGATTGCTACACCGTGTGCCCTCGACTTGCATGTGTTAGGCCTGTGCTAGCGTTCATCCTGAGC
CAGGATCAAACCTCTAGNGN

```

Figure 3.2: Pairwise alignment of the 16S rRNA gene sequences between *Proteiniphilum alaskensis* strain PE-10^T (query) and the nearest cultivated neighbor, *Proteiniphilum acetatigenes* strain TB107 (subject), showing 93.0% sequence similarity. 98% query coverage; 0.0 E value; 1523 bp sequence length.

```

TCAGGNACCCCCGGCTCCCATGGCTTGACGGGCGGTGNNNNCAAGGCCNNGGAACGTATT Query
||||| ||||| ||||| ||||| ||||| ||||| ||||| ||||| ||||| ||||| Sbjct
TCAGGCACCCCCAGCTTCCATGGCTTGACGGGCGGTGTGTACAAGGCCGGGAACGTATT
CACCGCGCGTGGCTGATGCGCGATTACTAGCGAATCCAGCTTCACGGAGTCGAGTTGCA
||||| ||||| ||||| ||||| ||||| ||||| ||||| ||||| ||||| |||||
CACCGCGCGTGGCTGATGCGCGATTACTAGCGAATCCAGCTTCACGGAGTCGAGTTGCA
GACTCCGATCCGAACCTGAGAGTGGTTTTGGAGATTAGCATCCTGTGCGCCAGGTAGCTGCC
||||| ||||| ||||| ||||| ||||| ||||| ||||| ||||| ||||| |||||
GACTCCGATCCGAACCTGAGAGTGGTTTTGGAGATTGGCATCATGTGCCATGTAGCTGCC
CTTTGTACCACCCATTGTAACACGTGTGTCGCCCCGGACGTAAGGGCCNGTGCTGATTTG
||||| ||||| ||||| ||||| ||||| ||||| ||||| ||||| ||||| |||||
CTTTGTACCACCCATTGTAACACGTGTGTCGCCCCGGACGTAAGGGCC-GTGCTGATTTG

```


The neighbor-joining tree shown in Figure 3.3 revealed that PE-10^T was affiliated with the Cytophaga- Flavobacterium- Bacteroides (CFB) group, and clustered firmly within the Bacteroidetes. Isolate PE-10^T was most closely related to *Proteiniphilum acetatigenes*, and clearly represented a novel species with greater than 3% 16S rRNA gene sequence divergence. Additionally, pyrosequencing of the PIG envelope community revealed that a tight phylogenetic relationship existed between PE-10 and a number of OTUs, including the *P. acetatigenes* type strain (Fig. 3.4).

Figure 3.3: Phylogenetic tree showing the relationship between members of *Proteiniphilum* and related taxa. The tree was constructed using the neighbor-joining methods based on 16S rRNA gene sequences. The numbers at node sites represent bootstrap values of 1000 replicates. Bar, 2.5 % range of sequence divergence over a 1300 nucleotide sequence. Genbank accession numbers are given in parentheses.

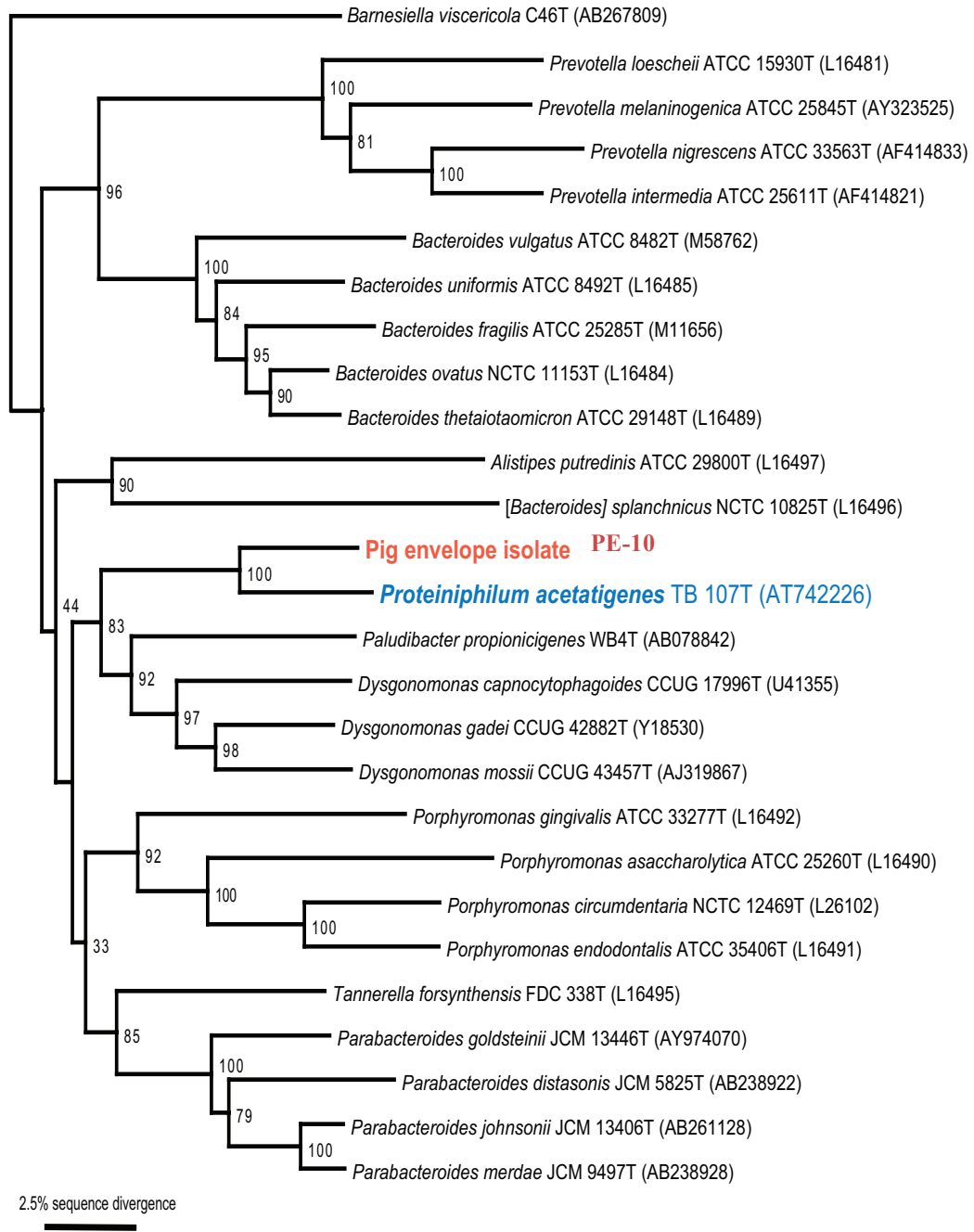
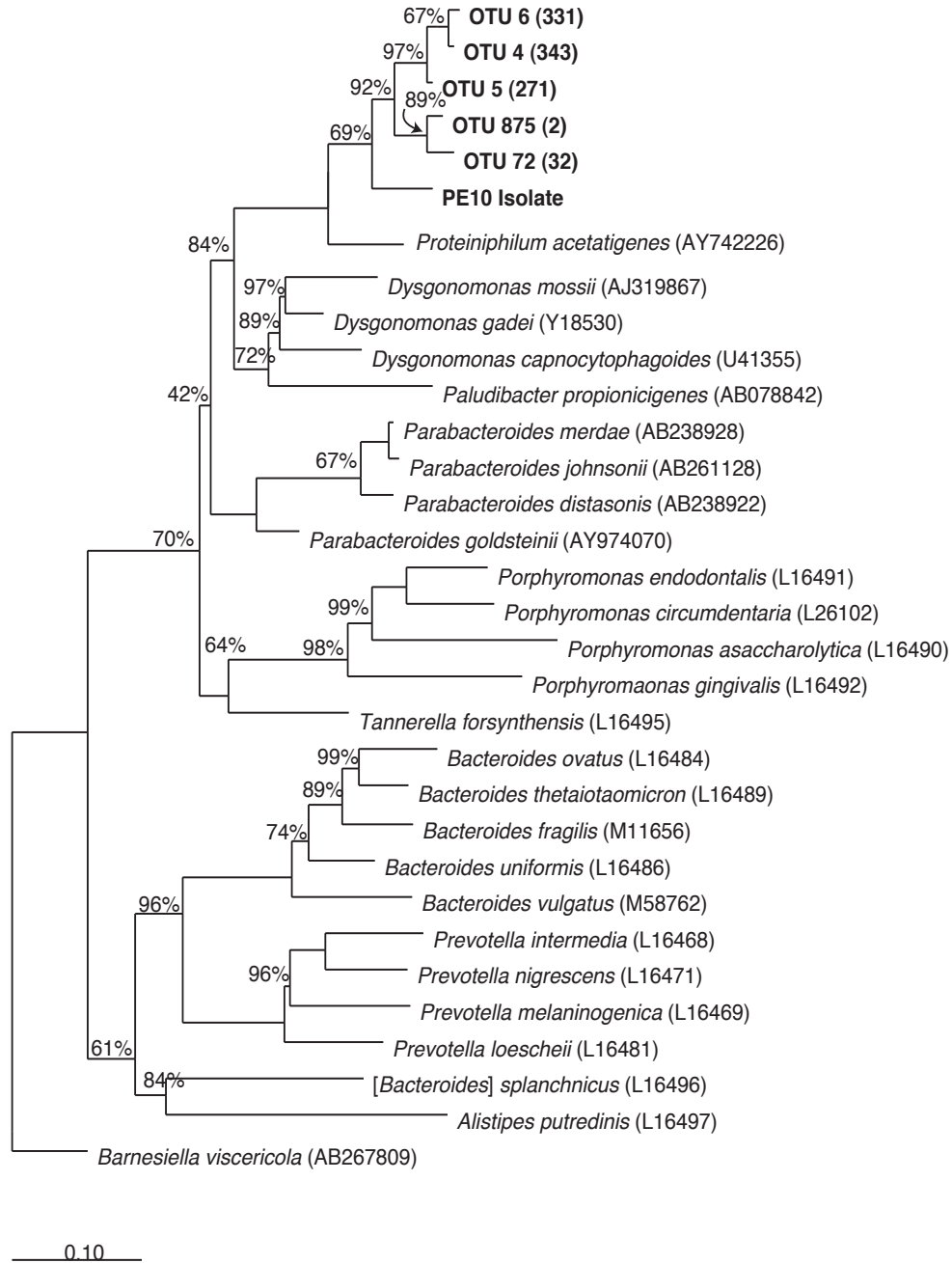


Figure 3.4: Phylogenetic analysis of a number of type strains, in addition to 16S rRNA sequence of PE-10^T and the OTUs obtained from the 454 pyrosequencing data. The numbers at node sites represent bootstrap values of 1000 replicates. Bar, 0.1 substitutions per nucleotide position. Genbank accession numbers given in parentheses.



The PIG biofilm was investigated through 454 pyrosequencing of 16S rRNA genes and found to contain a number of organisms belonging to the phylum Bacteroidetes. The PIG community had significantly higher abundances for Bacteroidetes, particularly the genera *Thermacetogenium* and *Proteiniphilum*. Within the Bacteroidetes, relevant *Proteiniphilum*-like organisms were represented by sequences unique to the PIG. Alternative samples, such as bulk production water, seawater, and injection well fluids lacked molecular signals for *Proteiniphilum*. Therefore, the bacterial community composition throughout the petroleum production facility revealed a greater relative abundance of *Proteiniphilum* in non-planktonic locations.

Chemotaxonomic characteristics

The results of fatty acid methyl ester analysis for strain PE-10^T and the type strains of closely related organisms have been listed in Table 3.1. Major fatty acids were identified as anteiso-C15:0 and C16:0, constituting 38.3% and 14.9% of the total lipids, respectively. Less predominant fatty acids included C15:0 (5.2%), iso-C16:0 3-OH (2.6%), iso-C15:0 (1.8%), and iso-C14:0 (1.8%). The fatty acid profiles of phylogenetic relatives were similar, with anteiso-C15:0 expression consistently highest followed by variable ratios of minor constituents.

Characterization of PE-10^T and comparisons between this novel strain, the closest cultivated and described species, *Proteiniphilum acetatigenes* TB107^T, and the nonvalidated *Proteiniphilum*-like strain MH5, are listed in Table 3.2. Based on the

results of the above phylogenetic and phenotypic analyses, it was proposed that strain PE-10^T be validated as a novel species, *Proteiniphilum alaskensis* sp. nov.

Table 3.1: Comparison of the cellular fatty acid compositions (% of total identified) of *Proteiniphilum alaskensis* sp. nov. PE-10^T and its phylogenetic relatives. Species: 1, PE-10^T; 2, *Proteiniphilum acetatigenes* TB107^T; 3, *Dysgonomonas capnocytophagoides* CCUG 17996^T; 4, *Dysgonomonas gadei* CCUG 42882^T; 5, *Tannerella forsythensis* FDC 338^T; 6, *Bacteroides distasonis* ATCC 8503^T; 7, *Bacteroides merdae* ATCC 43184^T. ND, Not detected; tr, trace.

Fatty Acids	1*	2	3	4	5	6	7
anteiso-C15:0	38.34	46.21	19.4-19.6	23.9	43.5-57.6	35.8	40.1
C15:0	5.16	8.9	11.3-14.2	2.9	tr to <1%	1.7	0.6
iso-C17:0 3-OH	ND	5.93	3.3-3.5	ND	6.4-17.7	19.2	23.5
C16:0	14.86	4.12	3.4-3.6	15.2	4.6-9.4	10.4	3.9
iso-C15:0	1.78	3.77	2.2-2.7	4.0	0.6-2.1	8.8	6.4
iso-C16:0 3-OH	2.64	1.96	9.3-12.3	10.5	<1%	ND	tr
iso-C14:0	1.81	0.97	12.3-19.8	12.9	tr	ND	tr
C16:0 3-OH	ND	0.59	4.6-5.3	7.9	14.4-20.6	7.5	5.6

* data generated from this study

data for strains 2-7 obtained from Chen, S. & Dong, X. (2005).

Table 3.2: Characteristics comparison of strain PE-10^T, type strain of *Proteiniphilum acetatigenes*, and strain MH5.

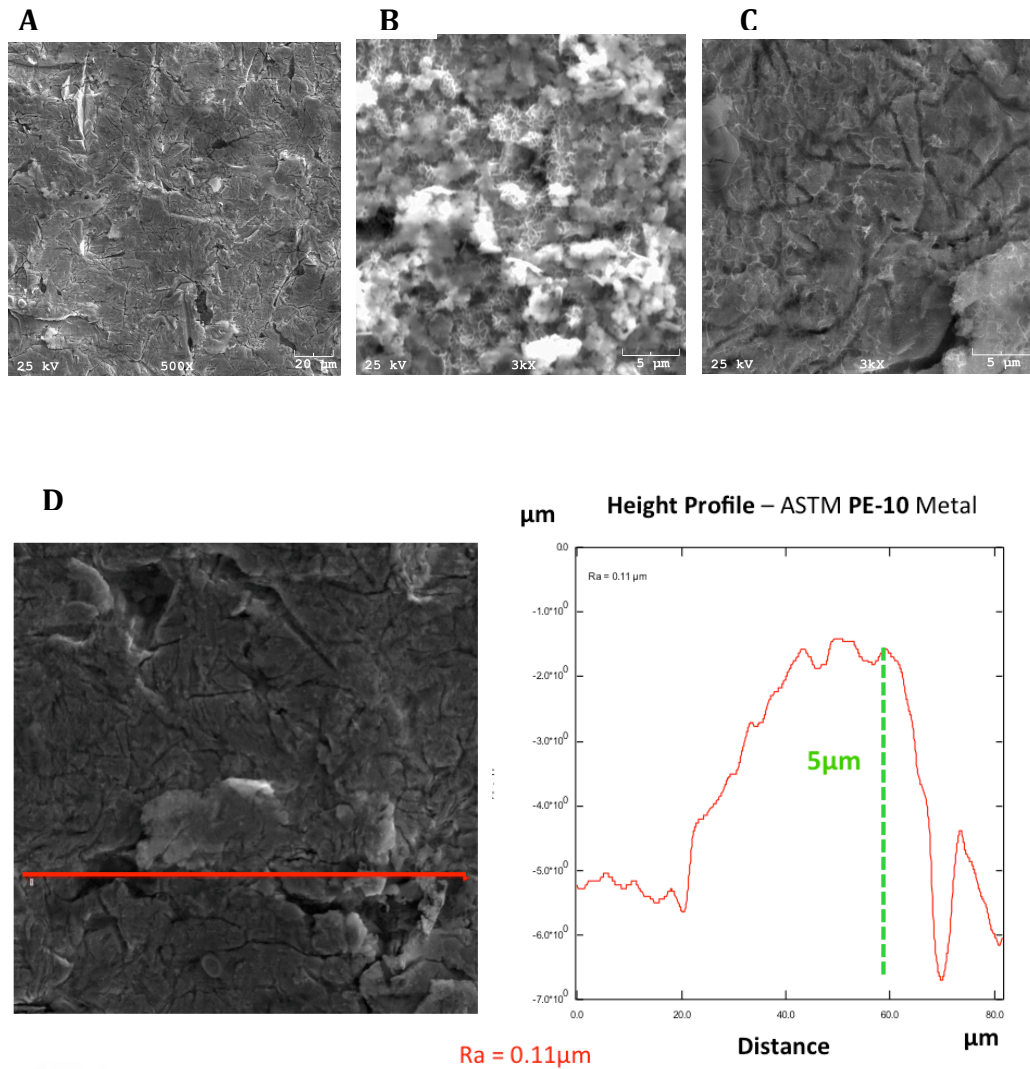
Characteristics	PE-10 ^T	TB107 ^T	MH5
Isolated from:	Produced water pipeline effluent	Brewery wastewater	Crude oil contaminated soil
Gram staining	G-	G-	G-
Cell Morphology	Rod-shaped, pleomorphic to round bodies	Rod-shaped	Irregular coccoid-shaped
Cell size	(0.4-0.9) x (0.8–4.0) μm	(0.6-0.9) × (1.9-2.2) μm	0.35-0.85 μm
Motility	Non-motile	Motile	Non-motile
Flagella	-	Peritrichous	-
Temp range (optimum °C)	20-65 (37)	20–45 (37)	20-65 (35)
pH range (optimum)	5.0-9.5 (7.5)	6.0–9.7 (7.5–8.0)	4.5-10 (7.5)
Toleration of (%w/v)	0-2.0	0–5	0-2.0 (0)
Doubling time under optimal condition/ hr	20.1	11.2	16.5
DNA G+C content (mol%)	48.2	46.6	53.7
Major cellular fatty acids	anteiso-C ₁₅ : 0 (38.34 %), C ₁₅ : 0 (5.16 %), iso-C ₁₆ :0 (12.49%), C ₁₆ :0 (14.86%), anteiso-C ₁₇ : 0 (11.45%)	anteiso-C ₁₅ : 0 (46.21 %), C ₁₅ : 0 (8.90 %), iso-C ₁₇ : 0 3-OH (5.93 %)	anteiso-C ₁₅ : 0 (40.79 %), C ₁₇ : 0 2-OH (5.93 %), (8.92%)
Major products from yeast extract	Formate, acetate	Acetate	Not determined
Carbon and energy sources	Growth: yeast extract and peptone, tryptone No growth: Carbohydrates	Growth: yeast extract and peptone, pyruvate, glycine and L-arginine; Weak growth: tryptone, L-serine, L-threonine and L-alanine; No growth: cellobiose, xylan,	Growth: cellobiose, tryptone, ethanol, xylan, salicylic acid, D- lactose, L- arabinose, gelatin, amylopectin and soluble starch; Weak growth:

<p>L-histidine, L-leucine, L-lysine, L-methionine, L- phenylalanine, L- valine, L- glutamine, tryptophan, L- tyrosine, L- isoleucine, L- proline, L- aspartate, L- cysteine, L- arabinose, aesculin, D-fructose, D- galactose, D- glucose, glycogen, inulin, D-lactose, D-maltose, mannose, melibiose, raffinose, rhamnose, ribose, sucrose, salicin, sorbose, starch, trehalose, D-xylose, adonitol, amygdalin, dulcitol, erythritol, inositol, mannitol, sorbitol, ribitol, methanol, ethanol, 1- propanol, citrate, fumarate, malate, succinate, malonate, hippurate, sodium gluconate, butane diacid, <i>b</i>- hydroxybutyric acid, phenylacetic acid and cellulose</p>	<p>Trehalose, D- glucose, sodium pyruvate, D- fructose and sorbitolum No growth: peptone, Sucrose, Sodium acetate, Sodium butyrate, L- sorbose, mannitol, cellulose, raffinose, maltose, glycerin, L- rhamnose, glycogen, L- Gly, L-Glu, L- Ala, L-Tyr, peptone, palmitic acid and citric acid</p>
--	--

Assessment of Corrosion potential

The genus *Proteiniphilum* was unique to the PIG sample, and in order to determine the role of PE-10^T within the pipeline, corrosion studies were performed. As seen in Figure 3.6 (A & B), SEM revealed the nature of metal topography after incubation with media-only (abiotic control) and PE-10^T. It was clear that coupon surfaces lent themselves to be colonized by PE-10^T cells, producing amorphous by-products that were presumed to be exopolysaccharidic material. The coupon-washing procedure failed to remove all evidence of the PE-10^T biofilm, as the same colonized-coupon was shown to still contain a cellular network on the metal surface after washing (Fig. 3.6, C). Previous experiments had not shown any residual biomass left after the wash procedure for any other organisms tested (data not shown). Using Scandium software, surface roughness profiles were obtained from a random area, which show a maximum/ minimum height difference of 5.0 μm , and an overall roughness calculation of 0.11 μm (Fig. 3.6, D)

Figure 3.5: Carbon steel coupons imaged with SEM at 25 kV. Medium-only control (A), PE-10^T surface biofilm (B), and PE-10^T following biofilm removal (C). Scandium-generated line scan of PE-10^T incubated coupon after ASTM cleaning revealing surface roughness (D).



Description of Proteiniphilum alaskensis sp. nov.

N.L. neut. n. *proteinum*, protein; N.L. adj. *philus -a -um* (from Gr. adj. *philos -ê -on*), friend, loving; N.L. neut. n. *Proteiniphilum*, protein loving. al.ask.en'sis. N.L. masc. adj. *alaskensis* from Alaska, referring to the place of isolation.

P. alaskensis strain PE-10^T stained Gram-negative and appeared rod-shaped. Cells were non-motile, non-spore-forming, and obligately anaerobic. Microaerophilic and aerobic growth did not occur. The length of rods was highly variable, with cells occasionally growing up to 4 µm for days at a time. Proteoplasts were also observed, where cells shrank in size and appeared coccus-shaped. Cells ranged from 0.4 x 0.8 µm to 0.6 x 4.0 µm, depending on growth phase, where log phase growth yielded longer rods and late stationary phase induced a pleomorphic transition to small reticulate bodies. Colonies on PY agar were a translucent-white, and appeared smooth, circular, entire, and very small. Optimum growth temperature, pH, and NaCl concentration of *P. alaskensis* were 47 °C, pH 7.5, and 0 g/L, respectively. The major end products of growth in PY were formate and acetate. Other end products included crotonate, methylsuccinate, butyrate, pyruvate, propionate, and lactate. Major fatty acids consisted of anteiso-C15:0 (38.3%) and C16:0 (14.9%). The genomic DNA G+C content was 48.2 mol%.

P. alaskensis represented a genetically divergent species, sharing 94% 16S rRNA sequence similarity to the nearest neighbor, *P. acetatigenes* TB107^T. Phenotypic and phylogenetic differences indicated that strain PE-10^T was distinct from the only other *Proteiniphilum* species, *P. acetatigenes* TB107^T. It was therefore proposed that strain

PE-10^T be classified as the type strain of a novel species within the genus *Proteiniphilum*, per the name *Proteiniphilum alaskensis* sp. nov.

Discussion

The recovery of previously uncultured bacteria allows researchers to explore the physiological and biochemical potential of microorganisms, which may have consequences far beyond the laboratory. Comparisons of distinguishing biomarkers, including descriptions of biochemical activities, aid in the assignment of phylogeny and help evaluate the general ecological role and environmental impact of pure culture isolates.

The isolation of strain PE-10^T represented the second validly described species within the genus *Proteiniphilum* and was significant because a cultivated molecular signal was now available with which to carry out corrosion studies. Having only one validated species of *Proteiniphilum*, *P. acetatigenes* TB107^T, provided very little context with regard to the role of this genus in the pipeline environment. Simultaneous to this study, however, two additional strains were recovered from oil tars of the Shengli oil field, China (Biogas Institute of Ministry of Agriculture, Sichuan University). The 16S rRNA gene sequences of these two strains, MH5 and MH1, were nearly identical (>99% sequence similarity) to *Proteiniphilum alaskensis* strain PE-10^T. MH5 and MH1 were isolated from a hexadecane-degrading methanogenic enrichment from a similar environment, implicating a potential unknown eco-physiological role in petroleum

production. For this reason, it is particularly interesting to have potentially linked its presence to another geographically distinct oil field.

Pyrosequencing data of the same Alaskan oil field sample showed that *Proteiniphilum*-like organisms represented a dominant fraction (up to 11%) of the microbial population (Stevenson *et. al*, 2011). The PIG community had significantly higher abundances for Bacteroidetes (16.9), specifically *Proteiniphilum* (49.2 -fold), compared to other field sites. According to 454 and qPCR data, the PIG sample had 4 to 6 orders of magnitude more cells than bulk fluids (Nunn, personal communication). This suggested that the PIG was likely to be an enrichment of surface associated organisms, not surprising given the nature of the sample. Furthermore, Figure 4.4 showed a tight phylogenetic relationship between PE-10^T and a number of OTUs from this PIG envelope sample, including the *Proteiniphilum acetatigenes* type strain. Within context of the oil production facility, *Proteiniphilum* was unique to the PIG sample, suggesting that PE-10^T may be involved in biofilm formation. SEM images showed that PE-10^T was indeed capable of colonizing the surface of carbon steel, and that the cellular network was difficult to remove with normal coupon-cleaning procedures. In laboratory studies, PE-10^T grew by fermenting proteins supplied in the medium. In its natural environment, the lysis of bacterial cells likely acts as a surrogate for proteinacious material. High protein content can also be found within EPS, another possible connection to biofilm activity. Topographical measurements of coupon roughness for PE-10^T incubated coupons were the same as abiotic control measurements (no statistical difference $p > 0.05$, $n=3$), suggesting that PE-10^T did not confer a biocorrosive risk to pipeline integrity.

It should be noted, however, that the abundance of *Proteiniphilum* within this sample may be an artifact of insufficient transportation and storage conditions. A consideration was made that mesophilic organisms could have grown during transit had refrigerated temperatures not been properly maintained. The integrity of the PIG sample handling was called into question once molecular and cultivation independent studies had been carried out. Therefore, the interpretation of relative abundance may represent a bloom of organisms whose growth conditions were enriched for during sample transport.

While taxonomic implications may not be important to industry, physiological properties associated with these particular organisms are fundamental in understanding the mechanisms of biocorrosion. Although important, it is not enough to simply identify the resident microflora using molecular methods to demonstrate the biodiversity of microbial communities. Rather, the physiological properties of the organisms present in the pipeline must be examined. Where a census of community composition offers an overall picture, it does not provide researchers with insight as to the metabolic capabilities of the assemblage, and therefore leaves an essential piece of the puzzle missing. Ultimately, the development of mitigation strategies depends on the characterization of these bacterial end products of metabolism in concert with physiological contributions such as biofilm formation. Additionally, involvement of other corrosive activities such as electrochemical interactions must be investigated more fully. As preliminary data confirms, there exists a wealth of taxonomic information to be discovered through the cultivation of organisms from corroded oil pipelines. However, this data also necessitates looking beyond the notion that key players have

already been identified based on their dominant existence. In future investigations, molecular data will be used as a “road-map” to selectively enrich for particular microbial targets, and microcosms of complex bacterial communities will be constructed to test the biocorrosive efficacy of key players with the ultimate goal being the chemical removal, control, or competitive inhibition of particularly important organisms involved in MIC. In conclusion, the cultivation of previously unknown organisms, particularly the isolation of *P. alaskensis* sp. nov. strain PE-10^T, provides new resources for the microbial library of pipeline colonization. Ultimately, the characterization of such cultivars increases the understanding of reservoir microflora composition, and may lead to better control of biocorrosive processes.

Acknowledgements

The authors would like to thank Heather Nunn for her molecular contributions to this effort, specifically in the generation of Figure 3.4. Pyrosequencing data provided an interesting snap-shot of the microbial population from which *Proteiniphilum alaskensis* strain PE-10^T was isolated. Furthermore, qPCR data revealed how much more abundant total bacteria were in the PIG compared to other fluid samples. Without this information, the cultivation of a dominant molecular signal would have been far less significant. This work was supported by OU Biocorrosion Center funding.

References

ASTM Standard G1-03.

Biezma, M. V. and J. R. San Cristóbal. (2005). Methodology to study cost of corrosion. *Corrosion Engineering, Science and Technology* **40**(4): 344-352.

Chen, S. and X. Dong. (2005). *Proteiniphilum acetatigenes* gen. nov., sp. nov., from a UASB reactor treating brewery wastewater. *Int J Syst Evol Microbiol* **55**(Pt 6): 2257-2261.

Felsenstein, Joseph. (1985). Confidence limits on phylogenies: an approach using the bootstrap. *Evolution* **39**: 783-791.

Holdeman, L. V. and W. C. Moore (ed.). (1975). Anaerobe laboratory manual, 3rd ed. Anaerobe Laboratory, Virginia Polytechnic Institute and State University, Blacksburg.

Kimura, M. (1980). A simple method for estimating evolutionary rates of base substitutions through comparative studies of nucleotide sequences. *J Mol Evol* 111-120.

Lawson, P. A., Gharbia, S. E., Shah, H. N. and Clark, D. R. (1989). Recognition of *Fusobacterium nucleatum* subgroups Fn-1, Fn-2 and Fn-3 by ribosomal RNA gene restriction patterns. *FEMS Microbiol Lett* **53**, 41-45.

Lipman, D. J. and W. R. Pearson. (1985). Rapid and sensitive protein similarity searches. *Science* **22**(227): 1435-1441.

Lloyd, J., Mabbett, A., Williams, D., and L. Macaskie. (2001). Metal reduction by sulphate-reducing bacteria: physiological diversity and metal specificity. *Hydrometallurgy* **59**(2): 327-337.

Melo, IRD., Urtiga Filho, S. L., Oliveira, FJS., and F. P. Franca. (2011). Formation of biofilms and biocorrosion on AISI-1020 carbon steel exposed to aqueous systems containing different concentrations of a diesel/biodiesel mixture. *International Journal of Corrosion* **2011**: 1-6.

Purish, L., Koptieva, Z. P., Asaulenko, L. and I. Kozlova. (2006). Adhesion of sulphate-reducing bacteria to steel under cathode polarization. *Mikrobiolohichnyi zhurnal*. Kiev, Ukraine. **68**(1): 54.

Ropital, F. (2010). Corrosion and degradation of metallic materials: Understanding of the phenomena and applications in petroleum and process industries. *IFP Publications* **2010**: 1-9.

Saitou, N. & Nei, M. (1987). The neighbor-joining method: a new method for reconstructing phylogenetic trees. *Mol Biol Evol* **4**, 406-425.

Sasser M. Identification of bacteria by gas chromatography of cellular fatty acids: Technical Note #101.

Sheng, X., Ting, Y. P. and S. O. Pehkonen. (2008). The influence of ionic strength, nutrients and pH on bacterial adhesion to metals. *J Colloid Interface Sci* **321**(2): 256-264.

Stevenson, B. S., Drilling, H. S., Lawson, P. A., Duncan, K. E., Parisi, V. A. and J. M. Suflita. (2011). Microbial communities in bulk fluids and biofilms of an oil facility have similar composition but different structure. *Environ Microbiol* **13**(4): 1078-1090.

Stipanicev, M., Turcu, F., Esnault, L., Rosas, O., Basseguy, R. and I. Beech. (2014). Corrosion of carbon steel by bacteria from North Sea offshore seawater injection systems: Laboratory investigation. *Bioelectrochemistry* **97**(0): 76-88.

Thompson, J. D., Higgins, D. G. and T.J. Gibson. (1994). Clustalw: improving the sensitivity for progressive multiple sequence alignment through sequence weighting, position-specific gap penalties and weight matrix choice. *Nucleic Acids Res.* **22**, 4673-4680.

Vu, B., Chen, M., Crawford, R. J. and E. P. Ivanova. (2009). Bacterial extracellular polysaccharides involved in biofilm formation. *Molecules* **14**(7): 2535-2554.

Zuo, R. (2007). Biofilms: strategies for metal corrosion inhibition employing microorganisms. *Appl Microbiol Biotechnol* **76**(6): 1245-1253.

Chapter 4

**Differential rates of corrosion measured between
Desulfovibrio alaskensis and *Desulfovibrio indonesiensis*,
a determination of microbial contributions to biocorrosion**

Abstract

Corrosion impacts many industrial processes including the production and transportation of petroleum, causing various economic and environmental concerns. Microbially influenced corrosion (MIC) or 'biocorrosion' is damage accelerated by interactions between bacterial cells, metal surfaces, and abiotic corrosion products. The investigation presented here was directed at assessing the efficacy of current corrosion detection, while comparing the corrosive capabilities of two model microorganisms associated with corrosion in petroleum production facilities. In this study, corrosion experiments were performed with two sulfate-reducing bacteria, *Desulfovibrio alaskensis* and *Desulfovibrio indonesiensis*. Although *D. alaskensis* had been labeled as having a less aggressive effect on metal corrosion, a direct comparison was lacking. For each organism, anaerobic incubations with carbon steel were assessed after 30 and 90 days. Biofilms were visualized with Scanning Electron Microscopy (SEM), compositionally compared with Energy Dispersive Spectroscopy (EDS), and the thickness measured with Fluorescence Reflectance via Confocal Microscopy. Replicate coupons were cleared of biofilm and corrosion products, weighed for mass loss determination, and the concentration of liberated iron in the culture medium was determined using Atomic Absorption Spectrometry (AAS). Finally, Scanning Electron Microscopy (SEM) and profilometry were used in order to analyze surface topography. Biofilms of *D. indonesiensis* appeared more flocculent than the smooth biofilms of *D. alaskensis*, contained more NaCl and FeO, and were significantly thicker than *D. alaskensis* after both 30 and 90 days ($p < 0.05$). Cultures of *D. indonesiensis* removed more material from the metal, resulting in a greater loss in mass after 30 days. However,

rates of weight loss were indistinguishable after 90 days. Distinguishable concentrations of liberated iron could not be measured with AAS, however, cultures of *D. indonesiensis* produced significantly greater surface roughness ($p < 0.05$) on metal surfaces than the less corrosive *D. alaskensis*. Profilometry data substantiated SEM roughness, revealing an increase in metal corrosion among *D. indonesiensis* cultures. The results reported here show that *D. indonesiensis* is more corrosive than *D. alaskensis* and demonstrate the use of SEM image analysis as a screening tool to measure the corrosive contributions of bacteria.

Introduction

Corrosion related issues affect many industrial processes including petroleum and energy related production and transportation. In particular, the pitting forms of iron corrosion have huge environmental and economic repercussions, as pits may reach depths that pose concerns of pipeline breaches (Olszewski, 2007). This phenomenon can be exacerbated when bacteria associate with metal surfaces in complex biofilms, resulting in direct microbial interactions that negatively affect infrastructure. This kind of microbiologically influenced corrosion (MIC, referred to here as “biocorrosion”) affects nearly every industry, costing the petroleum sector alone billions of US dollars (Iverson, 1987).

Carbon steel has been the primary source for pipeline construction and fuel transportation within the energy sector, and is susceptible to colonization by bacterial populations and subsequent deterioration due to metal loss (Neoh and Kang, 2011). Corrosive potential may be attributable to the ability of requisite organisms to form sustainable biofilms, including adhesion tendencies and symbiotic involvement (Boopathy, 1991; Zuo, 2007; Sheng, Ting *et al.*, 2008). Other bacterial characteristics that contribute to biocorrosion include the ability of microorganisms to a) travel to and locate metallic surfaces, b) colonize these surfaces with pili and produce exopolymeric substances (EPS), c) maintain metabolic functions as end products accumulate, d) live symbiotically, producing valuable energy sources for other bacteria and utilizing nutrients from surrounding bioenergetic processes, e) transfer electrons and directly oxidize metal, and 6) grow quickly and efficiently in dynamic environments (Videla, 2000). Anaerobic microorganisms, particularly sulfate reducing bacteria (SRB), have

long been implicated in biocorrosion because many possess the above physiological characteristics (Hamilton, 1985; Voordouw, 1995; Lloyd, Mabbett *et al.*, 2001; Zhou, He *et al.*, 2011). Damage to steel by SRB is usually localized, taking on the form of pits (Enning, Venzlaff *et al.*, 2012). The mechanism of pitting is believed to be an electrochemical interaction, where electrons are transferred from a small corroding area (the anode) to its non-corroding surroundings (the cathode) (Hamilton, 1985; Lovely, 2012). Chloride ions accumulate under the biofilm and establish electroneutrality, facilitating the autocatalytic stabilization of this biological galvanic cell. Chemically, sulfide can cause corrosion through cathodic depolarization via iron sulfur compounds, and the involvement of SRB perpetuate sulfide production and subsequent pitting corrosion (Cord-Ruwisch and Widdel, 1986; Lee, Lewandowski *et al.*, 1995). FeS encrustation occurs as sulfate anions become reduced to HS⁻ and interact with ferrous iron produced by the anodic reaction (Sherar, Power *et al.*, 2011). These black precipitates result in insoluble pipeline scalings which can cause damaging pipeline erosion and must be removed via costly pigging efforts. Additionally, SRB can produce harmful metabolic end products such as organic acids and H₂S which can intensify pitting through the souring process (Boopathy, 1991).

In order to better understand these mechanisms and to identify which organisms possess corrosive capabilities, associations of bacterial populations and their resulting surface properties must be investigated. However, the heterogeneous nature of biocorrosion presents a challenge when attempting to measure corrosion rates (Little, Lee *et al.*, 2006). The standard industry practice of measuring mass loss of metal coupons provides a coarse indication of corrosion rates but does not provide

information as to the nature of the corrosion itself (e.g. number, distribution, size, and shape of pits) (King, Gaylarde *et al.*, 1995). For instance, pits may be few and far between but reach depths that pose concerns about integrity, without considerable loss in weight. Studies have concentrated on the molecular detection of microbial communities and their metabolic activities associated with biocorrosion (Thauer, Stackebrandt *et al.*, 2007; Pham, Hnatow *et al.*, 2009; Suflita, Aktas *et al.*, 2012). Voordouw *et al.* (2006) compared oil field populations, and described a complex ecosystem dominated by sulfate reducing bacteria and a number of accessory species that play a role in SRB driven biocorrosion through their own sulfide utilization, fermentation or acetogenesis (Voordouw, Armstrong *et al.*, 1996). More recent studies have linked these community surveys to *in situ* metabolite profiles, demonstrating the potential to associate pipeline deterioration with key metabolic signatures (Stevenson, Drilling *et al.*, 2011). Where a census of community members may provide a snapshot of dominant phylotypes, further studies must be performed in order to investigate the underlying mechanisms of biocorrosion. Electrochemical studies have been performed in order to understand the acceleration of corrosion rates influenced by the electrochemical processes of SRB (Little, 1992; Peng and Park, 1994; Lovely, 2012). For example, authors Venzlaff *et al.* recently demonstrated the stimulation of the cathodic reaction by SRB species using potentiodynamic measurements, while also showing that the aforementioned FeS deposition actually mediated the connectivity between bacterial cells and the metal (Venzlaff, Enning *et al.* 2013).

The goal of this research was to explore alternative methods for measuring biocorrosion activity of two species of SRB, *Desulfovibrio alaskensis* and *Desulfovibrio*

indonesiensis. As well as sharing many physiological and metabolic characteristics, both organisms were originally isolated from petroleum production facilities and have been implicated in biocorrosive activity (Feio, Beech *et al.*, 1998; Beech, 2003; Feio, Zinkevich *et al.*, 2004). Although *D. indonesiensis* has been labeled an “aggressive corroder” relative to *D. alaskensis*, a direct laboratory comparison of their noticeably different corrosion rates was lacking. Thus, a polyphasic assessment was used to develop new parameters to differentiate corrosive abilities while also providing a baseline of descriptive tests for the characterization of biocorrosive activities of representative SRB. The dimensional analysis of pitting corrosion demonstrates the ability to distinguish between the corrosive capacity of microorganisms; and therefore has applications that may be applied to future industry mitigation strategies, quality control checks, and perhaps most importantly, an opportunity to investigate the mechanisms of this deleterious process.

Materials and Methods

Material and Solution Preparation

Cultures of *D. alaskensis* and *D. indonesiensis* were grown in VMI medium (modified Postgate medium) which contained, per liter: 0.5 g KH_2PO_4 , 1.0 g NH_4Cl , 4.5 g Na_2SO_4 , 0.04 g $\text{CaCl}_2 \cdot 2\text{H}_2\text{O}$, 0.06 g $\text{MgSO}_4 \cdot 7\text{H}_2\text{O}$, 0.004 g $\text{FeSO}_4 \cdot 7\text{H}_2\text{O}$, 0.3 g $\text{Na}_3\text{C}_6\text{H}_5\text{O}_7 \cdot 2\text{H}_2\text{O}$, 25.0 g NaCl , 2.0 g casamino acids, 2.0 g tryptone, and 6.0 g sodium lactate. The pH was adjusted to 7.5 with the addition of NaOH and 1.0 mL each of trace element and vitamin stock solutions were added. Anoxic conditions were obtained by purging the medium with N_2 for 15 min. while heating, followed by an additional amendment of 0.5 g of $\text{FeSO}_4 \cdot 7\text{H}_2\text{O}$, and further degassing with N_2 . After distribution, vials were butyl rubber stoppered, crimp sealed with aluminum, and autoclaved at 121 °C for 20 min. Metal coupons made of C1010 carbon steel were ordered from Metal Samples Company (Munford, AL), measuring 3 in. long X ½ in. wide X 1/16 in. thick, with a circular perforation and an exposed area of 3.38 in². Coupons were not pretreated or polished. Glassware and pre-weighed coupons were reduced for 48 hours in an anaerobic glove box, sealed with butyl rubber stoppers, and their headspace exchanged with N_2 . Vessels were then autoclaved, and the headspace again exchanged with N_2 . Separately, cell counts were performed for each bacterium after 72 hours growth using a hemocytometer, and dilutions were made in VMI medium such that 15 mL of seed cultures at a density of 10⁵ cells/mL could be distributed among biological replicates. Sets included 8 replicates of each *D. alaskensis*, *D. indonesiensis*, and an abiotic medium-only control. After 30 and 90 days incubation at 37 °C, corrosive activities were assessed in the following ways:

Biofilm Characteristics

The biological organic matter that had adhered to the surfaces of the metal was visualized with SEM, compared with EDS, and the thickness measured with Confocal Microscopy.

Scanning Electron Microscopy – One biological replicate was destructively sampled in an anaerobic chamber, where the coupon was placed in a sterile petri dish and left to dry. In order to evaluate bacterial interactions with the metal, the quality and quantity of biofilm deposition were studied by means of SEM, using a Zeiss NEON 40 EsB.

Energy Dispersive Spectroscopy – Corrosion products were analyzed for chemical identification on these same coupons. EDS of biofilm composition was performed on a Zeiss NEON high resolution SEM and analyzed with x-ray software (Aztec, Oxford). Quantitative chemical analysis was then used to make relative comparisons between *Desulfovibrio* species as well as changes over time.

Confocal Fluorescence Microscopy – Three additional tubes from each set were destructively sampled after 30 and 90 days for biofilm structure analysis using a Leica TCS SP2 SE, with a 63X dipping lens. Coupons were removed and placed in sterile petri dishes and carefully immersed in 2 mL TE buffer. Fluorescence reflectance mode was used to quantify biofilm thickness, including abiotic corrosion products, and pairwise comparisons made.

Iron Liberation

Three replicate coupons were cleared of biofilm and corrosion products (ASTM Standard G1-03), weighed for mass loss determination, and the concentration of liberated iron in the culture medium was determined using AAS.

Mass Loss – Sessile growth was removed by sonication in soapy water for five minutes followed by acid immersion for ten minutes. The acid solution consisted of 500 mL concentrated HCl, 500 mL DiH₂O, and 3.5 g hexamethylene tetramine. Coupons were rinsed with DiH₂O, acetone, then methanol, and finally blow-dried with nitrogen. Mass loss was measured for each metal coupon and used for classical corrosion rate calculations (CORCALC).

Atomic Absorption Spectrometry – The concentration of total liberated iron was measured spectrophotometrically at 248.3 nm with a Perkin Elmer AAnalyst 800 using air as the oxidant at a flow rate of 17.0 L/min and a 2.0 L/min flow of acetylene as fuel. Standards ranging from 0.1 mM to 10 mM ferric nitrate in 0.1 M HCl were used. Triplicate 0.5 mL culture samples were diluted to contain 0.1 M HCl in 0.25 M hydroxylamine HCl. Results were obtained using a standard nebulizer and flow spoiler, slit width of 0.2 nm, and relative noise 1.0, linear to 5 mg/L.

Surface Analysis

Scanning Electron Microscopy - The topography of triplicate coupons were visualized on a Zeiss DSM-960 SEM by magnification of one random site each. Stereo image pairs were taken at 20 kV on a +/-5° tilt, stacked, and analyzed for quantitative height reconstruction (Scandium Solution Height, Olympus). Surface profiles were

created in 3-dimension of stacked images from which line scans and height differences were mapped. Roughness measurements of the reconstructed surface were generated at random from poly line scans covering an approximately 1700 micron distance, averaged from three biological replicates, and reported as the value R_f (Table 4.1).

Profilometry – After imaging, the same coupons were stored anoxically and shipped to Nanovea for surface profiling. Metal topology was mapped at a resolution of $1\ \mu\text{m} \times 1\ \mu\text{m}$ with an ST400 optical profiler, including feature sizes, pit dimensions, and frequency. Grains measuring $>5\ \mu\text{m}$ deep and $>1\ \mu\text{m}$ in diameter below the average mean plane were designated as corrosion pits. This value was divided by the scanned surface area and reported as pit density (Table 4.2).

Results

The results presented here indicated that corrosion was indeed occurring and measurable. Both organisms produced biofilms on the surface of carbon steel that differed morphologically, but shared roughly the same chemical composition. Differential corrosion was measured, indicating that *D. indonesiensis* was more corrosive than *D. alaskensis*. Corrosion rates from mass-loss were differential (*D. alaskensis* vs *D. indonesiensis*; $p < 0.05$) and faster within the first 30 days, then slower and not different ($p > 0.05$) after 90 days.

Scanning Electron Microscopy

Over the course of the experiment, visible differences in biofilm formation and iron sulfide accumulation in the form of black precipitates within the culture medium was noted before tubes were sampled. Cultures of *D. alaskensis* produced a thin translucent film on the tube wall and relatively sparse biomass accumulation on the metal coupon. Cultures of *D. indonesiensis* contained visibly more precipitate, which did not adhere to the walls of the tube. SEM images revealed morphological differences between the two cultures (Fig. 4.1). Purish *et al.* (2006) found that, under cathodic depolarization, cultures of *D. indonesiensis* (*D. indonensis* at the time) adhered to metal more actively than *Desulfovibrio desulfuricans* Kiev-45 and *Desulfobulbus* sp. (Purish, Koptieva *et al.* 2006). At lower magnification, SEM images validate the ability of *D. indonesiensis* to aggressively colonize carbon steel (Fig. 4.2).

Figure 4.1: SEM images of (A) *D. alaskensis* and (B) *D. indonesiensis* biofilms formed on the surface of metal coupons after 30 days in VMI medium.

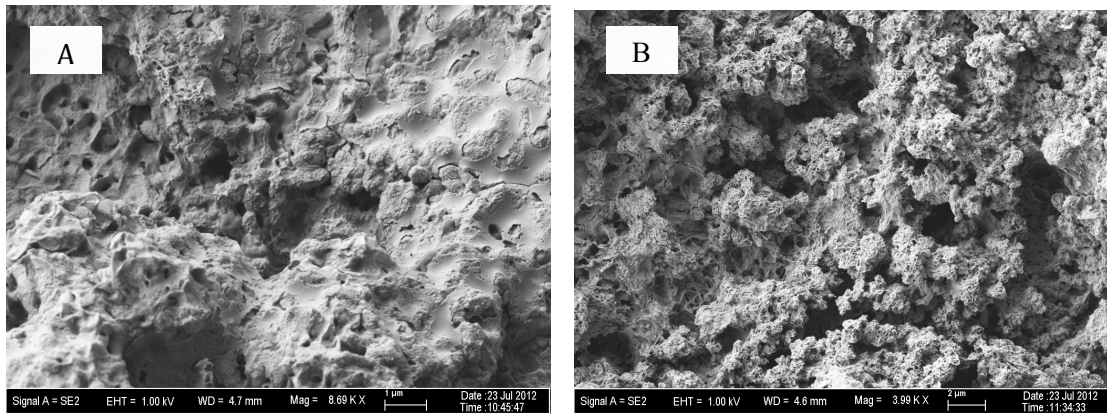
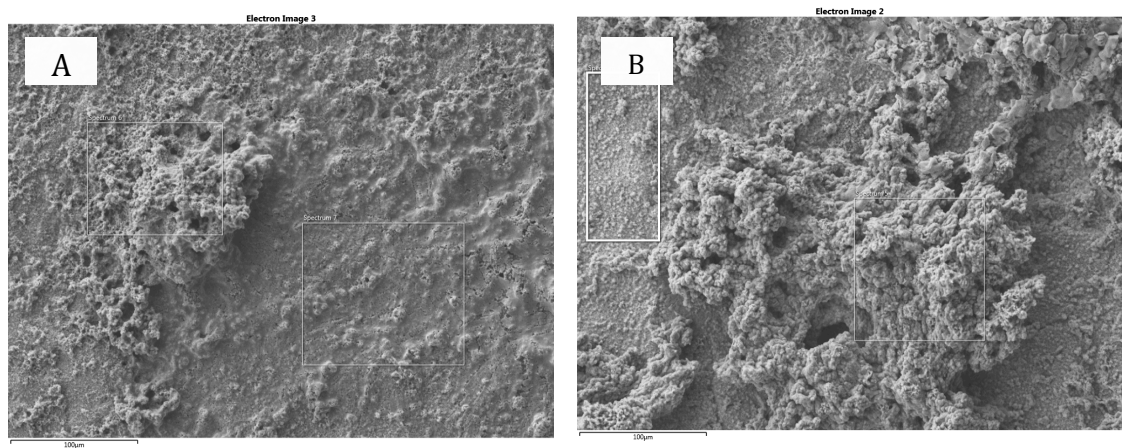


Figure 4.2: SEM images representative of all fields seen taken with an SE2 signal at 10 kV and 272 X magnification. (A) *D. alaskensis* and (B) *D. indonesiensis* colonized coupons after 90 days incubation. Boxes highlight areas for comparison, showing heavy biomass and less colonized areas.



Energy Dispersive Spectroscopy

EDS revealed subtle differences in the biofilms of *D. alaskensis* and *D. indonesiensis* after 30 days (Fig. 4.3). *D. indonesiensis* formed visibly denser biofilms that contained more Fe and O (perhaps existing as iron oxides), whereas *D. alaskensis* contained more Na and Cl. A comparison of the cultures' chemical composition after 30 days and 90 days was also made. Figure 4.4 shows that over time the organisms shared similar behavior. Both biofilms accumulated Na and Cl, and the concentrations of O species decreased. Similarly, both cultures demonstrated an inverse relationship between iron and sulfur, as Fe decreased over time, S increased within the EPS matrix.

Confocal Microscopy

D. alaskensis formed a biofilm that was thicker than the abiotic corrosion products deposited on the control coupon, but did appear to intensify over time. Biofilms of *D. indonesiensis* measured two orders of magnitude thicker than *D. alaskensis* and continued to grow (at a slower rate) over the 90 day incubation period (Fig. 4.5).

Figure 4.3: SEM images of bacterial growth taken with an SE2 signal at 10 kV and 272 X magnification. (A) *D. alaskensis* and (B) *D. indonesiensis* colonized coupons after 30 days incubation, including (C) EDS spectrum layered for comparison of *D. alaskensis* (red) and *D. indonesiensis* (yellow) biomass and corrosion products. Boxes indicate EDS scanned area.

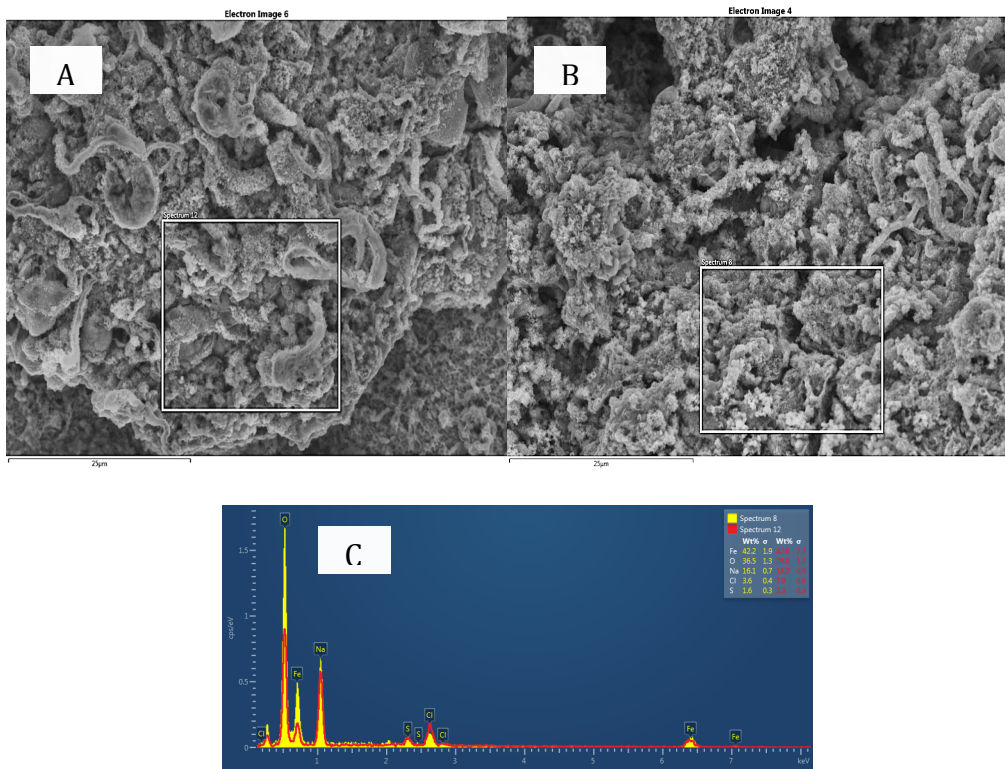


Figure 4.4: EDS comparison of biofilms (a) *D. alaskensis* spectra, 30 days (red) versus 90 days (yellow); (b) *D. indonesiensis* spectra, 30 days (red) versus 90 days (yellow).

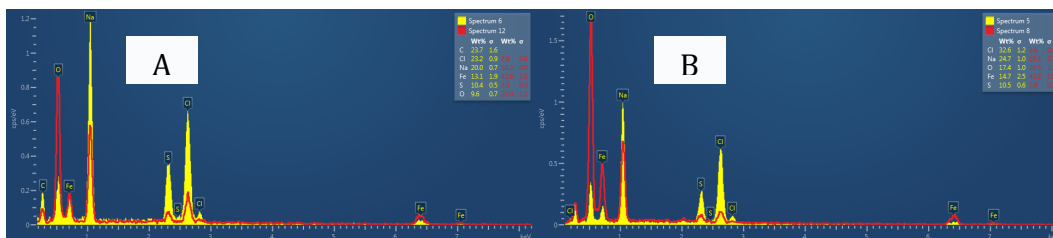
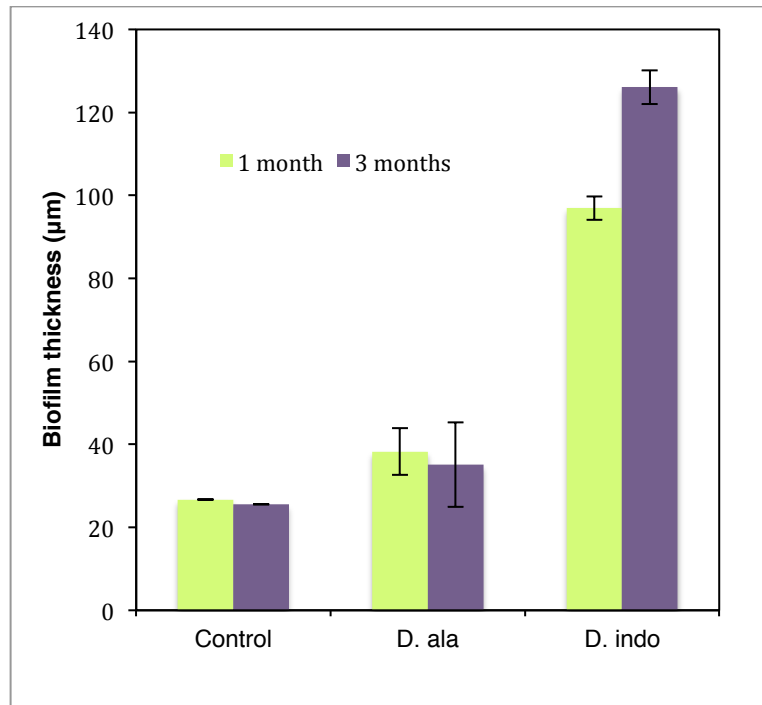


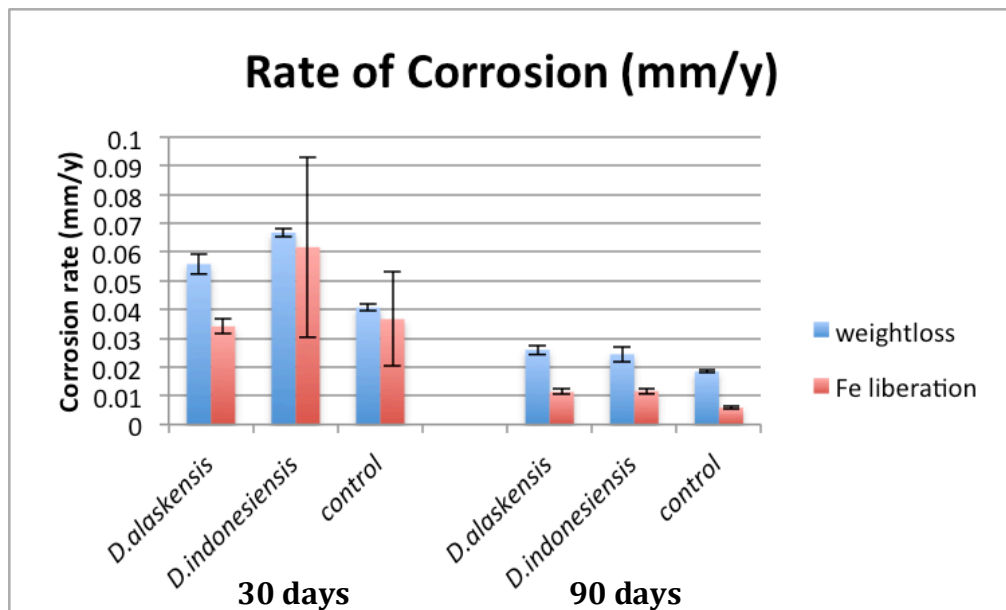
Figure 4.5: Biofilm thickness obtained from confocal microscopy using the reflective mode, showing statistically significant differences in colonization physiology between *D. alaskensis* and *D. indonesiensis* ($p < 0.05$) but not between *D. alaskensis* and the abiotic control (n=3).



Mass Loss and Atomic Absorption

After 30 days, more loss was measured from coupons incubated with *D. indonesiensis* than *D. alaskensis*. Figure 4.6 shows rates of corrosion for each organism, calculated from weight loss and solubilized iron content, respectively, after 30 days and 90 days incubation. Rates were differential and faster in the first 30 days of incubation (*D. alaskensis* vs *D. indonesiensis*; $p < 0.05$) calculated from weight-loss. However, differences in weight were not seen after 90 days, as corrosion rates coalesced. AAS differences in iron content were not statistically significant, due to the large deviation between biological replicates.

Figure 4.6: Rates of corrosion were differential and faster in the first 30 days of incubation (*D. alaskensis* vs *D. indonesiensis*; $p < 0.05$). Rates were slower and not different ($p > 0.05$) after 90 days.



Scanning Electron Microscopy

The use of SEM to map surface topography and measure the roughness of exposed metal proved useful for assessing the corrosive effects of *Desulfovibrio* sp. As seen in Figure 4.7 (A-D), images revealed less surface roughness on coupons incubated with *D. alaskensis* than coupons incubated with *D. indonesiensis*, indicative of less mass loss and less corrosion. Table 4.2 showed the roughness values obtained for biological replicates and the corresponding graph shows the averages of roughness values obtained for 30 and 90 day incubations.

Figure 4.7: Coupon topography using SEM (20kV at 500X) of metal surface after 30 days colonization with A₁) *D. alaskensis*, A₂) *D. indonesiensis*, showing; B_{1,2}) height profile for generating R_f, C_{1,2}) height thresholds (blue, depressed; red, elevated), and D_{1,2}) a 3-D plot of metal topography.

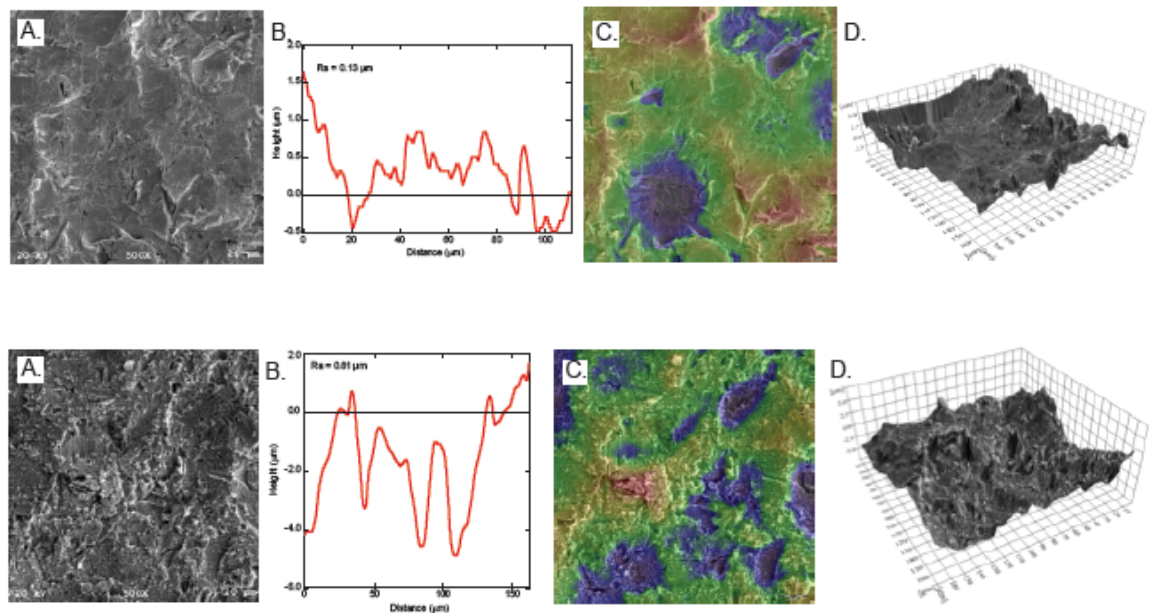
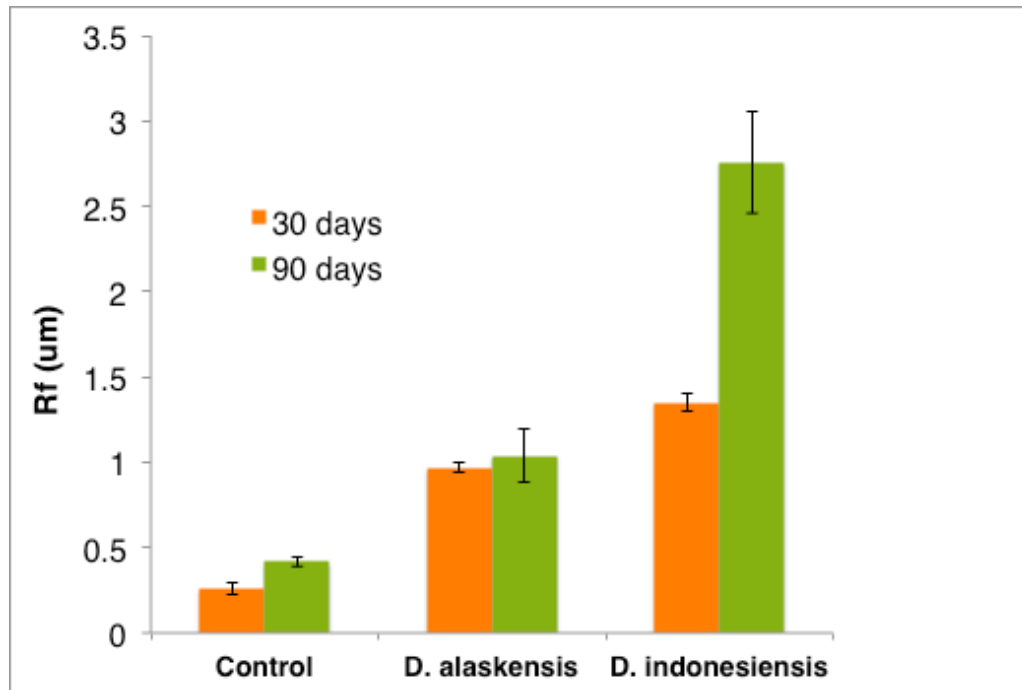
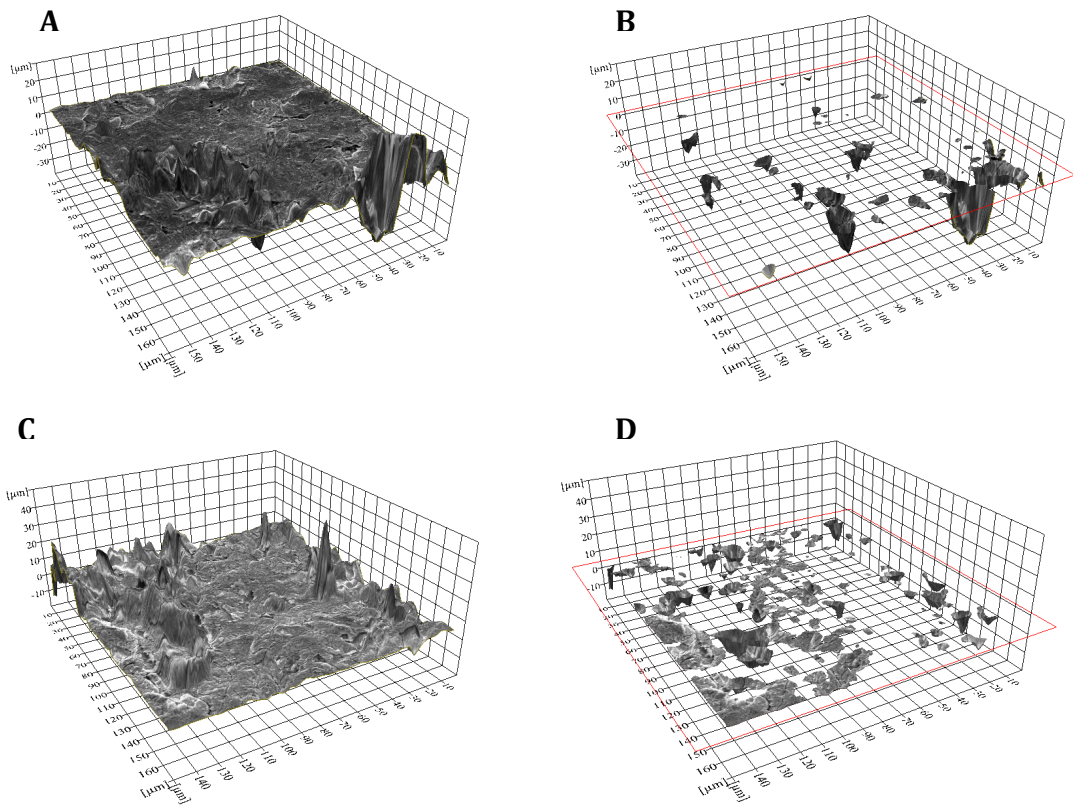


Figure 4.8: Roughness of metal shows differential corrosion were differential, between the control, *D. alaskensis*, and *D. indonesiensis* in the first 30 days of incubation (orange bars). The degree of roughness after 90 days incubation shows significantly greater topography changes for *D. indonesiensis* (green bars). (n = 3)



SEM stereo pairs were stacked and the resulting image plotted for topographical visualization (shown in Fig. 4.9, A & C). Digital removal of data above the average mean height revealed limited pitting corrosion from cultures incubated with *D. alaskensis* compared to more extensive surface damage caused by *D. indonesiensis* (Fig. 4.9, B & D).

Figure 4.9: A) 3-D contour map of *D. alaskensis* after 30 days B) *D. alaskensis* with thresholding at average mean height, revealing limited pitting corrosion. C) Contour map of *D. indonesiensis* after 30 days D) *D. indonesiensis* with thresholding at average mean height, revealing heavy pitting corrosion.



Profilometry

Topographical mapping of duplicate coupons with a white light profilometer corroborated SEM analysis of surface roughness. Biological interactions resulted in more metal disruption than seen with the uninoculated control. As can be seen from 3-D binary imagery, both the depth of pits and frequency of pits increase with bacterial involvement, particularly with cultures of *D. indonesiensis* (Fig. 4.10, A-C). Table 4.1 provides quantitative pit distribution whereby pits were identified as grains $> 5 \mu\text{m}$ deep and $> 1 \mu\text{m}$ in diameter.

Figure 4.10: Metal coupon surface topography after 30 days incubation showing the pit depth, frequency, and distribution of (A) abiotic control (B) *D. alaskensis* (C) *D. indonesiensis*.

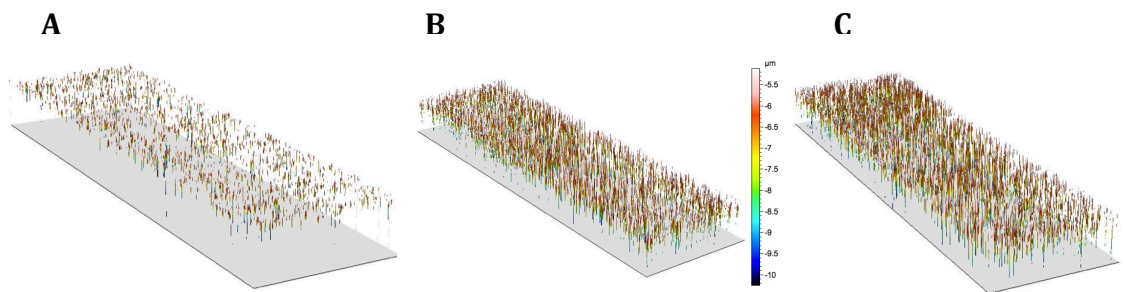


Table 4.1. Quantitative pit distribution obtained via profilometry for uninoculated control, *D. alaskensis*, and *D. indonesiensis*. Pit Density (grains/mm²). Grains > 5 µm deep and > 1 µm in diameter

Abiotic control	14.00
	10.65
<i>D. alaskensis</i>	17.75
	19.89
<i>D. indonesiensis</i>	22.57
	31.33

Discussion

In addition to traditional means of measuring corrosion such as weight loss and Fe accumulation, this assessment provides methods for measuring the corrosive capabilities of model microbes. This reproducible system allows for laboratory investigations to be conducted directly on metal surfaces, for the purpose of providing valuable information on potential corrosion mechanisms. The application of these methods has been demonstrated by the measurement of the differential corrosion activity between two species of SRB. Analysis of biofilms attached to the surface of metal coupons revealed differences in colonization behavior, and that under these culture conditions *D. alaskensis* produced a thinner biofilm than *D. indonesiensis*. *D. indonesiensis* is known to produce an extensive EPS matrix with a high binding affinity for iron (I. Beech, unpublished results). Corrosion rates calculated from mass-loss over time were differential (*D. alaskensis* vs *D. indonesiensis*; $p < 0.05$) and faster for *D. indonesiensis* ($p < 0.05$) within the first 30 days. A significantly greater loss in metal mass from *D. indonesiensis* may be attributable to this culture's initial colonization activity because rates were slower and not different ($p > 0.05$) after a 90 day period. It was suspected that corrosion either became controlled through the stability of iron sulfide accumulation on the metal surface as described by Videla, or because cells were no longer metabolically active (Videla 2000). Atomic Absorption did not appear to be sensitive enough to distinguish between concentrations of iron solubilized by bacteria. The large deviation between biological replicates measured by AAS may have been due to the nature of the slime aggregates and iron sulfide heterogeneity. However, SEM provided a direct analysis of pitting corrosion, and proved useful as a means to measure

the corrosive contributions of bacteria. Profilometry results showed the spatial and depth dimensions of pitting while validating SEM data and depicting the extent to which *Desulfovibrio* sp. liberate metal from carbon steel. A shorter time scale without excess ferrous sulfate is suspected to result in more corrosion of the coupon metal (Enning, Venzlaff *et al.* 2012). Additionally, Sherar *et al.* found that if nutrients are limited, particularly lacking a carbon substrate, nanowire-like pili are produced in order for cells to utilize energy directly from the metal itself (Sherar, Power *et al.* 2011). Therefore, use of a more minimal medium may also yield a greater extent of corrosion.

The results presented here suggest that SEM surface measurements offer a more sensitive means to measure differences in the rates of biocorrosion in laboratory studies. As a corrosion analysis tool, SEM complements commonly used practices/ approaches. In addition to the documentation of surface appearance, SEM aids in the evaluation of topographical roughness through the visualization of pit area, depth, and distribution. Other advantages include the visual characterization of pitting corrosion with 3-D information, and the quantification of feature sizes, providing a direct comparison of corrosive potential. More sophisticated SEM techniques allow us to visualize the surface topography while maintaining depth of field. In order to generate these images, the pixels per micron must be converted into distance matrices, a worth-while effort as the contrast of SEM images can be misleading, particularly when assessing 3-dimensional landscapes of metal. Therefore, a higher accelerating voltage was used in order to obtain a shorter wavelength and better diffraction-limited resolution for making precise measurements. The imagery of metal surfaces was complex due to the elastic scattering of the electrons used to perform SEM. The thicker or more dense (higher

atomic weight) portions of the coupon can appear as darker areas in an image due to less electrons from the beam passing through. The interpretation of such images is challenging, therefore quantitative mapping was performed using Scandium software. These calculations showed that the surface tomography of coupons incubated with *D. indonesiensis* was rougher than those incubated with *D. alaskensis*, and that the roughness of abiotic control coupons was minimal.

This micro-scale perspective will prove valuable for laboratory assessments of corrosion activities and mitigation strategies to control deleterious microorganisms. Future work could focus on developing an inventory of key players for reliable risk assessments, where model microbial assemblages could be maintained and manipulated for mechanistic investigations. Another application for these analytical tools is the ability to check quality control for industry maintenance, including the evaluation of current relief strategies and corrosion monitoring techniques. Furthermore, knowledge can be gained from the documentation of severity of pitting potential caused by controlled bacterial consortia, and these tools provide reproducible laboratory tests with which to investigate other MIC activities such as bacterial electron transfer, metabolic turnover, adhesion tendency, and quorum sensing.

Acknowledgements

This research was carried out with energy industry partner funding through the University of Oklahoma Biocorrosion Center. We gratefully thank Preston Larson of the Samuel Roberts Nobel Electron Microscopy Laboratory for providing guidance with SEM and to Heather Nunn for aiding in these analyses.

References

ASTM Standard G1-03.

Beech, I. B. (2003). Biocorrosion: Role of Sulfate Reducing Bacteria. Encyclopedia of Environmental Microbiology, John Wiley & Sons, Inc.

Boopathy, R. D., L. (1991). Effect of pH on Anaerobic Mild Steel Corrosion by Methanogenic Bacteria. *Applied and Environmental Microbiology* **57**(7): 2104-2108.

Cord-Ruwisch, R. and F. Widdel. (1986). Corroding iron as a hydrogen source for sulphate reduction in growing cultures of sulphate-reducing bacteria. *Appl Microbiol Biotechnol* **25**(2): 169-174.

Enning, D., Venzlaff, H., Garrelfs, J., Dinh, H. T., Meyer, V., Mayrhofer, K., Hassel, A. W., Stratmann, M. and F. Widdel. (2012). Marine sulfate-reducing bacteria cause serious corrosion of iron under electroconductive biogenic mineral crust. *Environ Microbiol* **14**(7): 1772-1787.

Feio, M. J., Beech, I. B., Carepo, M., Lopes, J. M., Cheung, C., Franco, R., Guezennec, J., Smith, J., Mitchell, J. I. and J. J. G. Moura. (1998). Isolation and Characterisation of a Novel Sulphate-reducing Bacterium of the *Desulfovibrio* Genus. *Anaerobe* **4**(2): 117-130.

Feio, M. J., Zinkevich, V., Beech, I.B., Llobet-Brossa, E., Eaton, P., Schmitt, J. and J. Guezennec. (2004). *Desulfovibrio alaskensis* sp. nov., a sulphate-reducing bacterium from a soured oil reservoir. *Int J Syst Evol Microbiol* **54**(Pt 5): 1747-1752.

- Hamilton, W. A.** (1985). Sulphate-reducing bacteria and anaerobic corrosion. *Annu Rev Microbiol* **39**: 195-217.
- Iverson, W. P.** (1987). Microbial corrosion of metals. *Adv. Appl. Microbiol.* **32**: 1-35.
- King, R. A., Gaylarde, C. and H. Videla.** (1995). Monitoring techniques for biologically induced corrosion. *Bioextraction and biodeterioration of metals* **1**: 271.
- Lee, W., Lewandowski, Z., Nielsen, P.H. and W.A. Hamilton.** (1995). Role of sulfate-reducing bacteria in corrosion of mild steel: A review. *Biofouling* **8**(3): 165-194.
- Little, B., Lee, J. and R. Ray.** (2006). Diagnosing microbiologically influenced corrosion: a state-of-the-art review. *Corrosion* **62**(11): 1006-1017.
- Little, B. and F. Mansfeld.** (1992). An Overview of Microbiologically Influenced Corrosion. *Electrochimica Acta* **37**(12): 2185-2194.
- Lloyd, J., Mabbett, A., Williams, D. and L. Macaskie.** (2001). Metal reduction by sulphate-reducing bacteria: physiological diversity and metal specificity. *Hydrometallurgy* **59**(2): 327-337.
- Lovely, D. R.** (2012). Electromicrobiology. *Annu Rev Microbiol* **66**(1).
- Neoh, K. G. and E. T. Kang** (2011). Combating bacterial colonization on metals via polymer coatings: relevance to marine and medical applications. *ACS Appl Mater Interfaces* **3**(8): 2808-2819.
- Olszewski, A. M.** (2007). Avoidable MIC-Related Failures. *Journal of Failure Analysis and Prevention* **7**(4): 239-246.
- Peng, C. G. and J. K. Park.** (1994). Electrochemical mechanisms of corrosion influenced by sulfate-reducing bacteria in aquatic systems. *Water Res* **28**(8): 1681-1692.
- Pham, V. D., Hnatow, L. L., Zhang, S., Fallon, R. D., Jackson, S. C., Tomb, J. F. and S. J. Keeler.** (2009). Characterizing microbial diversity in production water from an Alaskan mesothermic petroleum reservoir with two independent molecular methods. *Environ Microbiol* **11**(1): 176-187.
- Purish, L., Koptieva, Z. P., Asaulenko, L. and I. Kozlova.** (2006). Adhesion of sulphate-reducing bacteria to steel under cathode polarization. *Mikrobiologichnyi zhurnal.* Kiev, Ukraine. **68**(1): 54.
- Sheng, X., Ting, Y. P. and S. O. Pehkonen.** (2008). The influence of ionic strength, nutrients and pH on bacterial adhesion to metals. *J Colloid Interface Sci* **321**(2): 256-264.

- Sherar, B. W. A., Power, I. M., Keech, P. G., Mitlin, S., Southam, G. and D. W. Shoosmith.** (2011). Characterizing the effect of carbon steel exposure in sulfide containing solutions to microbially induced corrosion. *Corrosion Science* **53**(3): 955-960.
- Stevenson, B. S., Drilling, H. S., Lawson, P. A., Duncan, K. E., Parisi, V. A. and J. M. Suflita.** (2011). Microbial communities in bulk fluids and biofilms of an oil facility have similar composition but different structure. *Environ Microbiol* **13**(4): 1078-1090.
- Suflita, J. M., Aktas, D. F., Oldham, A. L., Perez-Lbarra, B. M. and K. Duncan.** (2012). Molecular tools to track bacteria responsible for fuel deterioration and microbiologically influenced corrosion. *Biofouling* **28**(9): 1003-1010.
- Thauer, R. K., Stackebrandt, E. and W. A. Hamilton.** (2007). Energy metabolism phylogenetic diversity of sulphate-reducing bacteria. *Sulphate-Reducing Bacteria: Environmental and Engineered Systems*. Cambridge: Cambridge University Press. p. 137.
- Venzlaff, H., Enning, D., Srinivasan, J., Mayrhofer, K. J. J., Hassel, A. W., Widdel, F. and M. Stratmann.** (2013). Accelerated cathodic reaction in microbial corrosion of iron due to direct electron uptake by sulfate-reducing bacteria. *Corrosion Science* **66**: 88-96.
- Videla, H. A.** (2000). An overview of mechanisms by which sulphate-reducing bacteria influence corrosion of steel in marine environments. *Biofouling* **15**(1-3): 37-47.
- Voordouw, G.** (1995). The genus *Desulfovibrio*: the centennial. *Appl Environ Microbiol* **61**(8): 2813.
- Voordouw, G., Armstrong, S. M., Reimer, M. F., Fouts, B., Telang, A. J., Shen, Y. and D. Gevertz.** (1996). Characterization of 16S rRNA genes from oil field microbial communities indicates the presence of a variety of sulfate-reducing, fermentative, and sulfide-oxidizing bacteria. *Appl Environ Microbiol* **62**(5): 1623-1629.
- Zhou, J., He, Q., Hemme, C. L., Mukhopadhyay, A., Hillesland, K., Zhou, A., He, Z., Van Nostrand, J. D., Hazen, T. C. and D. A. Stahl.** (2011). How sulphate-reducing microorganisms cope with stress: lessons from systems biology. *Nat Rev Microbiol* **9**(6): 452-466.
- Zuo, R.** (2007). Biofilms: strategies for metal corrosion inhibition employing microorganisms. *Appl Microbiol Biotechnol* **76**(6): 1245-1253.

Appendix A

***Fodinicurvata halophilus* sp. nov., a moderately halophilic bacterium
from a marine saltern**

Abstract

A Gram-stain-negative, rod-shaped, facultatively anaerobic, moderately halophilic bacterium, designated strain BA45AL^T, was isolated from water of a saltern in Santa Pola, Alicante, Spain. Cells were motile, catalase and oxidase positive. Strain BA45AL^T grew at temperatures in the range of 14-45 °C (optimally at 37 °C) and at pH 5.0-9.0 (optimally at pH 7.5). It grew in media containing 5-20 % (w/v) salts and optimally in media containing 10 % (w/v) salts. Phylogenetic analysis based on the comparison of 16S rRNA gene sequences revealed that strain BA45AL^T is a member of the genus *Fodinicurvata*. The closest relatives to this strain were *Fodinicurvata fenggangensis* YIM D812^T and *Fodinicurvata sediminis* YIM D82^T with sequence similarities of 98.2 % and 97.4 %, respectively. DNA-DNA hybridization between the novel isolate and these phylogenetically related species revealed relatedness of 15 % and 30 %, respectively, with respect to the aforementioned species. The major cellular fatty acids of strain BA45AL^T were C_{18:1}ω7c, C_{16:0} and iso-C_{15:0}. Its polar lipid pattern consisted of diphosphatidylglycerol, phosphatidylmethylethanolamine, phosphatidylinositol, and a number of unknown phospholipids. Based on the phenotypic, chemotaxonomic and phylogenetic data presented in this study, strain BA45AL^T constitutes a novel species of the genus *Fodinicurvata*, for which the name *Fodinicurvata halophilus* sp. nov. is suggested. The type strain of *Fodinicurvata halophilus* is strain BA45AL^T (= CCM 8504^T = CECT 8472^T = JCM 19075^T = LMG 27945^T).

Introduction

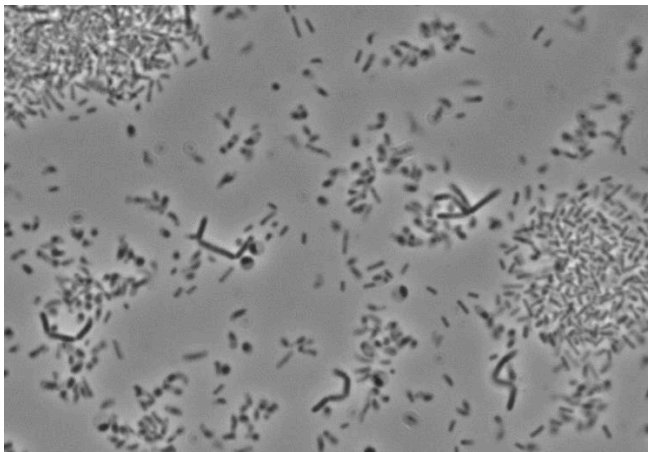
The genus *Fodinicurvata* belongs to the family *Rhodospirillaceae*, within the order *Rhodospirillales* (Pfening & Trüper, 1971) of the class *Alphaproteobacteria*. This genus was originally proposed by Wang *et al.* (2009) and to date it comprises two species, *Fodinicurvata sediminis* (Wang *et al.*, 2009) and *Fodinicurvata fenggangensis* (Wang *et al.*, 2009). Both species were isolated from a sediment sample collected from a salt mine in Yunnan, south-west China. The species of the genus *Fodinicurvata* stain Gram-negative, are facultatively anaerobic, non-motile, vibrioid or rod-shaped. Catalase and oxidase are produced and polyhydroxybutyrate (PHB) granules are observed. The predominant polar lipids consist of diphosphatidylglycerol, phosphatidylmethyl-ethanolamine and phosphatidylcholine. Phosphatidylinositol is variable between species. Their DNA G+C content ranges from 61.5 – 62.3 mol% (Wang *et al.*, 2009). Recent metagenomic studies have provided new insights into the microbial diversity along the salinity gradient of salterns located in Santa Pola and Isla Cristina in Spain (Ghai *et al.*, 2011; Fernández *et al.*, 2014 a,b; León *et al.*, 2014; Ventosa *et al.*, 2014). During the course of a study to search for the most abundant microorganisms in these salterns, a novel, moderately halophilic, yellow to cream pigmented, Gram-stain-negative bacterium, strain BA45AL^T, was isolated from a water sample. The pH of the water was 7.4 and its salinity was 12 % (w/v) salts. At the time of sampling, the temperature of the water was 28 °C. In this paper we describe the taxonomic features of this novel bacterium and propose it as a new species of the genus *Fodinicurvata*, as *Fodinicurvata halophilus* sp. nov.

Methods and Results

Aliquots of the water sample were diluted with a sterile salt solution, where 100 microliters was plated on saline media and incubated aerobically at 37° C. The isolation medium used was prepared with a 15% (g l⁻¹) salts mixture: NaCl, 117; MgCl₂.6H₂O, 19.5; MgSO₄.7H₂O, 30.5; CaCl₂.2H₂O, 0.3; KCl, 3; NaHCO₃, 0.06; NaBr, 0.23 (Subow, 1931), supplemented with 0.25 % (w/v) yeast extract (Difco) and 1.8 % (w/v) agar (Difco). The pH of the medium was adjusted to 7.5 with 1 M KOH. A pure culture of strain BA45AL^T was obtained after several transfers on the same medium. For routine growth, the strain was cultivated in the same medium but prepared with 10 % (w/v) total salts. The culture was maintained at -80 °C in the routine medium containing 50 % (v/v) glycerol. *Fodinicurvata fenggangensis* DSM 21159^T and *Fodinicurvata sediminis* DSM 21160^T obtained from the DSMZ (German Collection of Microorganisms and Cell Cultures) were used as reference strains and were grown following the recommendations of the culture collection.

Cell morphology and motility were examined using an Olympus CX41 microscope equipped with phase-contrast optics. Cells were motile, both rod- and vibrioid-shaped (Fig. A1.1). Colony morphology was observed on routine medium under optimal growth conditions after incubation at 37° C for 5 days. Colonies of strain BA45AL^T that formed on agar plates were circular, smooth, entire, opaque, yellow-cream pigmented, with a size of 0.3-0.5 mm. The strain was able to accumulate PHB, as was observed by using an Olympus CX41 microscope equipped with phase-contrast optics.

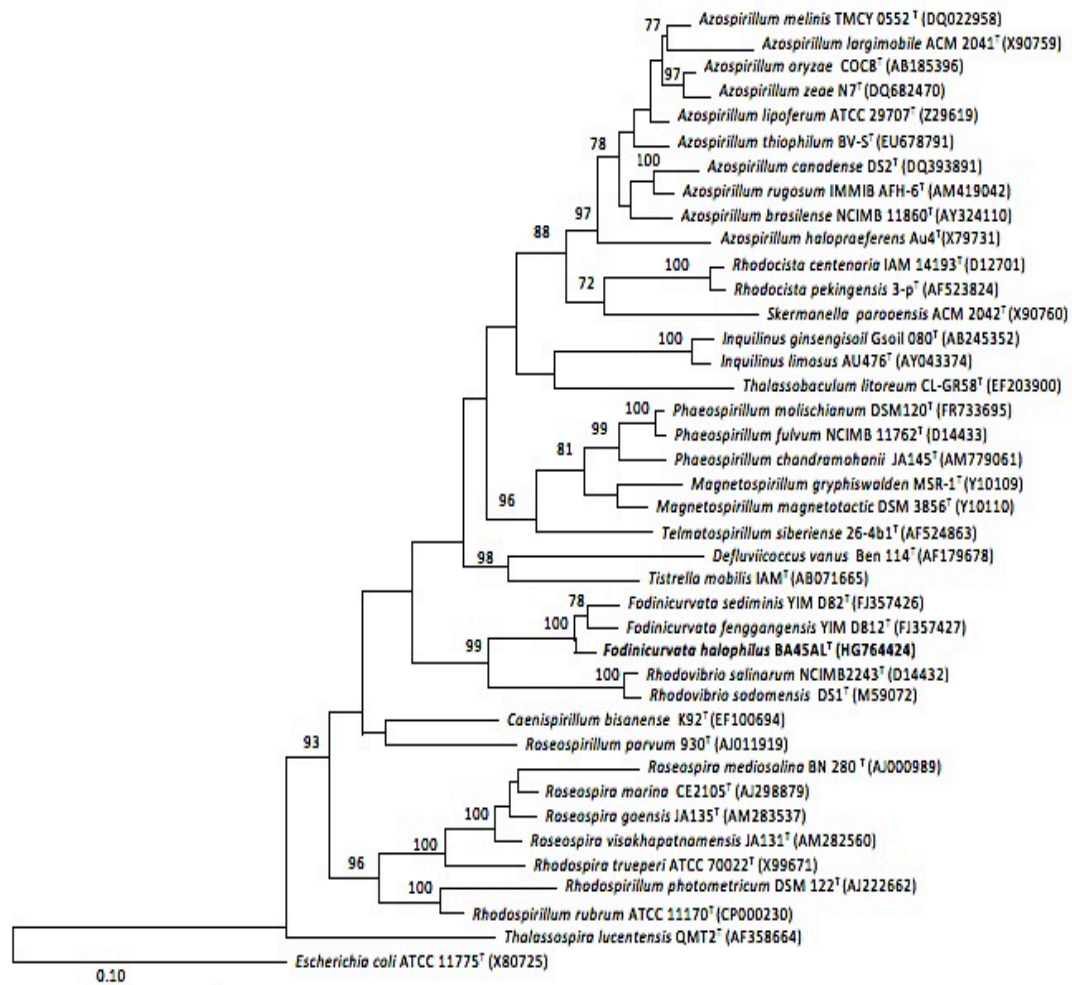
Figure A1.1. Phase-contrast micrograph of cells of strain BA45AL^T grown in liquid medium under optimal conditions. Scale bar, 1 μ m.



Genomic DNA from strain BA45AL^T was obtained using the method described by Marmur (1961). The 16S rRNA gene of the isolate was amplified by PCR using forward primer 16F27 and reverse primer 16R1488 (Mellado *et al.*, 1995). An almost complete 16S rRNA gene sequence (1392 nt) of strain BA45AL^T was obtained. The identification of the closest phylogenetic neighbours and calculation of pairwise 16S rRNA gene sequence similarity were achieved using the EzTaxon-e tool (Kim *et al.*, 2012). The 16S rRNA gene sequence similarities between BA45AL^T and the most closely related *Fodinicurvata* type strains, *Fodinicurvata fenggangensis* YIM D812^T and *Fodinicurvata sediminis* YIM D82^T were 98.2 and 97.4 %, respectively. The 16S rRNA gene sequence was aligned and checked against both primary and secondary structures of the 16S rRNA molecule using the alignment tool of the ARB software package. Phylogenetic trees were constructed using three different methods, namely the maximum-likelihood (Felsenstein, 1981), maximum-parsimony (Fitch, 1971) and

neighbour-joining (Saitou & Nei, 1987) algorithms integrated in the ARB software. The maximum-likelihood phylogenetic tree is presented in Figure A1.2.

Figure A1.2: Maximum-likelihood phylogenetic tree based on 16S rRNA gene sequences, showing the relationships between strain BA45AL^T and representatives of the family *Rhodospirillaceae*. Bootstrap percentages (based on 1000 replications) ≥ 70 % are shown at branch points. Bar represents 0.1 substitutions per nucleotide position.



Although no precise correlation exists between the percentage of 16S rRNA sequence divergence and species delineation, it is generally recognized that divergence values of 1.3% or more are significant (Stackebrandt & Goebel, 1994). However, due to the high sequence similarity values to its close relatives, DNA-DNA hybridization studies were performed. These studies were carried out using the competition procedure of the membrane method (Johnson, 1994) as described by Ventosa *et al.* (2004). The levels of DNA-DNA relatedness for strain BA45AL^T with respect to *Fodinicurvata fenggangensis* DSM 21160^T and *Fodinicurvata sediminis* DSM 21159^T were 30 and 15 %, respectively. These data confirmed that strain BA45AL^T represents a novel species of the genus *Fodinicurvata*, having DNA-DNA hybridization values <70 % with respect to the type strains of the most closely related species of the genus *Fodinicurvata* (Waine *et al.*, 1987; Stackebrandt & Goebel, 1994).

Optimal conditions for growth and range were determined by growing the strain in the routine medium prepared at the following salinity values: 0.5, 3, 5, 7, 7.5, 8, 10, 12, 15, 20 and 25% (w/v) total salts and at temperatures from 5 to 45 °C (in increments of 5 °C) and from 35 to 40 °C in increments of one unit. The pH range for isolate was determined in the routine medium at optimal salinity adjusted to pH values ranging from 4 to 10 (in increments of one pH unit). The growth was determined by monitoring the optical density using a spectrophotometer at 600 nm.

Strain BA45AL^T grew in media containing 5-20 % (w/v) salts and optimally in media containing 10 % (w/v) salts. No growth was observed in the absence of NaCl. It grew at temperatures in the range 14-45 °C (optimally at 37 °C) and at pH 5.0-9.0

(optimally at pH 7.5). The strain was able to grow anaerobically, determined after incubation in an anaerobic chamber (GasPak Anaerobic system, BBL).

All phenotypic features were carried out growing the strain in the routine medium prepared at 10% (w/v) total salts, pH 7.5 and at 37 °C. The production of acid from different carbohydrates was tested in a medium with 0.5 % (w/v) yeast extract and supplemented with 1% (w/v) of the carbohydrate tested (sterilized separately) (Ventosa *et al.*, 1982). To determine the utilization of different organic substrates as carbon and energy sources, a medium containing 0.05 % (w/v) yeast extract and supplemented with 1 % (w/v) of the tested substrate, was used (Ventosa *et al.*, 1982). The results for the utilization of different substrates are included in the species description.

Catalase activity was determined by adding a 1% (w/v) H₂O₂ solution to colonies on solid medium. The oxidase test was performed using a DrySlide assay (Difco). Strain BA45AL^T was catalase and oxidase positive. The following tests were conducted as described by Cowan and Steel (1977): hydrolysis of aesculin, casein, gelatin, Tween 80, and starch; urease and indole production; the methyl red, Voges-Proskauer test; nitrate and nitrite reduction, and Simmons citrate. The following tests were negative: methyl red, Voges-Proskauer, indole production from tryptone and Simmons's citrate, casein and starch hydrolysis. The strain was positive for nitrate reduction but nitrite was not reduced. Both gelatin and aesculin were hydrolyzed and the urease test was positive. Other phenotypic characteristics of strain BA45ALT are included in the species description.

Antimicrobial compounds sensitivity tests were performed by spreading the culture suspension on solid medium plates and applying discs impregnated with

antimicrobial compounds following the technique of Bauer-Kirby (Bauer *et al.*, 1966). Susceptibility to antimicrobial compounds was determined on agar plates using antimicrobial agent discs with the following concentrations: ampicillin (10 µg), chloramphenicol (30 µg), erythromycin (15 µg), gentamicin (10 µg), nalidixic acid (30 µg), neomycin (10 µg), novobiocin (30 µg), penicillin G (10 U) and rifampicin (30 µg). Strain BA45AL^T was resistant to ampicillin, erythromycin, gentamicin, nalidixic acid, neomycin, novobiocin, penicillin G, and rifampicin but susceptible to chloramphenicol. Several phenotypic differences were observed between strain BA45AL^T and the two closely related *Fodinicurvata* species, including those concerning motility, physiological and cultural features, nitrate reduction, hydrolysis of gelatin and aesculin, H₂S production, and utilization of several carbohydrates (Table A1.1).

Table A1.1: Characteristics that differentiate strain BA45AL^T from related species of the genus *Fodinicurvata*.

Taxa: 1, strain BA45AL^T; 2, *Fodinicurvata fenggangensis* DSM 21160^T; 3, *Fodinicurvata sediminis* DSM 21159^T. All data are from the present study, except where indicated. +, Positive reaction; -, negative reaction.

Characteristic	1	2	3
Colony pigmentation	Yellow-cream	Cream-white	Cream-white
Cell size (width x length; μm)	0.05-0.1 x 0.2-1.5	0.2-0.4 x 0.5-1.3	0.3-0.5 x 0.7-1.5
Motility	+	-	-
Temperature range ($^{\circ}\text{C}$)	14-45	15-42	15-42
NaCl range (% w/v)	5-20	1.5-20	1.5-20
pH range	5-9	6.5-8.5	6.5-8.5
Nitrate reduction	+	-	-
Hydrolysis of:			
Aesculin	+	-	+
Gelatin	+	-	-
Utilization of carbon sources:			
Fructose	+	-	-
Lactose	+	-	-
Fumarate	+	-	-
Hippurate	+	-	-
L-ornithine	+	-	-
Simmons citrate	-	+	+
H ₂ S production	+	-	-
Major fatty acids	C _{18:1} ω 7c, iso-C _{16:0} and iso-C _{15:0}	C _{18:1} ω 7c, 2-OH-C _{18:1} and C _{16:0}	C _{18:1} ω 7c, 2-OH-C _{18:1} and C _{16:0}
Polar lipids	Diphosphatidylglycerol, phosphatidylmethyl-ethanolamine, phosphatidylinositol and seven unknown phospholipids	Diphosphatidylglycerol, phosphatidylmethyl-ethanolamine, phosphatidylcholine, phosphatidylinositol and three unknown phospholipids	Diphosphatidylglycerol, phosphatidylmethyl-ethanolamine, phosphatidylcholine and an unknown phospholipid
Source	Salt water	Deposit of salt mine*	Deposit of salt mine*

*Data from Wang *et al.* (2009).

Cell biomass for fatty acid, polar lipid analyses and quinone composition of strain BA45AL^T, *Fodinicurvata sediminis* DSM 21159^T and *Fodinicurvata fenggangensis* DSM 21160^T was obtained by cultivation in nutrient agar (NA) supplemented with 5 % NaCl, incubated at 28 °C for 5 days. The whole-cell fatty acid composition of strain BA45AL^T and the reference strains was determined on cultures reaching the late-exponential stage of growth according to the four quadrants streak method (Sasser, 1990). Fatty acid methyl esters were prepared and analyzed according to the standard protocol of the Microbial Identification System (MIDI, Version 6.1; Identification Library TSBA40 4.1; Microbial ID). Extracts were analyzed using a Hewlett Packard model HP6890A gas chromatograph equipped with a flame-ionization detector as described by Kämpfer & Kroppenstedt (1996). The fatty acid profiles of strain BA45AL^T included C_{18:1} ω7c (35.6 %), iso-C_{16:0} (16.3 %) and iso-C_{15:0} (10.1 %) as the major fatty acids, followed by iso-C_{17:1} ω9c (5.8 %), C_{17:0} (5.5 %), C_{16:0} (3.3 %), C_{18:1} 2OH (3 %). The fatty acid profile of strain BA45AL^T was clearly different from those of the related taxa. Although all three species produce C_{18:1} ω7c as a major product, the novel organism also produces major amounts of iso-C_{16:0} and iso-C_{15:0} which are lacking in *Fodinicurvata sediminis* DSM 21159^T and *Fodinicurvata fenggangensis* DSM 21160^T (Table A1.2).

Table A1.2: Cellular fatty acid contents (percentages) of strain BA45AL^T and the type strains of phylogenetically closely related species.

Taxa: 1, strain BA45AL^T; 2, *Fodinicurvata fenggangensis* DSM 21160^T; 3, *Fodinicurvata sediminus* DSM 21159^T. All data are from this study. ND, Not detected; TR, traces.

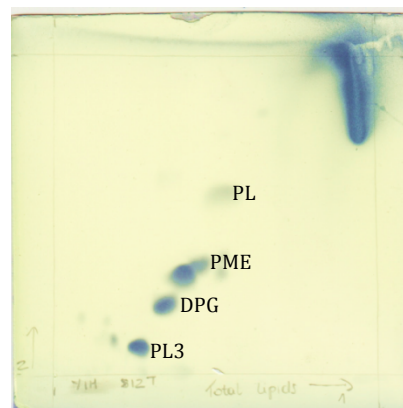
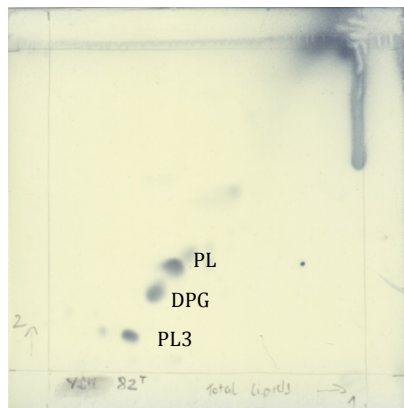
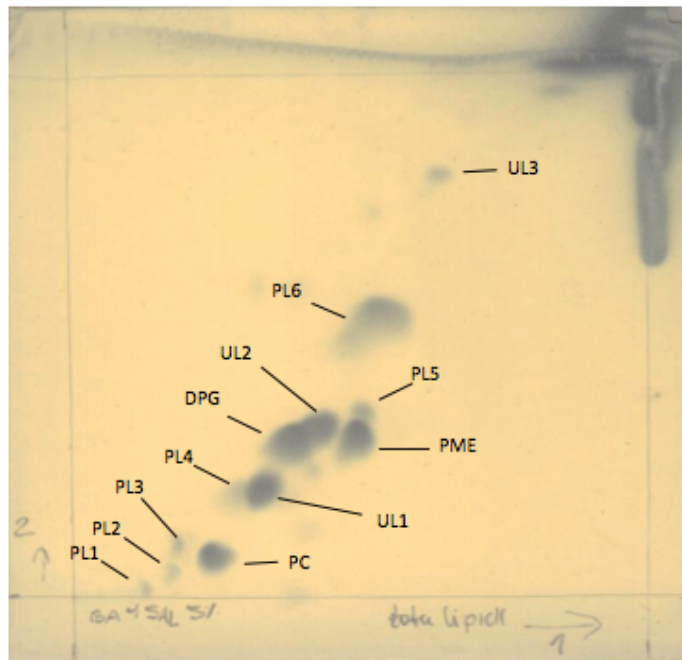
Fatty acids	1	2	3
C _{11:0}	2.9	ND	ND
C _{12:0}	1.1	ND	ND
iso-C _{12:0}	1.4	ND	ND
iso-C _{13:0} 3-0H	1.5	ND	ND
C _{14:0}	ND	1.4	1.4
iso-C _{15:0}	10.1	ND	ND
iso-C _{16:0}	16.3	ND	ND
C _{16:0}	3.3	10.6	11.8
C _{16:1} ω7c/ C _{16:1} ω6c	1.6	1.5	traces
C _{17:0}	5.5	traces	traces
Iso-C _{17:1} ω9c	5.7	ND	ND
C _{17:0} cyclo/ C _{18:0}	1.8	ND	ND
C _{18:0}	ND	6.9	9.3
C _{18:1} 2-OH	3	14.7	12.2
C _{18:1} ω7c	35.6	46.6	48.6
C _{18:0} 3-OH	ND	1.8	1.3
C _{18:1} ω7c 11-methyl	0.3	5	1
C _{18:1} ω9c	ND	1.3	2
C _{19:0} cyclo w8c	2	7.4	7.9
C _{20:2} w6,9c	0.3	1	traces

Major products are shown in bold type.

The polar lipids of strain BA45AL^T and the reference strains were analyzed as described by Groth *et al.* (1996). The polar lipids detected in strain BA45AL^T were diphosphatidylglycerol, phosphatidylmethylethanolamine, phosphatidylinositol and a number of unknown phospholipids (Fig. A1.3). It is important to note that in our hands TLC plates from the novel strain, BA45AL^T, or neighbours, *Fodinicurvata sediminis* DSM 21159^T and *Fodinicurvata fenggangensis* DSM 21160^T, did not possess choline-containing lipids as previously described (Wang *et al.*, 2009). The total polar lipid pattern, along with other physiological properties, more closely resembles *Fodinicurvata sediminis* DSM 21159^T but clear differences are also observed.

Quinone analyses were carried out by the protocol Identification of the DSMZ, Braunschweig, Germany (Tindall *et al.*, 2007). The novel strain contained a ubiquinone with ten isoprene units (Q-10) that is commonly found in species belonging to the genus *Fodinicurvata* (Wang *et al.*, 2009). Based on the phenotypic, chemotaxonomic and phylogenetic data presented in this study, strain BA45AL^T represents a novel species of the genus *Fodinicurvata*, for which the name *Fodinicurvata halophilus* sp. nov. is proposed.

Figure A1.3: Two-dimensional thin layer chromatograms of the polar lipids of strain BA45AL^T, *Fodinicurvata fenggangensis* DSM 21160^T; 3, *Fodinicurvata sediminis* DSM 21159^T. DPG, diphosphatidylglycerol; PME, phosphatidylmethylethanolamine; PI, phosphatidylinositol; PL1-7, unknown phospholipids, UL, unknown lipids.



Description of *Fodinicurvata halophilus* sp. nov.

Fodinicurvata halophilus (ha.lo'phi.lus. Gr. masc. n. *hals*, *halos* salt; Gr. adj. *philos* loving; N.L. masc. adj. *halophilus* salt loving).

Cells are motile, rod to vibrioid shaped, 0.05-0.1 x 0.2-1.5 μm in size and stain Gram-negative. Endospores are not produced. Colonies are circular, smooth, entire, opaque, yellow-cream pigmented, with a size of 0.3-0.5 mm in diameter after 5 days at 37 °C on plates containing 10 % (w/v) total salts. In liquid medium, growth has a strong tendency to form aggregates at the bottom. Grows over a wide range (5-20 %, w/v) of salts concentrations, with optimal growth at (10 %, w/v) salts. No growth in the absence of NaCl. Grows at 14-45 °C (optimally at 37 °C) and pH 5.0-9.0 (optimally at pH 7.5). PHB is accumulated. Facultatively anaerobic. Catalase and oxidase positive. Nitrate but not nitrite is reduced. Aesculin and gelatin are hydrolyzed. DNA, starch, Tween 80 or casein are not hydrolyzed. H₂S is produced. Indole, Simmons citrate, methyl red, and Voges-Proskauer tests are negative. Urease is positive. Acid is not produced from various carbohydrates including: glycerol, D-arabinose, D-glucose, D-fructose, D-mannitol, galactose, lactose, sucrose, maltose, D-mannose, D-melezitose, melibiose, D-raffinose and sorbitol. The following compounds are utilized as sole source of carbon and energy: D-glucose, D-galactose, D-fructose, D-arabinose, maltose, D-lactose, xylose, L-valine, L-ornithine, L-glutamine, L-serine, L-threonine, formate, fumarate, propionate, hippurate, butanol, dulcitol, ethanol and glycerol. The following compounds are not utilized as sole source of carbon and energy: D-cellobiose, D-ribose, D-mannose, D-melibiose, D-trehalose, sucrose, D-raffinose, D-melezitose, salicine, L-isoleucine, L-methionine, L-cysteine, L-phenylalanine, L-lysine, benzoate, citrate, DL-

malate, DL-tartrate, succinate, D-mannitol, myo-inositol, propanol, D-sorbitol, xylitol and methanol. The predominant fatty acids are C_{18:1} ω7c, iso-C_{16:0} and iso-C_{15:0}. Polar lipids include diphosphatidylglycerol, phosphatidylmethylethanolamine, phosphatidylinositol and seven unknown phospholipids. Respiratory quinone is Q10. The type strain of *Fodinicurvata halophilus* is strain BA45AL^T (= CCM 8504^T = CECT 8472^T = JCM 19075^T = LMG 27945^T), isolated from water of a marine saltern.

Acknowledgements

This work represents the collaborative efforts of taxonomic laboratories as a means to spread the use of classical characterization techniques. *Fodinicurvata halophilus* was isolated by C. Infante-Dominguez, a post-graduate fellow with the Spanish Ministry of Science and Innovation who visited the Lawson Laboratory for advisory completion of descriptive tests. This research was supported by grants from the Spanish Ministry of Science and Innovation (CGL2013-46941-P and BIO2011-12879-E), and the Junta de Andalucía (P10-CVI-6226). FEDER funds and the Plan Andaluz de Investigación also supported this project.

References

- Barrow, G. I. & Feltham, R. K. A. (editors)** (2003). *Cowan and Steel's Manual for the Identification of Medical Bacteria*. 3rd edition. Cambridge: Cambridge University Press.
- Bauer, A. W., Kirby, W. M. M., Sherris, J. C. & Turck, M.** (1966). Antibiotic susceptibility testing by a standardized single disk method. *Am J Clin Pathol* **45**, 493-496.
- Bowman, J. P. & McMeekin, T. A.** (2005). Order X. *Alteromonadales*. In *Bergey's Manual of Systematic Bacteriology*, 2nd edn, vol. 2, *The Proteobacteria*, part B, *The Gammaproteobacteria*, pp. 443–490. Edited by D. J. Brenner, N. R. Krieg, J. T. Staley & G. M. Garrity. New York: Springer.
- Cowan ST, & Steel KJ.** (1977). *Manual for the identification of medical bacteria*. Cambridge University Press, London, United Kingdom.
- Felsenstein, J.** (1985). Confidence limits on phylogenies: an approach using bootstrap. *Int J Org Evol* **39**, 783–791.
- Fernández, A.B., Ghai, R., Martín-Cuadrado, A.B., Sánchez-Porro, C., Rodríguez-Valera, F. & Ventosa, A.** (2014a). Prokaryotic taxonomic and metabolic microbial diversity of an intermediate salinity hypersaline habitat assessed by metagenomics. *FEMS Microbiol Ecol* **88**, 623-635.
- Fernández, A. B., Vera-Gargallo, B., Sánchez-Porro, C., Ghai, R., Papke, R. T., Rodríguez-Valera, F. & Ventosa.** (2014b). Comparison of prokaryotic community structure from Mediterranean and Atlantic saltern concentrator ponds by a metagenomic approach. *Front Microbiol* **5**: 196.
- Fitch, W. M.** (1971). Toward defining the course of evolution: minimum change for a specific tree topology. *Syst Zool* **20**: 406-416.
- Ghai, R., Pašić, L., Fernández, A. B., Martín-Cuadrado, B., Mizuno, C. M., McMahon, K.D., Papke, R.T., Stepanauskas, R., Rodríguez-Brito, B., Rohwer, F., Sánchez-Porro, C., Ventosa, A. & Rodríguez-Valera, F.** (2011). New abundant microbial groups in aquatic hypersaline environments. *Sci Rep* **1**: 135.
- Groth, I., Schumann, P., Weiss, N., Martin, K. & Rainey, F. A.** (1996). *Agrococcus jenensis* gen. nov., sp. nov., a new genus of actinomycetes with diaminobutyric acid in the cell wall. *Int J Syst Bacteriol* **46**: 234–239.
- Johnson, J. L.** (1994). Similarity analysis of DNAs. In *Methods for General and Molecular Bacteriology*, pp. 655–681. Edited by P. Gerhardt, R. G. E. Murray, W. A. Wood & N. R. Krieg. Washington, DC: American Society for Microbiology.

- Kim, O.-S., Cho, Y.-J., Lee, K., Yoon, S.-H., Kim, M., Na, H., Park, S.-C., Jeon, Y. S., Lee, J.-H., Yi, H., Won, S. & Chun, J.** (2012). Introducing EzTaxon-e: a prokaryotic 6S rRNA gene sequence database with phylotypes that represent uncultured species. *Int J Syst Evol Microbiol* **62**: 716-721.
- Kampfer, P. & Kroppenstedt, R. M.** (1996). Numerical analysis of fatty acid patterns of coryneform bacteria and related taxa. *Can J Microbiol* **42**: 989–1005.
- Kushner, D. J. & Kamekura, M.** (1988). Physiology of halophilic eubacteria. In *Halophilic Bacteria*, vol. I, pp. 109–140. Edited by F. Rodríguez. Boca Raton, FL: CRC Press.
- León, M. J., Fernández, A. B., Ghai, R., Sánchez-Porro, C., Rodríguez-Valera, F. & Ventosa, A.** (2014). From metagenomics to pure culture: isolation and characterization of the moderately halophilic bacterium *Spiribacter salinus* gen. nov., sp. nov. *Appl Environ Microbiol* **80**: 3850-3857.
- Marmur, J.** (1961). A procedure for the isolation of deoxyribonucleic acid from microorganisms. *J Mol Biol* **3**: 208–218.
- Mata, J. A., Martínez-Cánovas, J., Quesada, E. & Béjar, V.** (2002). A detailed phenotypic characterization of the type strains of *Halomonas* species. *Syst Appl Microbiol* **25**: 360–375.
- Mesbah, M., Premachandran, U. & Whitman, W. B.** (1989). Precise measurement of the G+C content of deoxyribonucleic acid by high-performance liquid chromatography. *Int J Syst Evol Bacteriol* **39**: 159-167.
- Murray, R. G. E., Doetsch, R. N. & Robinow, C. F.** (1994). Determinative and cytological light microscopy. In *Methods for General and Molecular Bacteriology*, pp. 21–41. Edited by P. Gerhardt, R. G. E. Murray, W. A. Wood & N. R. Krieg. Washington, DC: American Society for Microbiology.
- Saitou, N. & Nei, M.** (1987). The neighbor joining method: a new method for reconstructing phylogenetic trees. *Mol Biol Evol* **4**: 406-425.
- Sasser, M.** (1990). *Identification of bacteria by gas chromatography of cellular fatty acids*. MIDI Technical Note 101. Newark, DE: MIDI Inc.
- Stackebrandt, E. & Goebel, B. M.** (1994). Taxonomic note: a place for DNA-DNA reassociation and 16S rRNA sequence analysis in the present species definition in bacteriology. *Int J Syst Bacteriol* **44**: 846–849.
- Tamura, K., Peterson, D., Peterson, N., Stecher, G., Nei, M. & Kumar. S.** (2011). MEGA5: Molecular evolutionary genetics analysis using maximum likelihood, evolutionary distance, and maximum parsimony methods. *Mol Biol Evol* **28**, 2731-2739.

- Thompson, J. D., Gibson, T. J., Plewniak, F., Jeanmougin, F. & Higgins, D. J.** (1997). The clustral X windows interface: Flexible strategies for multiple sequence alignment aided by quality analysis tools. *Nucleic Acids Res* **24**: 4876–4882.
- Tindall, B. J., Rosselló-Móra, R., Busse, H.-J., Ludwig, W. & Kämpfer, P.** (2010). Notes on the characterization of prokaryote strains for taxonomic purposes. *Int J Syst Evol Microbiol* **60**: 249–266.
- Tindall, B. J., Sikorski, J., Smibert, R. A. & Krieg, N. R.** (2007). Phenotypic characterization and the principles of comparative systematics. In *Methods for General and Molecular Microbiology*, pp. 330-393. Edited by C. A. Reddy, T. J. Beveridge, J. A. Breznak, G. A. Marzluf, T. M. Schmidt and R. L. Snyder. Washington, D. C.: ASM Press.
- Torreblanca, M., Rodríguez-Valera, F., Juez, G., Ventosa, A., Kamekura, M. & Kates, M.** (1986). Classification of non-alkaliphilic halobacteria based on numerical taxonomy and polar lipid composition, and description of *Haloarcula* gen. nov. and *Haloferax* gen. nov. *Syst Appl Microbiol* **8**: 89–99.
- Ventosa, A., Quesada, E., Rodríguez-Valera, F., Ruiz-Berraquero, F. & Ramos-Cormenzana, A.** (1982). Numerical taxonomy of moderately halophilic Gram-negative rods. *J Gen Microbiol* **128**: 1959–1968.
- Ventosa, A., Gutiérrez, M. C., Kamekura, M., Zvyagintseva, I. S. & Oren, A.** (2004). Taxonomic study of *Halorubrum distributum* and proposal of *Halorubrum terrestre* sp. nov. *Int J Syst Evol Microbiol* **54**: 389–392.
- Ventosa, A., Fernández, A. B., León, M. J., Sánchez-Porro, C. & Rodríguez-Valera, F.** (2014). The Santa Pola saltern as a model for studying the microbiota of hypersaline environments. *Extremophiles* **18**: 811-824.
- Wang, Y. X., Liu, J.-H., Zhang, X. X., Chen, Y.-G., Wang, Z. G., Chen, Y., Li, Q. Y., Peng, Q. & Cui, X. L.** (2009). *Fodinicurvata sediminis* gen. nov., sp. nov. and *Fodinicurvata fenggangensis* sp. nov., poly- β -hydroxybutyrate-producing bacteria in the family *Rhodospirillaceae*. *Int J Syst Evol Microbiol* **59**: 2575–2581.
- Wayne, L. G., Brenner, D. J., Colwell, R. R., Grimont, P. A. D., Kandler, O., Krichevsky, M. I., Moore, L. H., Moore, W. E. C., Murray, R. G. E., Stackebrandt, E., Starr, M. P. & Trüper, H. G.** (1987). Report of the ad hoc committee on reconciliation of approaches to bacterial systematics. *Int J Syst Bacteriol* **37**: 463-464.

Appendix 2

Peptostreptococcus canis sp. nov., isolated from subgingival plaque
from canine oral cavity

Abstract

A polyphasic taxonomic study was performed on two strains of an unknown Gram-positive, assacharolytic, nonspore-forming, obligately anaerobic coccus-shaped bacterium isolated from oral subgingival plaque of Labrador retriever dogs. Comparative 16S rRNA gene sequencing confirmed that these isolates were highly related to each other and formed a hitherto unknown lineage within the clostridial rRNA XI cluster of organisms. Pairwise analysis demonstrated that the novel organism to be most closely related to members of the genus *Peptostreptococcus* with 16S rDNA gene sequence similarity values between 92.8% and 96.7%, respectively. The G+C DNA base composition was 30.8 mol% and the major cellular fatty acids included iso-C_{14:0}, iso-C_{16:0}, and iso-C_{16:0 DMA}. Based on biochemical, chemotaxonomic, and phylogenetic evidence it is proposed that the unknown bacterium be classified as a new species, *Peptostreptococcus canis* sp. nov. The type strain is CCUG 57081^T.

1. Introduction

The genus *Peptostreptococcus* was created in 1936 by Kluver and van Niel, and by the 1990's contained 18 species comprised of obligately anaerobic, Gram-positive, non-sporeforming, coccoid and coccobacillary bacteria that were physiologically and biochemically diverse [1]. The advent of 16S rRNA sequencing confirmed the heterogeneity of the genus and subsequently underwent a major revision with many former species being transferred to a number of genera that include

Anaerococcus, *Peptoniphilus*, *Finegoldia*, *Micromonas*, *Gallicola*, *Slackia*, *Ruminococcus* and *Atopobium* [1, 2]. The result of these reclassifications was that *Peptostreptococcus anaerobius* remained as the only validly named *Peptostreptococcus* species. More recently, two additional species were described, *P. stomatis* isolated from the human oral cavity [3], and *P. russellii* originating from underground swine manure pits [4].

In a recent study, Dahlén and colleagues undertook an investigation into the predominant bacterial microflora in subgingival plaque in dogs [5]. Two Gram-positively staining coccus-shaped strains were isolated and deposited with the CCUG for identification. Almost identical biochemical profiles demonstrated that these isolates resembled members of peptostreptococci. While 16S rRNA gene sequencing confirmed that these isolates were almost identical, forming a hitherto unknown lineage within the Clostridial rRNA XI cluster of organisms [6]. Pairwise analysis demonstrated that the novel organism was most closely related to *P. anaerobius*, *P. russellii*, and *P. stomatis* with 16S rRNA gene sequence similarity values of 95.8%, 92.8%, and 96.7%, respectively. Based on phenotypic, chemotaxonomic, and phylogenetic considerations, it was proposed that the unknown organism originating from the oral plaque of a dog be classified as novel species of *Peptostreptococcus* as *Peptostreptococcus canis* sp. nov. (type strain CCUG 57081^T).

2. Materials and Methods

2.1. Cultures and cultivation

Two isolates designated CCUG 57081^T and CCUG 57313 were recovered from the subgingival plaque of two 1 year old Labrador retriever dogs as described previously [5]. Samples was diluted into a series of 1:10 and 1:1000 and spread uniformly over the entire surface of a Brucella agar plate (BBL Microbiological Systems, Cockeysville, MD, USA) enriched with 5% defibrinated horse blood, 0.5% hemolysed horse blood and 5 mg/L of menadione. The plates were anaerobically incubated for 7 days in jars at 37 °C with an atmosphere of 95% H₂ and 5% CO₂. Colonies were picked and streaked repeatedly to purity. The strains were deposited with CCUG for identification.

2.2. Phenotypic characterization

Gram staining was performed with a commercial kit (Sigma, St. Louis, IL) according to manufacturer's instructions. The strains were biochemically characterized by using a combination of conventional tests, API ID 32A, and API ZYM systems, according to the manufacturer's instructions (API bioMérieux, Mary I'Etoile, France). All biochemical tests were performed in duplicate. Fourteen dietary sugars and two sugar alcohols were tested; glucose (Merck, Darmstadt, Germany), fructose (Merck), lactose (Difco Laboratories, Detroit, Michigan, US), sucrose (Merck), maltose (Merck), mannose (Merck), arabinose (Merck), cellobiose (Sigma-Aldrich, Stockholm, Sweden), melezitose (ICN Biochemicals, Inc., Cleveland, Ohio, US), melibiose (Sigma-Aldrich), raffinose (Merck), rhamnose (Merck), salicin (Merck), trehalose (Merck), mannitol

(Difco) and sorbitol (Merck). They were prepared in 2% aqueous solutions and sterile filtered by Whatman® Puradisc™ 25 mm PES 0.2 µm grade filters (Sigma-Aldrich). Brucella agar plates (BBL Microbiology Systems, Cockeysville, MD, USA) and 8 ml of Brain Heart Infusion broth (BHI, Difco) plus 1% glucose medium were used for anaerobic culturing of the two *Peptostreptococcus canis* strains (CCUG 57081 and CCUG 57314). A modified BHI broth without addition of carbohydrates was employed in the fermentation assay (pH 7.4). The *Peptostreptococcus* strains were grown in an anaerobic atmosphere for 72 hours at 37 °C. Pure colonies were picked and subcultured in 8 ml BHI broth plus 1% glucose for 48 hours. To eliminate traces of glucose from the culture medium, the bacteria were centrifuged at 3500 rpm and the medium discarded. The bacterial cell pellets were suspended in sterile phosphate- buffered saline (PBS), sodium chloride 85 mM, potassium phosphate 25 mM (pH 7.4), centrifuged and resuspended in PBS. The optical densities were adjusted to 1.0 (650 nm) and these suspensions were immediately used in the fermentation assay. The fermentation assay was performed in microtiter plates (96 Microwell™ Plates Nunclon™Δ; Nunc, Roskilde, Denmark); 50 µl of modified BHI broth (without addition of sugar) was mixed with 50 µl of each of the 16 carbohydrates in the wells. A sterile filtered 3% solution of bromocresol purple was used as pH indicator in the assay. The pH indicator was mixed with each of the bacterial strains (1:1) and 10 µl of the blend was added to each well with the different carbohydrates. The plates were incubated at 37 °C in anaerobic conditions with 10% H₂, 5% CO₂ in N₂ and were examined for color changes after 24 and 48 hours of incubation. For the negative control, PBS replaced bacterial cells. Coagulase activity was determined using a commercial kit (Sigma, St. Louis, IL)

according to manufacturer's instructions. *Staphylococcus aureus* was used as a positive control. Hemagglutination using horse erythrocytes was also tested and other phenotypic tests were performed as described by Tindall *et al.* [7].

2.3 DNA isolation and 16S rRNA gene sequencing and phylogenetic analysis

To provide a rapid means of identification and determine the phylogenetic position of the canine oral isolates, 16S rRNA gene sequence analysis was performed as described previously [5]. The closest known relatives of the new isolates were determined by performing database searches using the program FASTA [8]. These sequences and those of other related strains were retrieved from EMBL / GenBank and aligned with the newly determined sequences using the program SEQtools [9]. The resulting multiple sequence alignment was corrected manually using the program GeneDoc [10], and a phylogenetic tree was constructed according to the neighbor-joining method with the programs SEQtools and Treeview [11]. The stabilities of the groupings were estimated by bootstrap analysis (1000 replications) using the same programs. All major branching nodes were confirmed by maximum parsimony (data not shown). Determination of mol % G+C was carried out by thermal denaturation of chromosomal DNA using a Beckman model DU 640 spectrophotometer equipped with a high performance temperature controller and T_m analysis software [12].

2.4. GenBank accession numbers

The GenBank/EMBL accession numbers for the 16S rRNA gene sequence of strain CCUG 57081^T is HE687281.

2.5 Cellular fatty acid analysis

Fatty acid methyl ester (FAME) analysis was performed via gas chromatography, using a standardized protocol and a system similar to that of the MIDI Sherlock MIS system (www.ccug.se/pages/CFA_method_2008.pdf) as described previously [13-15]. Cells were grown for 3 days on agar Chocolate agar (Brain Heart Infusion, Difco 241830) under anaerobic conditions for 72 hours at 37 °C. Analysis was carried out with a Hewlett Packard HP 5890 GC equipped with a phenyl methyl silicone fused silica capillary column (HP-5 25m x 0.2 mm x 0.33 mm film thickness) and a flame ionization detector. Hydrogen was used as the carrier gas. The temperature program was initiated at 170 °C and increased at 5 °C min⁻¹ to a final temperature of 270 °C. Integration of peaks and further calculations was performed by a HP 3396A integrator. Fatty acid methyl esters were identified and quantified, and the relative amount of each fatty acid was expressed in terms of the percentage of total fatty acids in the profile of the strain.

3. Results and Discussion

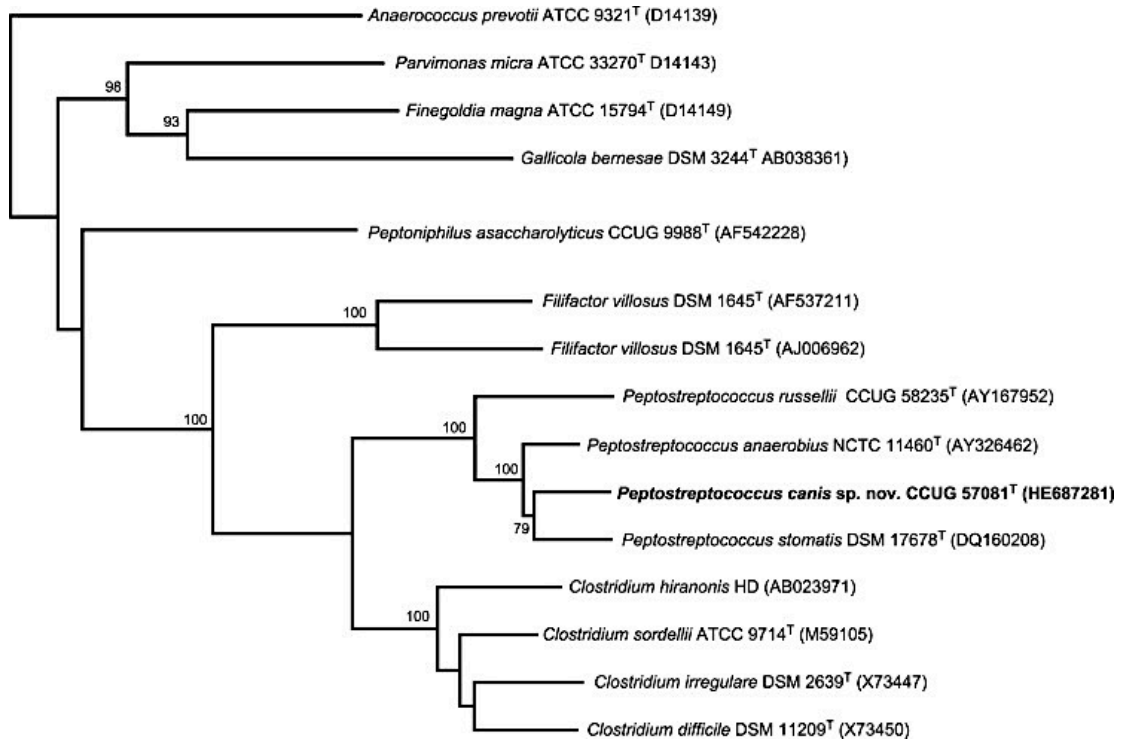
3.1. Identification and phylogenetic analysis

The unknown organism recovered from canine subgingival plaque consisted of Gram-positive, catalase- and oxidase-negative, non-motile coccid or ovoid-shaped cells. After 72 hours of anaerobic growth on Brucella and chocolate agar plates at 37 °C, colonies were 1-1.5 mm in diameter, grey-white color, round, smooth, shiny and non-hemolytic. No growth was observed after 24 hours in static or shaking aerobic BHI broth, and no growth on aerobic BHI agar plates. Anaerobic growth occurs in Brain Heart Infusion broth (BHI, Difco) plus 1% glucose medium but is improved by replacing glucose with 5-10% horse serum. The organism was able to grow in liquid culture at 25- 45 °C with an optimum temperature of 37 °C. No growth was observed at 4 °C or at 50 °C. Using the API rapid ID32An, only α -glucosidase, proline arylamidase, and mannose were found to be positive. All reactions in the API ZYM test system were negative except for α -glucosidase. Using the API rapid ID32An test kit a profile of 0 4 0 2 0 2 0 0 0 0 was obtained that corresponds to positive reactions for α -glucosidase, mannose, and proline arylamidase. All other reactions were negative. Employing the API ZYM system, a positive reaction was obtained only for β -glucosidase, all other tests in the test gallery were negative. The profiles for each test system employed are given in the species description. Nitrate was not reduced and indole was not produced. Neither of the two peptostreptococcal strains were able to utilize any of the 16 carbohydrates used in the fermentation assay supporting a proteolytic mode of nutrition. The pH was found to be slightly alkaline ranging between 7.9 and 8.1. Presence of spores was determined by visual examination, as well as by incubation of cultures in

95% ethanol followed by plating onto anaerobic agar medium. No spores were identified by either method. Coagulase activity was investigated at 4 hours and 24 hours and was found to be negative. Cellular fatty acid analysis demonstrated that the novel organism contained major amounts of iso-C_{14:0}, iso-C_{16:0}, and iso-C_{16:0} DMA. The full profile is given in Table B1.1.

On the basis of pairwise 16S rRNA gene sequence comparisons, the 2 isolates were highly related to each other genetically (99.5 %). Sequence searches of DNA Database libraries revealed that the unknown organism was a member of the *Firmicutes* phylum within the rRNA cluster XI [6]. Pairwise comparisons based on almost the full length of 16S rRNA gene sequences (=1400 nt) revealed significant sequence divergence values between the unknown bacterium and the type strains of its closest species, *P. anerobius* (95.8% sequence similarity), *P. russellii* (92.8% sequence similarity), and *P. stomatis* (96.7 % sequence similarity), respectively. A phylogenetic tree, constructed by the neighbor-joining method, depicting the phylogenetic affinity of the novel bacterium as exemplified by strain CCUG 57081^T, is shown in Figure B1.1. There is no precise correlation between 16S rRNA gene sequence divergence and species delineation, but it is generally recognized that divergence values of 3% or more are significant [16] . Recent data demonstrates that this value can be decreased to 1.3% without loss of resolution [17]. Tree topology and sequence divergence values (>3.3%) show that the unidentified coccus-shaped organism clearly represents a novel lineage within the genus *Peptostreptococcus*.

Figure B1.1: Unrooted tree showing the phylogenetic relationships of *Peptostreptococcus canis* sp. nov., and some other organisms within rRNA clusters XI and XIII. The tree constructed using the neighbor-joining method was based on a comparison of approx. 1320 nucleotides. Bootstrap values, expressed as a percentage of 1000 replications, are given at branching points; only significant values are shown. The bar represents a sequence divergence range of 1%.



The novel organism shares a branching node with *P. stomatis*, recovered from a human oral cavity that contained sites of dento-alveolar abscesses, endodontic infections, periodontal pockets and pericoronal infections. It is noteworthy to mention that *P. stomatis* processes an additional 25 bases in the 16S rRNA secondary structure of the variable region 1 when compared to *P. anaerobius* and *P. russellii*, as reported by Downs *et al.* (2006) [3] and Whitehead *et al.* (2011) [4], respectively. The sequences of the two strains of novel organisms from canine plaque described here showed that they

too contain these additional nucleotide bases (although with some slight changes in the nucleotides present) (Fig. B1.2). *Peptostreptococcus stomatis* and *P. canis* are both derived from the oral cavity, albeit from different host species, and both contain this modification to their 16S RNA secondary structure. Therefore, it will be interesting to see if future species recovered from the oral cavity of different animals also contain this feature, perhaps proving to be a useful diagnostic signature for oral peptostreptococci. In a recent study using 51 canines, Dewhirst *et al.* [18] recovered over 100 cloned sequences that were almost identical to that described in this study, all of which included the identical 25 base insertion. Although this study suggests that this organism is not a dominant member of the canine oral microbiota, it demonstrates that the novel species described here is commonly found within this ecosystem. Strains CCUG 57081^T and CCUG 57313 were recovered from subgingival plaque in close proximity to inflamed gingival tissue; their assaccarolytic nature may support a role in the destruction of tissue. The description of this novel species will facilitate its future isolation and a closer examination of its role in disease processes. Based on phenotypic, chemotaxonomic, and phylogenetic evidence that demonstrates its separateness from other members of the genus *Peptostreptococcus*, we consider the unidentified organism merits classification in a new species, for which the name *Peptostreptococcus canis* sp. nov. is proposed. In addition to its unique 16S sequence, *Peptostreptococcus canis* sp. nov. may be differentiated from *Peptostreptococcus anerobius*, *Peptostreptococcus russellii*, and *Peptostreptococcus stomatis* by characteristics shown in Table B1.1 and Table B1.2.

Figure B1.2: 16 rRNA gene sequence alignment of variable region 1 for *Peptostreptococcus canis*, *P. anaerobius*, *P. russellii*, and *P. stomatis*.

```

P. russellii    CAAGTCGAGCG-----CGCTCCCTTTG  GTGCTTGCAC-----CAAAGAAGA
P. anaerobius CAAGTCGAGCG-----CGTCTGATTG   ATGCTTGCAT-----NTATGAAAG
P. stomatis    CAAGTCGAGCGAGGGTTTGCTCAGTATTGAGTATTCTA  AGACTAGAATGTTCAATTCTGAGCAAAA
P. canis       CAAGTCGAGCGCGTTGTGCTTAGTATTGAGTGTTTTATTGATATAAAACATTGAATTCTATGCACAA
                16 bases                               9 bases

```

Table B1.1: Cellular fatty acid compositions (%) of *Peptostreptococcus canis* sp. nov., *Peptostreptococcus anaerobius*, *Peptostreptococcus russellii*, and *Peptostreptococcus stomatis*.

Fatty acid ^a	CCUG 57081 ^T	<i>P. anaerobius</i> CCUG 7835 ^T	<i>P. russellii</i> CCUG 58235 ^T	<i>P. stomatis</i> CCUG 51858 ^T
C _{10:0}		1.1	–	–
anteiso-C _{11:0}		–	0.8	–
C _{12:0}		3.5	–	–
iso-C _{12:0}	3.2	4.5	5.7	0.4
iso-3OH-C _{13:0}	8.3	2.4	–	5.5
anteiso-C _{13:0}		1.8	2.7	–
C _{14:0}	1.2	7.0	–	0.5
C _{14:0} 2,4 dimethyl	2.6		1.5	1.8
iso-C _{14:0}	14.9	5.5	1.2	23.3
2OH-C _{14:0}		0.5	–	–
anteiso-C _{15:0}		1.4	–	0.5
C _{16:0}	6.1	19.3	2.2	7.7
C _{16:0} aldehyde	1.3	–	–	0.9
iso-C _{16:0}	14.2	4.4	17.3	11.2
iso-C _{16:0} DMA	10.7	2.8	6.5	7.6
iso-C _{17:1} /C _{16:0} DMA	5.1	7.5	9.2	3.5
anteiso-C _{17:0}	0.9	1.0	4.4	1.7
anteiso-C _{17:0} DMA		–	2.1	–
iso-3OH-C _{17:0}	3.0	–	–	–
C _{18:0}	1.7	1.2	2.2	3.3
iso-C _{18:0}		–	2.6	1.8
C _{18:0} ω9c	4.0	17.8	2.1	2.8
C _{18:1} ω9c DMA	2.7	5.4	2.9	4.2
C _{18:2} ω6,9c/anteiso-C _{18:0}	6.2	4.5	–	3.9
C _{18:2} DMA		5.4	4.8	6.6
Iso-C _{19:1}	2.8	–	1.8	1.8
Unknown		11.9	9.7	7.9
Unidentified		2.5	3.8	2.3

a Data obtained from CCUG, all growth conditions were identical. Bold values represent major products.

Table B1.2: Differential characteristics of *Peptostreptococcus canis* sp. nov., *Peptostreptococcus anaerobius*, *Peptostreptococcus russellii*, and *Peptostreptococcus stomatis*.

Characteristic	<i>P. canis</i> sp. nov. CCUG 57081 ^T	<i>P. russellii</i> CCUG 58235 ^T	<i>P. anaerobius</i> CCUG 7835 ^T	<i>P. stomatis</i> CCUG 51858 ^T
Rapid ID 32A profile	0402 0200 00	0000 0200 00	0400 0200 00	0400 0000 00
α-glucosidase	+	-	+	+
Mannose	+	-	+	+
Proline arylamidase	+	+	+	-
Hippurate	-	-	+ ^w	-
Major fatty acid	iso-C _{14:0} , iso-C _{16:0} , iso-C _{16:0} DMA,	iso-C _{16:0}	C _{16:0} , C _{18:1} ω9c	iso-C _{16:0} , iso-C _{14:0}
Source	Canine subgingival plaque	Swine manure	Human clinical material	Human oral cavity (Dento-alveolar abscess, periodontal infections)

+, positive; -, negative; w, weak. Major fatty acid constitutes >10% of total fatty acids.

Description of *Peptostreptococcus canis* sp.nov.

ca'nis. L. gen. n. *canis* of a dog. Colonies consist of Gram-positive, non-motile coccoid or ovoid-shaped cells. After 72 hours of anaerobic growth on brucella and chocolate agar plates at 37 °C, colonies were 1-1.5 mm in diameter, grey-white color, round, smooth, shiny and non-hemolytic. Growth is observed at 10 °C and 45 °C and in presence of 6.5% NaCl. Obligately anaerobic. Anaerobic growth occurs in Brain Heart Infusion broth plus 1% glucose medium but is improved by replacing glucose with 5-10% horse serum. Indole production is negative. Catalase, urease and nitrate reduction activity are negative. Hydrolyze esculin and starch but not indole or hippurate. Positive for hemagglutination of horse erythrocytes. Coagulase activity is negative at 4 and 24

hours. Using the API rapid ID32AN test kit, positive reactions are obtained for α -glucosidase, proline arylamidase, and mannose. Negative reactions are obtained with *N*-acetyl- β -glucosaminidase, alanine arylamidase, alkaline phosphatase, α -arabinosidase, arginine arylamidase, arginine dihydrolase, β -galactosidase, β -glucuronidase, glutamic acid decarboxylase, glutamyl glutamic acid arylamidase, α - fucosidase (weak reaction), α -galactosidase, β -galactosidase 6-phosphatase, β -glucosidase, glycine arylamidase, histidine arylamidase, leucine arylamidase, leucyl glycine arylamidase, phenyl alanine arylamidase, pyroglutamic acid arylamidase, raffinose, serine arylamidase, and tyrosine arylamidase, indole hydrolysis, nitrate reduction, and urease. Using the API ZYM system, a positive reaction is obtained for β -glucosidase. No activity is detected for *N*-acetyl- β -glucosaminidase, acid phosphatase, alkaline phosphatase, cystine arylamidase, α -chymotrypsin, esterase (C4), esterase lipase (C8), α -fucosidase α -galactosidase, β -galactosidase, α -glucosidase, β -glucuronidase, leucine arylamidase, and *N*-AS-BI-phosphohydrolase, lipase (C14), α -mannosidase, trypsin, or valine arylamidase. Using conventional methods glucose, fructose, lactose, sucrose, maltose, mannose, arabinose, cellobios, melezitose, melibiose, raffinose, rhamnose, salicin, trehalose, mannitol and sorbitol were not utilized. Major fatty acids are iso-C_{14:0}, iso-C_{16:0}, and iso-C_{16:0} DMA. The G + C content of the DNA of the type strain is 30.8 mol%. Isolated from canine oral subgingival plaque. Habitat not known. The type strain is CCUG 57081^T.

References

- [1] **Ezaki T, Ezaki T.** Genus I. *Peptostreptococcus*. . Bergey's Manual of Systematic Bacteriology, Vol 3 The Firmicutes New York: Springer-Verlag; 2009 In: De Vos P, Garrity GM, Jones D, Krieg NR, Ludwig W, Rainey FA, Schleifer K-H, Whitman WB, editors 2009: 1008-9.
- [2] **Ezaki T, Kawamura Y, Li N, Li ZY, Zhao LC, Shu SE.** Proposal of the genera *Anaerococcus* gen. nov., *Peptoniphilus* gen. nov and *Gallicola* gen. nov for members of the genus *Peptostreptococcus*. International Journal of Systematic and Evolutionary Microbiology 2001;**51**:1521-8.
- [3] **Downes J, Wade WG.** *Peptostreptococcus stomatis* sp. nov., isolated from the human oral cavity. Int J Syst Evol Microbiol 2006;**56**:751-4.
- [4] **Whitehead TR, Cotta MA, Falsen E, Moore E, Lawson PA.** *Peptostreptococcus russellii* sp. nov., isolated from a swine-manure storage pit. International Journal of Systematic and Evolutionary Microbiology 2011;**61**:1875-9.
- [5] **Dahlén G, Charalampakis G, Abrahamsson I, Bengtsson L, E. F.** Predominant bacterial species in subgingival plaque in dogs. Journal of Periodontal Research 2011;doi:10.1111/j.1600-0765.20011.01440.x.
- [6] **Collins MD, Lawson PA, Willems A, Cordoba JJ, Fernandezgarayzabal J, Garcia P, et al.** The phylogeny of the genus clostridium - proposal of 5 new genera and 11 new species combinations. International Journal of Systematic Bacteriology 1994;**44**:812-26.
- [7] **Tindall BJ, Sikorski J, Smibert RM, Kreig NR.** Phenotypic characterization and the principles of comparative systematics. Methods for General and Molecular Microbiology 2007;Editors: C. A. Reddy, T. J. Beveridge, J. A. Breznak, G. Marzluf, T. M. Schmidt, L. R. Snyder ASM Press, Washington DC, USA:330-93.
- [8] **Pearson WR, Lipman DJ.** Improved tools for biological sequence comparison. Proceedings of the National Academy of Sciences of the United States of America 1988;**85**:2444-8.
- [9] **Rasmussen SW.** SEQtools, a software package for analysis of nucleotide and protein sequences. Published on the internet at <http://wwwseqtoolsdk>. 2002.
- [10] **Nicholas KB, Nicholas HBJ, Deerfield DWI.** GeneDoc, analysis and visualization of genetic variation. EMBNEW News 1997;4:14.
- [11] **Page RDM.** TreeView: An application to display phylogenetic trees on personal computers. Computer Applications in the Biosciences 1996;**12**:357-8.

- [12] **Johnson JL.** Similarity analysis of DNAs. *Methods for General and Molecular Bacteriology* 1994;Gerhardt, P., Murray, R.G.E., Wood, W.A., and Krieg, N.R. (eds.) ASM, Washington, D.C.:656-82.
- [13] **Miller LT.** Single derivatization method for routine analysis of bacterial whole-cell fatty acid methyl esters, including hydroxy acids. *J Clin Microbiol* 1982;**16**:584-6.
- [14] **Sasser M.** Identification of bacteria by gas chromatography of cellular fatty acids. MIDI Technical Note 101. Newark, DE: MIDI, Inc.; 1990.
- [15] **Kämpfer P, Kroppenstedt RM.** Numerical analysis of fatty acid patterns of coryneform bacteria and related taxa. *Canadian Journal of Microbiology* 1996;**42**:989-1005.
- [16] **Stackebrandt E, Goebel BM.** Taxonomic Note: A place for DNA-DNA reassociation and 16S rRNA sequence analysis in the present species definition in bacteriology. *International Journal of Systematic Bacteriology* 1994;**44**:846-9.
- [17] **Stackebrandt E, Ebers J.** Taxonomic parameters revisited: tarnished gold standards. *Microbiol Today* 2006;**33**:152-5.
- [18] **Dewhirst FE, Klein EA, Thompson EC, Blanton JM, Chen T, Milella L.** The Canine Oral Microbiome. *PLoS ONE* 2012;**7**:e36067.